[redacted]

NASA TECHNICAL MEMORANDUM

UB
NASA TM X-1504

UB
NASA TM X-1504

[redacted]

AERODYNAMIC CHARACTERISTICS OF THE HL-10 MANNED LIFTING ENTRY VEHICLE AT A MACH NUMBER OF 10.5

by Charles L. Ladson

Langley Research Center
Langley Station, Hampton, Va.

NATIONAL AERONAUTICS AND SPACE ADMINISTRATION • WASHINGTON, D. C. • JANUARY 1968

[redacted]

[redacted]

NASA TM X-1504

N70-78337

AERODYNAMIC CHARACTERISTICS OF THE HL-10 MANNED LIFTING ENTRY VEHICLE AT A MACH NUMBER OF 10.5

By Charles L. Ladson

Langley Research Center
Langley Station, Hampton, Va.

[redacted]

[redacted]

[redacted]

[redacted]

NATIONAL AERONAUTICS AND SPACE ADMINISTRATION

1\3

[redacted]

AERODYNAMIC CHARACTERISTICS OF THE HL-10 MANNED LIFTING ENTRY VEHICLE AT A MACH NUMBER OF 10.5*

By Charles L. Ladson
Langley Research Center

SUMMARY

The longitudinal, directional, and lateral stability and control characteristics of a model of a manned lifting entry vehicle with negative camber, a flat bottom, blunt leading edges, and a delta planform (designated HL-10) have been determined at a Mach number of about 10.5. The configuration was stable about all axes throughout the trim angle-of-attack range of 27° to 51°. The maximum trimmed lift coefficient was about 0.48 and the maximum trimmed lift-drag ratio was about 1.08. These trimmed values are in close agreement with data previously obtained at a Mach number of 6.8, but the trim angle-of-attack range is much less because of a loss in longitudinal control effectiveness with increasing Mach number. In general, lateral control effectiveness increased with increasing positive elevon deflection and angle of attack, and the data show fair agreement with data for a Mach number of 6.8. Although the center-fin rudder is ineffective in the trim angle-of-attack range, directional control can be provided by use of tip-fin rudders if desired.

INTRODUCTION

General studies of lifting bodies have been underway at the Langley Research Center for several years. In early 1962, a specific study was undertaken to develop a manned lifting entry vehicle having a maximum hypersonic lift-drag ratio of about 1. As a result of preliminary work, a configuration with negative camber, a flat bottom, blunt leading edges, and a delta planform was selected for testing throughout the Mach number range. Aerodynamic results of this investigation, most of which are published in references 1 to 33, show that this body shape (designated HL-10) in combination with toed-in, rolled-out tip fins and a vertical center fin (designated I_4 and E_2, respectively, in the references) has static stability and is controllable throughout the range of test variables investigated for values of lift coefficient up to about 0.50. For Mach numbers from low subsonic to

---

[redacted]

[redacted]

[redacted]

supersonic, the range of test variables studied has included most of the control deflections necessary for the definition of the characteristics of a flight vehicle. At hypersonic speeds, however, the data available with fins I_4 and E_2 are limited to tests at a Mach number of 6.8 in air (ref. 15) and 20 in helium (ref. 13). The data obtained in air do not include detailed directional and lateral stability characteristics or roll-control characteristics at angles of attack above about 30°. The data obtained in helium are for an elevon deflection angle of 0° only. Several different elevon planform shapes have been tested on the HL-10 and the shape used herein was the current elevon at the time the tests were conducted. The sweep of the outer elevon chord is different from that of the elevons on the flight vehicle being tested at the NASA Flight Research Center. A comparison of the subsonic longitudinal characteristics with the various elevon planform shapes is presented in reference 33.

The purpose of this report is to present detailed longitudinal, directional, and lateral stability and control characteristics of the HL-10 vehicle with tip fins I_4 and center fin E_2 at a Mach number of 10.5. The data were obtained at angles of attack up to about 60° at a Reynolds number based on model length of about 1.6×10^6. Some additional data for low angles of attack and positive elevon deflection angles are presented at Reynolds numbers of 1.1×10^6 and 2.3×10^6. Where possible, the summary curves are compared with previous hypersonic data on this configuration from references 13 and 15.

SYMBOLS

b	span, inches (centimeters)
C_A	axial-force coefficient, Axial force/qS
C_D	drag coefficient, Drag/qS
C_L	lift coefficient, Lift/qS
C_l	rolling-moment coefficient, Rolling moment/qSb
$C_{l_\beta} = \Delta C_l / \Delta\beta$	per degree
C_m	pitching-moment coefficient, Pitching moment/qSl
$\Delta C_m = (C_m)_{\delta_e \neq 0} - (C_m)_{\delta_e = 0}$	
C_N	normal-force coefficient, Normal force/qS

[redacted]

[redacted]

[redacted]

C_n yawing-moment coefficient, Yawing moment/qSb

$C_{n_\beta} = \Delta C_n/\Delta\beta$ per degree

C_Y side-force coefficient, Side force/qS

$C_{Y_\beta} = \Delta C_Y/\Delta\beta$ per degree

L/D lift-drag ratio

l body length, inches (centimeters)

M free-stream Mach number

p_t stagnation pressure, pounds/inch^2 (meganewtons/meter^2)

q free-stream dynamic pressure, pounds/inch^2 (newtons/centimeter^2)

R Reynolds number based on body length l

S reference area equal to projected planform area with elevons, inches^2 (centimeters^2)

T_t stagnation temperature, degrees Rankine (degrees Kelvin)

X,Y,Z body axes

x,y,z distances along body axes, inches (centimeters)

α angle of attack, degrees

β angle of sideslip, degrees

δ_a aileron deflection angle, equal to right-elevon deflection angle minus left-elevon deflection angle, degrees

δ_e resultant angle of elevon deflection (positive when trailing edge is down), $(\delta_{e,right} + \delta_{e,left})/2$ measured relative to aft lower surface of model and normal to hinge line, degrees

[redacted]

δ_r rudder deflection angle, angle between rudder outer surface and tail outer surface ahead of rudder, measured in plane normal to rudder hinge line, positive for trailing edge left, degrees

MODEL AND DESIGNATIONS

A two-view drawing showing the basic dimensions of the HL-10 vehicle in combination with tip fins I_4 and center fin E_2 is presented in figure 1(a). Cross sections of the vehicle with the tip fins off and on are presented in figure 1(b). All fin designations used herein are a continuation of those established for the HL-10 program in the references.

Nondimensional ordinates of the body and tip fins of the 12-inch-long (30.48-cm) model are presented in table I. Ordinates for the basic body have previously been published in reference 1 for the 8-inch (20.32-cm) model and in reference 5 for the 12-inch (30.48-cm) model. These measurements were not as detailed and were not obtained by as precise a method as were the present measurements. In scaling these values up to larger-sized vehicles, some scatter in the points will be noted because of the small size of the model measured and the accuracy of the machining of the model.

Three rudder configurations were tested and details of these are shown in figure 1(c). The center-fin rudder is identical to that used on the vehicle in tests at lower Mach numbers, while the tip-fin rudders have been tested in the present program only.

The model and all components were constructed of stainless steel because of the high model-equilibrium temperatures expected during the tests. As much of the model interior as was practical was removed to reduce weight and keep the balance tare loads low. The elevons were hinged and the various deflection angles were obtained by placing dowel pins in appropriate holes. The rudder deflections were simulated by solid wedges mounted on the fin surface.

Two different sting-support configurations were used to obtain the data throughout the range of angle of attack. For angles from 0° to about 30°, a straight sting was inserted through the base of the model. For tests at angles of attack from about 30° to 60°, an offset sting was inserted through the model upper surface. In both cases, the balance was housed inside the model. Drawings of the two support systems are shown in figure 2(a) and a photograph of the model with bent sting is shown in figure 2(b). Shadowgraphs of the vehicle with the two support systems are shown in figure 3. When mounted on the bent sting, the model was tested without the center fin E_2. This omission of the center fin at the high angles of attack (30° to 60°) is justified by data obtained at low angles of attack (0° to 30°); these data have shown that the center fin has no aerodynamic contribution above an angle of attack of 25° because the fin is shielded from the flow. Therefore, throughout this paper the term "complete configuration" is used to

[redacted]

define the vehicle with tip and center fins on at low angles of attack and with only tip fins on at the high angles of attack.

All coefficients are based on the total projected planform area, the span, and the length of the model without tip fins. The moment center is located at 53 percent of the body length behind the nose and at 1.25 percent of the body length below the reference center line. The reference areas and lengths are as follows:

$$S = 51.40 \text{ inches}^2 \quad (331.61 \text{ centimeters}^2)$$

$$b = 7.73 \text{ inches} \quad (19.64 \text{ centimeters})$$

$$l = 12.00 \text{ inches} \quad (30.48 \text{ centimeters})$$

APPARATUS, TESTS, AND PROCEDURE

The data contained herein were obtained in the Mach 10 test section of the Langley continuous-flow hypersonic tunnel. This 31-inch-square (79-cm-square) test section operates at stagnation pressures from about 20 to 150 atmospheres (2.03 MN/m^2 to 15.20 MN/m^2). A description and calibration of the facility is presented in the appendix.

Tests were made at three stagnation pressures, and the following table presents the stagnation temperature, Mach number, and Reynolds number based on model length for each pressure:

p_t		T_t		M	R
psi	MN/m^2	^{o}R	^{o}K		
850	5.86	1760	978	10.41	1.1×10^6
1200	8.28	1760	978	10.46	1.6
1800	12.42	1760	978	10.49	2.3

Most of the data were obtained at the intermediate stagnation pressure.

The angles of attack and sideslip of the model were determined from the measured strut angles and calibrations of the deflection of balance and sting due to aerodynamic load. The data were obtained on a six-component, internal, electrical strain-gage balance. Both the balance housing and sting-support system were water cooled to protect the balance from the high air temperatures. Base-pressure measurements were made for several of the configurations tested and, in general, varied from about one-half stream static pressure (about 0.5 mm Hg) to about twice stream pressure (2 mm Hg). The

[redacted]

contribution of base pressure to axial force, based on these measurements, is small compared with the measured axial force; thus, the data presented have not been corrected

The lateral and directional stability data were obtained at sideslip angles between 0° and 10°. Since the data for some configurations were nonlinear with β, the basic results have been presented in this paper. The directional and lateral stability parameters, determined from the two lowest sideslip angles tested, are presented in tabular form in table II. Longitudinal data are presented for both body- and stability-axis systems, whereas the directional and lateral data are referred to the body-axis system only.

ACCURACY OF RESULTS

Two balances were used in order to obtain more accurate results throughout the angle-of-attack range. The accuracy of each balance in terms of the aerodynamic coefficients at a stagnation pressure of 1200 psia (8.28 MN/m^2) is presented in the following table:

α, deg	Accuracy of static balance calibration in terms of –					
	C_N	C_A	C_m	C_l	C_n	C_Y
0 to 30	0.0048	0.0011	0.0004	0.0002	0.0002	0.0011
30 to 60	.0085	.0032	.0007	.0002	.0004	.0032

The data are also subject to an error caused by a shift in the balance zero reading with time. This shift in zero was due to the heat load on the balance even though the balance housing and sting were water cooled. The resultant error is about equal in magnitude to the balance accuracy for all cases except C_l in the high angle-of-attack range, where the error is several times the balance accuracy. The accuracy in angles of attack and sideslip is estimated to be $\pm 0.1^{\circ}$.

PRESENTATION OF RESULTS

The results of this investigation are presented in figures 4 to 29:

[redacted]

[redacted]

[redacted]

RESULTS AND DISCUSSION

Longitudinal Stability and Control

The effects of addition of tip fins and center fin on the longitudinal aerodynamic characteristics are presented in figure 4. Addition of the tip fins increased the axial-force coefficient throughout the test range of angle of attack and produced a negative increment in the normal-force coefficient at the lower angles of attack (see fig. 4(a)). The increase in axial force is the result of the blunt leading edge of the fin (which becomes shielded from the flow as the angle of attack is increased) and the outer surface of the fin. The orientation of the outer surface of the fin would also produce a positive incremental normal force, but this is overcome by the stronger negative normal-force contribution of the leading edge of the fin and a possible high-pressure area on the upper surface due to the tip-fin flow field. These changes in normal- and axial-force coefficients result in about a 0.1 loss in maximum lift-drag ratio for 0^o elevon deflection and essentially no change in stability or trim angle of attack (see fig. 4(b)). The effects of adding the center fin are small and are evident only at angles of attack below about 20^o.

The effects of elevon deflections on the characteristics of the vehicle with fins on are presented in figure 5. Minimum axial force occurs for an elevon deflection angle of 0^o. For both positive and negative elevon deflection angles, the axial force increases because of the inclination of the aft portion of the lower surface of the vehicle to the model reference plane. At the higher angles of attack the axial force is negative because of the lower-surface inclination (see fig. 5(a)). As seen in figure 5(b), elevon deflection has a very small effect on the lift-drag ratio of the vehicle for any angle of attack.

[redacted]

[redacted]

The trim characteristics at a Mach number of 10.5, presented in figure 6, are compared with data for the HL-10 vehicle at $M = 6.8$ from reference 15. At $M = 10.5$, the maximum lift-drag ratio is 1.08 at a lift coefficient of 0.26, and the maximum lift coefficient is about 0.48 at a lift-drag ratio of 0.80. These maximum trimmed values are about the same as those obtained at $M = 6.8$.

The maximum trim angle of attack is 51° with an elevon deflection angle of -45°. At hypersonic speeds, elevon effectiveness is essentially zero once the elevon is deflected above the streamwise direction so that it is shielded from the flow. Thus, this same trim angle of attack might be obtained with an elevon deflection angle of -36° and the fairing of the $\delta_{e,trim}$ curve in figure 6 is arbitrary at the high negative deflection angles.

For most trim angles of attack, higher values of lift and drag were obtained at $M = 10.5$ than at $M = 6.8$. An analysis based on one modified Newtonian theory, in which the values of normal force are assumed to be proportional to the ratios of the stagnation pressure coefficient at the two Mach numbers, indicates that the $M = 10.5$ data should be only a fraction of 1 percent higher than the $M = 6.8$ data. Although the exact reason for the larger differences in the data is not known, they are probably due to the uncertainty in Mach number and balance accuracy and the differences in elevon effectiveness. For example, the untrimmed normal force at $\delta_e = 0^{\circ}$ is 5 percent higher at $M = 10.5$ than at $M = 6.8$, but can be brought into agreement by a change in either or both Mach numbers of only 0.10. (For a calibration of the Langley 11-inch hypersonic tunnel, in which the data at $M = 6.8$ were obtained, see refs. 34 and 35.)

The incremental pitching moment ΔC_m due to elevon deflection angle is presented in figure 7 for both $M = 10.5$ and $M = 6.8$. In general, ΔC_m is less at $M = 10.5$ than at $M = 6.8$. The lower value of ΔC_m results in higher trim angles of attack at positive elevon deflection angles (or higher trimmed lift coefficient) and lower trim angles for negative deflection angles.

The data in figure 7 are also compared with Newtonian theory for an isolated flat plate in free-stream flow. Although Newtonian theory was not expected to predict the forces on the elevons because of the flow separation over the elevons and double-shock flow fields (see schlieren and oil-flow photographs in refs. 13 and 15), it does serve as a useful guideline in evaluating the elevon effectiveness. As expected, the theory overpredicts the experimental data throughout most of the range of angle of attack for the positive deflection angles. At $\alpha = 59^{\circ}$, the double-shock flow field in combination with reduced amounts of separation results in ΔC_m being slightly higher than that of theory.

In reference 15, ΔC_m data at negative elevon deflection angles and oil-flow photographs show that for some combinations of elevon deflection angle and angle of attack, where the elevon should be shielded from the flow, high pressures exist on the lower-surface tips of the elevons. This high pressure on the elevons in the shielded region is

[redacted]

probably the result of a vortex formed by the difference in pressure ac. the body-elevon chord plane, and thus the effectiveness of the elevons is reduced. From the data at $M = 10.5$ in figure 7, it appears that this same flow pattern probably exists at the higher Mach number also, since ΔC_m at negative elevon deflections is much less than theory for cases where the elevon is shielded from the flow.

Directional and Lateral Stability

The basic directional and lateral data are presented as a function of sideslip angle for the configuration with fins off, with tip fins on, and with tip and center fins on in figures 8, 9, and 10, respectively. These basic data are presented in detail to show where nonlinear trends occurred. For an elevon deflection angle of 0°, rolling-moment and yawing-moment coefficients are nonlinear with sideslip angle for low angles of attack (see figs. 8(a), 9(a), and 10(a)). The data become linear as the angle of attack is increased above 10°. These same trends are also noted at low angles of attack for the positive elevon deflection angles presented in figures 10(b), 10(c), and 10(d). For the case of $\delta_e = 45^\circ$ (fig. 10(d)) the nonlinearity in rolling moment also exists at the highest angle of attack of the tests.

Since several cases of nonlinear data exist, the stability derivatives presented are based on the slope between the two lowest sideslip angles of the test (usually 0° and about 2°). These slopes are presented in tabular form in table II for all data obtained and some of the typical results are plotted in figures 11, 12, and 13.

The effects of tip fins and center fin on the directional and lateral stability characteristics are shown in figure 11 for $\delta_e = 0^\circ$. As would be expected, the center fin increases both directional and lateral stability but its effects are limited to angles of attack below about 25°. The tip fins give a positive increment in directional stability and also provide the vehicle with stability throughout the test range of angle of attack. The tip fins provide a positive increment in lateral stability at low angles of attack (which is unexpected when area is added above the vehicle center of gravity) and a negative increment in lateral stability at angles of attack above about 10°. Within the envisioned operational trim angle-of-attack range of the vehicle (27° to 51°), however, the configuration has lateral stability.

The effects of elevon deflection angle on the directional and lateral stability characteristics are presented in figure 12. At angles of attack of 20° and 30°, positive elevon deflection produces a large negative increment in C_{l_β} and has only a small effect on C_{n_β}. Evidently the differential normal force is enough to result in the large effects on rolling moment, while the differential axial force and side force combine to produce only a small effect on yawing moment because of the swept hinge line.

[redacted]

Figure 13 presents directional and lateral stability data for the complete vehicle ($\delta_e = 0^\circ$) and a comparison with data obtained at $M = 6.8$ from reference 15 and at $M = 20.3$ from reference 13. Throughout the trim angle-of-attack range of the vehicle, the agreement is within the accuracy of the data. At low angles of attack, however, differences are noted between the $M = 6.8$ and $M = 10.5$ results. The $M = 6.8$ data of reference 15 were stated to be linear with sideslip angle whereas the $M = 10.5$ data are nonlinear with sideslip angle. Good agreement between the slopes of the data for the two Mach numbers at these low angles of attack is obtained at the higher sideslip angles.

Lateral Control Characteristics

Aileron deflection, which was produced by a differential deflection of the elevons, has essentially no effect on the longitudinal aerodynamic characteristics as shown in figure 14. The incremental rolling moments and yawing moments produced are presented in figure 15. As was the case with elevon effectiveness, little or no lateral control is available at low angles of attack (below the trim limit of the vehicle). Within the trim angle-of-attack range, however, lateral control is available and the yaw due to lateral control is small. The lateral control effectiveness as a function of elevon deflection is presented in figure 16 and compared with results at $M = 6.8$ at $\alpha = 0^\circ$ and 25°. The agreement between the data at the two Mach numbers is fair. In general, the control effectiveness increases with increasing positive elevon deflection angle and angle of attack, as would be expected. At $\alpha = 55^\circ$, however, the control effectiveness at $\delta_e = 30^\circ$ is about the same as at $\delta_e = 0^\circ$. This is probably due to the large amount of separation at this high deflection angle (up to 85°), or the flow over the elevon could be subsonic for this condition.

The effects of sideslip on the lateral characteristics are presented for elevon deflection angles of -30°, 0°, and 30° and aileron deflection angles of 0°, 10°, and 20° in figures 17, 18, and 19, respectively. The incremental rolling and yawing moments do not seem to be affected by sideslip angle, and thus aileron deflection has little effect on directional and lateral stability characteristics.

Directional Control Characteristics

Three rudder configurations (see fig. 1(c)) were tested to determine the directional control characteristics of the vehicle throughout the test range of angle of attack. The center-fin rudder, designated R_1, was tested because it is used on the HL-10 vehicle from subsonic to low supersonic speeds (see refs. 24, 29, and 31). Since it was anticipated that this rudder would have low effectiveness because it was shielded from the flow at the higher angles of attack, two tip-fin rudders were also tested. The first of these, designated R_4, has the same planform shape and location as the outer-surface tip-fin flap

[redacted]

which is used at subsonic speeds to improve the lift-drag ratio by reducing base area (see ref. 16).

The hinge line of this rudder, R_4, is swept back about 30^o from the vertical so that at the higher angles of attack, the hinge line is nearly parallel to the free-stream direction, and its effectiveness would be expected to be low in this case. The last rudder considered, R_5, has the hinge line swept forward 13^o so that it would retain effectiveness at the higher angles of attack and also reduce the pitching moment due to rudder deflection. The planform areas of R_4 and R_5 are essentially the same.

The effects of rudder deflection on the longitudinal characteristics are presented in figure 20. The center-fin rudder (fig. 20(a)) has little effect, whereas the two tip-fin rudders (figs. 20(b) and 20(c)) cause noticeable increases in drag, and thus losses in lift-drag ratio, at the higher rudder deflection angle. This increase in drag is limited to angles of attack below about 40^o for rudder R_4, but exists throughout the test range of angle of attack (26^o to 58^o) for rudder R_5. The incremental rolling and yawing moments due to rudder deflection are shown in figure 21 and the results are as expected. The center-fin rudder, R_1, loses its control capability at an angle of attack of about 20^o while the two tip-fin rudders show control capability throughout the test range of angle of attack. The rudder with the forward swept hinge line, R_5, has a higher yawing moment than rudder R_4, as would be expected, but also shows a large adverse rolling moment at a rudder deflection angle of 40^o because the rudder center of pressure is located well above the vehicle center of gravity.

The effects of sideslip angle on the directional control data are shown in figures 22, 23, and 24 for rudders R_1, R_4, and R_5. These detailed data show that for positive rudder deflection angles the control effectiveness increases with negative sideslip angles, because of the increase in flow deflection angle. This will also lead to increased directional and lateral stability due to rudder deflection.

It can be concluded that to provide aerodynamic directional control for the HL-10 vehicle at $M = 10.5$ at the envisioned operational angles of attack, the existing center-fin rudder is not adequate and tip-fin rudders could be used. Since tip-fin rudders require extra actuators and control systems on the vehicle, it is necessary to determine the merits of aerodynamic control as compared with reaction control for the directional-control system. Factors such as weight, complexity, and reliability must be considered in determining the best control system. The directional-control data presented herein can be used as inputs to this type of comparison.

Effects of Reynolds Number

The effects of increasing the Reynolds number from 1.1×10^6 to 2.3×10^6 are shown in figures 25 and 26 for various elevon deflection angles. The effects of Reynolds number

[redacted]

on C_N and C_m for any elevon angle are small. The axial-force coefficient shows the expected decrease with increasing Reynolds number. The magnitude of the decrease in axial force becomes larger as the elevon deflection angle increases. This is a result of the large area of separation which exists ahead of the elevons when they are deflected into the flow. At $\delta_e = 0^{\circ}$, the lower surface of the vehicle is continuous and no separation area exists. For this case, the change in axial force with Reynolds number is probably due only to the change in skin friction. At $\delta_e = 45^{\circ}$ very little change in axial force is noted at the higher angles of attack (fig. 25(d)). The area of separated flow is probably so large that it is unaffected by the changes in Reynolds number. These differences in axial force are reflected in the lift-drag ratio presented in figure 26. Varying the Reynolds number by a factor of 2 resulted in a maximum change in lift-drag ratio of about 0.1, or about 10 percent.

Sting Effects

As mentioned previously and shown in figure 2, two types of stings were used to obtain the data: a straight sting entering the model base for tests at low angles of attack ($\alpha = 0^{\circ}$ to 30°) and a bent sting entering the model upper surface for tests at high angles of attack ($\alpha = 30^{\circ}$ to 60°). To provide an indication of the effects of the bent sting, the model was tested with this sting in the low angle-of-attack range, and the data are compared with data obtained with the straight sting. Figures 27(a) and 27(b) show that the bent sting produced a small negative incremental normal force and a slight positive incremental pitching moment. This is probably the result of a high-pressure region on the upper surface of the model caused by a shock on the sting. At higher angles of attack with the sting shielded, these differences would be negligible because of the low dynamic pressure and/or separated flow in this region. The bent sting also produces a positive increment in axial force, which leads to a reduction in lift-drag ratio. The cause of this incremental axial force is unknown.

The effects of sideslip angle on the directional and lateral data are presented in figure 28 for the bent-sting configuration. The same nonlinear trends of rolling and yawing moment as observed on the straight sting at the lower angles of attack are evident (compare figs. 9(a) and 28). There is essentially no difference in the directional and lateral stability derivatives when the two sting supports are used, as is shown in figure 29.

CONCLUDING REMARKS

The longitudinal, directional, and lateral stability and control characteristics of a model of a manned lifting entry vehicle with negative camber, a flat bottom, blunt leading edges, and a delta planform (designated HL-10) have been determined at a Mach number

[redacted]

of about 10.5. The configuration was stable about all axes throughout the trim angle-of-attack range of 27° to 51°. The maximum trimmed lift coefficient was about 0.48 and the maximum trimmed lift-drag ratio was about 1.08. These trimmed values are in close agreement with data previously obtained at a Mach number of 6.8, but the trim angle-of-attack range is much less because of a loss in longitudinal control effectiveness with increasing Mach number. In general, lateral control effectiveness increased with increasing positive elevon deflection and angle of attack and the data show fair agreement with data at a Mach number of 6.8. Although the center-fin rudder is ineffective in the trim angle-of-attack range, directional control can be provided by use of tip-fin rudders if desired.

Langley Research Center,
National Aeronautics and Space Administration,
Langley Station, Hampton, Va., June 22, 1967,
124-07-02-56-23.

[redacted]

APPENDIX

CALIBRATION OF THE LANGLEY CONTINUOUS-FLOW HYPERSONIC TUNNEL

The Langley continuous-flow hypersonic tunnel was first placed in operation as a blowdown facility in 1963. By mid-1964 the compressors and drive system were completed and the facility was capable of continuous-flow operation. During this time period, the Mach 10 nozzle was equipped with a water-cooled stainless-steel throat section. Because of the high air temperatures and cooling-water pressure, this nozzle was subject to frequent, costly, and time-consuming repairs. In early 1965, the stainless-steel throat section was replaced by a beryllium-copper throat section which is still in operation. The copper throat is slightly smaller than the original stainless-steel throat and thus the test section Mach number is higher. A brief description and schematic diagram of this facility with the steel throat is contained in reference 36.

The Mach number distributions obtained in the test section with the beryllium-copper throat section are presented in figures 30 to 33 for several stagnation pressures. These Mach numbers are based on total-pressure measurements obtained on a 10-tube rotating and translating total-pressure rake which was air cooled to protect it from the high stagnation temperature of the tunnel. All Mach numbers in these figures have been corrected for real-gas effects by the method presented in reference 37. Based on the accuracy of the instrumentation used, it is estimated that the maximum error in any individual data point is about ±0.02 in Mach number or about 1 percent in dynamic pressure.

[redacted]

[redacted]

REFERENCES

1. Rainey, Robert W.; and Ladson, Charles L.: Preliminary Aerodynamic Characteristics of a Manned Lifting Entry Vehicle at a Mach Number of 6.8. NASA TM X-844, 1963.

2. Ware, George M.: Aerodynamic Characteristics of Models of Two Thick 74° Delta Manned Lifting Entry Vehicles at Low-Subsonic Speeds. NASA TM X-914, 1964.

3. Ladson, Charles L.: Aerodynamic Characteristics of a Manned Lifting Entry Vehicle at a Mach Number of 6.8. NASA TM X-915, 1964.

4. Dunavant, James C.; and Everhart, Philip E.: Investigation of the Heat Transfer to the HL-10 Manned Lifting Entry Vehicle at a Mach Number of 8. NASA TM X-998, 1964.

5. Rainey, Robert W.; and Ladson, Charles L.: Aerodynamic Characteristics of a Manned Lifting Entry Vehicle at Mach Numbers From 0.2 to 1.2. NASA TM X-1015, 1964.

6. McShera, John T., Jr.; and Campbell, James F.: Stability and Control Characteristics of a Manned Lifting Entry Vehicle at Mach Numbers From 2.29 to 4.63. NASA TM X-1019, 1964.

7. Ware, George M.: Effect of Fin Arrangements on Aerodynamic Characteristics of a Thick 74° Delta Manned Lifting Entry Vehicle at Low-Subsonic Speeds. NASA TM X-1020, 1965.

8. Harris, Julius E.: Longitudinal Aerodynamic Characteristics of a Manned Lifting Entry Vehicle at a Mach Number of 19.7. NASA TM X-1080, 1965.

9. Everhart, Philip E.; and Hamilton, H. Harris: Investigation of Roughness-Induced Turbulent Heating to the HL-10 Manned Lifting Entry Vehicle at a Mach Number of 8. NASA TM X-1101, 1965.

10. Campbell, James F.; and McShera, John T., Jr.: Stability and Control Characteristics From Mach Number 1.50 to 2.86 of a Model of a Manned Lifting Entry Vehicle. NASA TM X-1117, 1965.

11. McShera, John T., Jr.; and Campbell, James F.: Aerodynamic Characteristics From Mach 1.50 to 2.86 of a Lifting Entry Vehicle Alone, With Adapter Sections, and With a Saturn Launch Vehicle. NASA TM X-1125, 1965.

12. Harvey, William D.: Pressure Distribution on HL-10 Manned Lifting Entry Vehicle at a Mach Number of 19.5. NASA TM X-1135, 1965.

13. Johnston, Patrick J.: Stability Characteristics of a Manned Lifting Entry Vehicle at a Mach Number of 20.3 in Helium. NASA TM X-1156, 1965.

 [redacted]

[redacted]

14. Spencer, Bernard, Jr.: An Investigation of Methods of Improving Subsonic Performance of a Manned Lifting Entry Vehicle. NASA TM X-1157, 1965.

15. Ladson, Charles L.: Aerodynamic Characteristics of a Manned Lifting Entry Vehicle With Modified Tip Fins at Mach 6.8. NASA TM X-1158, 1965.

16. Rainey, Robert W.: Summary of an Advanced Manned Lifting Entry Vehicle Study. NASA TM X-1159, 1965.

17. Ware, George M.: Full-Scale Wind-Tunnel Investigation of the Aerodynamic Characteristics of the HL-10 Manned Lifting Entry Vehicle. NASA TM X-1160, 1965.

18. Silvers, H. Norman; and Campbell, James F.: Stability Characteristics of a Manned Lifting Entry Vehicle With Various Fins at Mach Numbers From 1.50 to 2.86. NASA TM X-1161, 1965.

19. Moul, Martin T.; and Brown, Lawrence W.: Some Effects of Directional Instability on Lateral Handling Qualities of an Early Version of a Manned Lifting Entry Vehicle. NASA TM X1162, 1965.

20. Campbell, James F.: Effects of Tip-Fin Geometry on Stability Characteristics of a Manned Lifting Entry Vehicle From Mach 1.50 to 2.86. NASA TM X-1176, 1965.

21. Harris, Charles D.: Effect of Elevon Deflection and of Model Components on Aerodynamic Characteristics of a Manned Lifting Entry Vehicle at Mach Numbers of 0.20 to 1.20. NASA TM X-1226, 1966.

22. Spencer, Bernard, Jr.; and Fox, Charles H., Jr.: Subsonic Longitudinal Control Characteristics of Several Elevon Configurations for a Manned Lifting Entry Vehicle. NASA TM X-1227, 1966.

23. Harris, Charles D.: Control-Surface Hinge-Moment and Elevon Normal-Force Characteristics at Transonic Speeds on a Manned Lifting Entry Vehicle. NASA TM X-1241, 1966.

24. Harris, Charles D.: Transonic Aerodynamic Characteristics of a Manned Lifting Entry Vehicle With and Without Tip Fins. NASA TM X-1248, 1966.

25. Campbell, James F.; and Jernell, Lloyd S.: Effects of Various Center-Fin and Tip-Fin Arrangements on Aerodynamic Characteristics of a Manned Lifting Entry Vehicle From Mach Numbers 1.50 to 2.86. NASA TM X-1299, 1966.

26. Stubbs, Sandy M.: Landing Characteristics of a Dynamic Model of the HL-10 Manned Lifting Entry Vehicle. NASA TN D-3570, 1966.

27. Campbell, James F.; and Watson, Carolyn B.: Stability and Control, Hinge-Moment, and Pressure-Coefficient Data for the HL-10 Manned Lifting Entry Vehicle at Mach Numbers From 1.41 to 2.16. NASA TM X-1300, 1966.

[redacted]

[redacted]

28. Harvey, William D.: Experimental Investigation of Laminar Heat-Transfer Characteristics of a Manned Lifting Entry Vehicle at a Mach Number of 20. NASA TM X-1306, 1966.

29. Ware, George M.: Investigation of the Flight Characteristics of a Model of the HL-10 Manned Lifting Entry Vehicle. NASA TM X-1307, 1967.

30. Campbell, James F.; and Grow, Josephine W.: Stability and Control Characteristics of a Manned Lifting Entry Vehicle at Mach Numbers From 1.50 to 2.16 Including Hinge Moment and Pressure Distribution Data. NASA TM X-1314, 1966.

31. Ladson, Charles L.: Effects of Various Canopies on the Aerodynamic Characteristics of a Manned Lifting Entry Vehicle at Mach 0.06 to 6.8. NASA TM X-1321, 1966.

32. Johnson, Joseph L., Jr.; Chambers, Joseph R.; and White, Lucy C.: Analytical Study of the Subsonic Dynamic Stability and Response of the HL-10 Entry Vehicle. NASA TM X-1348, 1967.

33. Spencer, Bernard, Jr.: Effects of Elevon Planform on Low-Speed Aerodynamic Characteristics of the HL-10 Manned Lifting Entry Vehicle. NASA TM X-1409, 1967.

34. Bertram, Mitchel H.: Exploratory Investigation of Boundary-Layer Transition on a Hollow Cylinder at a Mach Number of 6.9. NACA Rept. 1313, 1957. (Supersedes NACA TN 3546.)

35. Neal, Luther, Jr.: A Study of the Pressure, Heat Transfer, and Skin Friction on Sharp and Blunt Flat Plates at Mach 6.8. NASA TN D-3312, 1966.

36. Schaefer, William T., Jr.: Characteristics of Major Active Wind Tunnels at the Langley Research Center. NASA TM X-1130, 1965.

37. Erickson, Wayne D.; and Creekmore, Helen S.: A Study of Equilibrium Real-Gas Effects in Hypersonic Air Nozzles, Including Charts of Thermodynamic Properties for Equilibrium Air. NASA TN D-231, 1960.

[redacted]

TABLE I.- ORDINATES FOR HL-10

(a) Body ordinates

y/l	z/l	z/l
x/l = 0.046875		
0	-0.05717	0.05675
.00833	-.05700	.05583
.01667	-.05600	.05267
.02500	-.05367	.04667
.02917	-.05158	.04258
.03333	-.04867	.03750
.03750	-.04475	.03150
.04167	-.03933	.02408
.04583	-.03142	.01217
.04792	-.02450	.00333
.04875	-.01750	-.00242
.04892	--------	-.00708
.04917	-.01433	-.01433
x/l = 0.088541		
0	-0.07708	-------
.01250	-.07692	0.06658
.02083	-.07650	.06242
.02500	--------	.05958
.02917	-.07500	.05608
.03333	--------	.05200
.03750	-.07200	.04692
.04167	-.06967	.04092
.04583	-.06650	.03400
.04792	--------	.03000
.05000	-.06242	.02567
.05208	--------	.02058
.05417	-.05658	.01458
.05625	--------	.00750
.05833	-.04808	.00075
.06042	-.04017	-.01117
.06125	-.03267	-------
.06142	-.02633	-.02633
x/l = 0.13021		
0	-0.09192	0.07408
.00833	--------	.07325
.01250	-.09200	-------
.01667	--------	.07083
.02500	-.09183	.06675
.02917	--------	.06400
.03333	-.09117	.06075
.03750	--------	.05692
.04167	-.08950	.05242
.04583	--------	.04725
.04792	--------	.04442
.05000	-.08617	.04142
.05208	--------	.03808
.05417	--------	.03450
.05625	--------	.03058
.05833	-.08058	.02633
.06042	--------	.02150
.06250	-.07667	.01600
.06458	--------	.00958
.06667	-.07117	.00250
.06875	--------	-.00808
.07083	-.06258	-.01475
.07292	-.05292	-.02600
.07358	-.04042	-.04042
.07500	--------	-.03025
x/l = 0.17187		
0	-0.10375	0.07717
.00833	--------	.07650
.01250	-.10375	-------
.01667	--------	.07467
.02500	-.10383	.07158
.02917	--------	.06967
.03333	--------	.06725
.03750	-.10367	.06425
.04167	--------	.06092
.04583	--------	.05700
.04792	--------	.05483
.05000	-.10225	.05267
.05208	--------	.05025
.05417	--------	.04767
.05625	--------	.04492
.05833	--------	.04200
.06042	--------	.03892
.06250	-.09767	.03550
.06458	--------	.03192
.06667	--------	.02808
x/l = 0.17187 – Continued		
0.06875	--------	0.02383
.07083	--------	.01942
.07292	--------	.01442
.07500	-0.08833	.00858
.07708	--------	.00192
.07917	-.08267	-.00567
.08125	--------	-.01475
.08333	-.07358	-.02425
.08500	-.06483	-------
.08542	--------	-.03742
.08600	-.05392	-.05392
x/l = 0.21354		
0	-0.11333	0.07933
.00833	--------	.07883
.01250	-.11333	-------
.01667	--------	.07742
.02500	-.11333	.07508
.02917	--------	.07358
.03333	--------	.07175
.03750	-.11333	.06967
.04167	--------	.06725
.04583	--------	.06433
.04792	--------	.06275
.05000	-.11317	.06117
.05208	--------	.05933
.05417	--------	.05750
.05625	--------	.05550
.05833	--------	.05317
.06042	--------	.05083
.06250	-.11158	.04850
.06458	--------	.04592
.06667	--------	.04317
.06875	--------	.04033
.07083	--------	.03717
.07292	--------	.03392
.07500	-.10700	.03042
.07708	--------	.02683
.07917	--------	.02283
.08125	--------	.01883
.08333	--------	.01392
.08542	--------	.00858
.08750	-.09725	.00225
.08958	--------	-.00492
.09167	-.09133	-.01308
.09375	-.08725	-.02225
.09583	-.08142	-.03383
.09708	-.07450	-------
.09767	-.06600	-------
.09792	--------	-.04967
.09817	--------	-.06600
x/l = 0.25521		
0	-0.12108	0.08067
.00833	--------	.08033
.01250	-.12108	-------
.01667	--------	.07933
.02500	-.12108	.07767
.03333	--------	.07525
.03750	-.12108	-------
.04167	--------	.07175
.05000	-.12108	.06742
.05833	--------	.06158
.06250	-.12092	-------
.06667	--------	.05400
.07500	-.11942	-.04500
.08333	--------	.03367
.08750	-.11458	.02675
.09167	--------	.01858
.09583	-.10867	.00867
.10000	-.10408	-.00392
.10208	--------	-.01142
.10417	-.09775	-.02008
.10625	--------	-.03033
.10833	-.08683	-.04275
.10917	-.08133	-.05275
.10950	-.07108	-.07108
x/l = 0.29687		
0	-0.12708	0.08150
.00833	--------	.08117
.01250	-.12708	-------
.01667	--------	.08050
.02500	-.12708	.07925
x/l = 0.29687 – Continued		
0.03333	--------	0.07758
.03750	-0.12700	-------
.04167	--------	.07525
.50000	-.12708	.07200
.05833	--------	.06792
.06250	-.12708	-------
.06667	--------	.06250
.07500	-.12692	.05575
.08333	--------	.04775
.08750	-.12517	.04292
.09167	--------	.03733
.09583	--------	.03100
.10000	-0.12033	.02367
.10208	--------	.01942
.10417	--------	.01467
.10625	--------	.00958
.10833	-.11392	.00367
.11042	--------	-.00283
.11250	-.10917	-.00983
.11458	--------	-.01775
.11667	-.10258	-.02683
.11875	-.09783	-.03758
.11958	-.09525	-.04283
.12042	-.09183	-------
.12083	--------	-.05117
.12125	-.08692	-------
.12150	-.07867	-.07867
x/l = 0.33854		
0	-0.13100	0.08200
.00833	--------	.08192
.01250	-.13100	-------
.01667	--------	.08108
.02500	-.13108	.08017
.03333	--------	.07900
.03750	-.13108	-------
.04167	--------	.07733
.05000	-.13100	.07492
.05833	--------	.07200
.06250	-.13100	-------
.06667	--------	.06833
.07500	-.13100	.06350
.08333	--------	.05767
.08750	-.13083	.05417
.09167	--------	.05033
.09583	--------	.04575
.10000	-.12908	.04083
.10208	--------	.03800
.10417	--------	.03508
.10625	--------	.03183
.10833	--------	.02842
.11042	--------	.02467
.11250	-.12358	.02050
.11458	--------	.01583
.11667	--------	.01075
.11875	--------	.00492
.12083	--------	-.00167
.12292	--------	-.00800
.12500	-.11225	-.01575
.12708	--------	-.02400
.12917	-.10525	-.03342
.13125	-.10017	-.04508
.13208	--------	-.05058
.13250	-.09533	-------
.13333	-.08917	-.06033
.13367	-.08067	-.08067
.13417	--------	-.07367
x/l = 0.38021		
0	-0.13317	0.08192
.01250	-.13317	.08150
.02500	-.13317	.08050
.03750	-.13308	.07892
.05000	-.13308	.07658
.06250	-.13308	.07308
.07500	-.13317	.06817
.08750	-.13308	.06133
.10000	-.13292	.05200
.10833	--------	.04350
.11250	-.13092	-------
.11667	--------	.03242
.12083	--------	.02567
.12500	-.12550	.01725
.12917	--------	.00675
x/l = 0.38021 – Continued		
0.13125	--------	0.00083
.13333	-0.11875	-.00583
.13542	--------	-.01333
.13750	--------	-.02133
.13958	--------	-.03017
.14167	-.10642	-.04017
.14375	-.10075	-.05283
.14458	-.09692	-.05883
.14567	-.08683	-.08683
.14583	--------	-.07158
x/l = 0.42187		
0	-0.13350	0.08158
.01250	-.13342	.08125
.02500	-.13350	.08042
.03750	-.13350	.07917
.05000	-.13350	.07717
.06250	-.13350	.07458
.07500	-.13350	.07092
.08750	-.13342	.06600
.10000	-.13342	-------
.11250	-.13317	.04950
.11667	--------	.04550
.12083	--------	.04092
.12500	-.13092	.03567
.12917	--------	.02967
.13333	--------	.02267
.13750	-.12542	.01417
.14167	--------	.00367
.14375	--------	-.00258
.14583	-.11850	-.00950
.14792	--------	-.01717
.15000	-.11342	-.02567
.15208	-.11008	-.03508
.15417	-.10575	-.04617
.15542	-.10225	-.05392
.15625	-.09883	-.05967
.15708	-.09300	-.06700
.15750	--------	-.08033
.15767	-.08575	-.08575
x/l = 0.46354		
0	-0.13158	0.08008
.01250	-.13158	.07983
.02500	-.13158	.07933
.03750	-.13150	.07850
.05000	-.13158	.07700
.06250	-.13150	.07492
.07500	-.13158	.07200
.08750	-.13167	.06842
.10000	-.13167	.06342
.11250	-.13167	.05650
.12500	-.13133	.04700
.13333	--------	.03842
.13750	-.12892	.03342
.14167	--------	.02750
.14583	--------	.02050
.15000	-.12292	.01217
.15417	--------	.00158
.15625	--------	-.00467
.15750	--------	-.00858
.15833	-.11583	-.01133
.15917	--------	-.01450
.16000	--------	-.01767
.16083	--------	-.02100
.16167	--------	-.02433
.16250	-.11067	-.02783
.16333	--------	-.03175
.16417	--------	-.03592
.16458	-.10708	-------
.16500	--------	-.04000
.16583	--------	-.04483
.16667	-.10242	-.04975
.16750	-.09975	-.05533
.16833	-.09617	-.06175
.16917	-.09050	-.06875
.16958	--------	-.07983
.16975	-.08100	-.08100
x/l = 0.50521		
0	-0.12775	0.07817
.01250	-.12775	.07808
.02500	-.12775	.07775
.03750	-.12783	.07717
.05000	-.12783	.07617

[redacted]

[redacted]

TABLE I.- ORDINATES FOR HL-10 – Continued

(a) Body ordinates – Continued

y/l	z/l	z/l
x/l = 0.50521 – Continued		
0.06250	-0.12783	0.07450
.07500	-.12783	.07233
.08750	-.12783	.06950
.10000	-.12775	.06575
.11250	-.12775	.06075
.12500	-.12783	.05392
.13750	-.12758	.04450
.14583	--------	.03633
.15000	-.12467	-------
.15417	--------	.02583
.15833	--------	.01917
.16250	-.11833	.01108
.16458	--------	.00625
.16667	--------	.00100
.16875	--------	-.00550
.17083	-.11108	-.01233
.17292	--------	-.02025
.17500	-.10550	-.02908
.17708	--------	-.03942
.17917	-.09675	-.05158
.18042	--------	-.06017
.18125	--------	-.06842
.18150	-.08475	-.08475
x/l = 0.54687		
0	-0.12192	0.07617
.01250	-.12192	.07608
.02500	-.12192	.07592
.03750	-.12192	.07550
.05000	-.12192	.07475
.06250	-.12200	.07367
.07500	-.12200	.07208
.08750	-.12192	.06983
.10000	-.12200	.06700
.11250	-.12200	.06317
.12500	-.12200	.05825
.13750	-.12200	.05150
.15000	-.12158	.04258
.15833	--------	.03483
.16250	-.11867	-------
.16667	--------	.02467
.17083	--------	.01842
.17500	-.11175	.01075
.17917	--------	.00108
.18125	--------	-.00467
.18333	--------	-.01133
.18542	--------	-.01883
.18750	-.09842	-.02767
.18958	-.09433	-.03792
.19083	--------	-.04483
.19167	-.08858	-.05008
.19208	--------	-.05283
.19250	--------	-.05592
.19292	-.08175	-.05950
.19333	--------	-.06433
.19350	--------	-.07117
.19367	-.07600	-.07600
x/l = 0.58854		
0	-0.11450	0.07400
.01250	-.11450	.07392
.02500	-.11450	.07383
.03750	-.11450	.07358
.05000	-.11450	.07308
.06250	-.11458	.07233
.07500	-.11458	.07133
.08750	-.11450	.06975
.10000	-.11450	.06758
.11250	-.11450	.06467
.12500	-.11458	.06092
.13750	-.11458	.05592
.15000	-.11450	.04942
.15833	--------	.04408
.16250	-.11400	-------
.16667	--------	.03750
.17500	-.11092	.02925
.18333	--------	.01850
.18750	-.10392	.01117
.19167	--------	.00233
.19583	-.09592	-.00925
.19792	--------	-.01633
.20000	-.08967	-.02483
.20208	-.08583	-.03517
.20417	-.07900	-.04725
.20500	--------	-.05358
.20533	--------	-.05783
.20567	-.07125	-.07133

y/l	z/l	z/l
x/l = 0.63021		
0	-0.10617	0.07142
.01250	-.10617	.07142
.02500	-.10625	.07133
.03750	-.10625	.07117
.05000	-.10625	.07092
.06250	--------	.07042
.07500	-.10617	.06967
.08750	-.10625	.06867
.10000	-.10617	.06725
.11250	-.10617	.06517
.12500	-.10617	.06242
.13750	-.10617	.05875
.15000	-.10608	.05383
.16250	-.10617	.04767
.17500	-.10550	.03975
.18333	--------	.03300
.18750	-.10233	-------
.19167	--------	.02425
.20000	-.09500	.01217
.20417	--------	.00375
.20833	-.08675	-.00700
.21042	--------	-.01400
.21250	-.08050	-.02225
.21458	-.07558	-.03200
.21583	--------	-.03917
.21667	-.06700	-.04533
.21708	--------	-.05483
.21733	-.06133	-.06133
x/l = 0.67187		
0	-0.09725	0.06850
.01250	-.09725	.06850
.02500	-.09733	.06842
.03750	-.09733	.06842
.05000	-.09733	.06825
.06250	-.09725	.06800
.07500	-.09725	.06750
.08750	-.09733	.06683
.10000	-.09733	.06592
.11250	-.09733	.06458
.12500	-.09733	.06275
.13750	-.09733	.06033
.15000	-.09733	.05708
.16250	-.09733	.05283
.17500	-.09733	.04717
.18750	-.09667	.03983
.20000	-.09300	.03008
.20833	--------	.02067
.21250	-.08550	.01442
.21667	--------	.00667
.22083	-.07700	-.00392
.22292	-.07383	-.01050
.22500	-.07008	-.01842
.22708	-.06450	-.02850
.22833	--------	-.03608
.22900	-.06350	-.06350
.22917	--------	-.04408
x/l = 0.68750		
0	-0.09383	0.06733
.01250	-.09383	.06733
.02500	-.09383	.06725
.03750	-.09383	.06717
.05000	-.09392	.06708
.06250	-.09392	.06692
.07500	-.09392	.06650
.08750	-.09383	.06600
.10000	-.09392	.06517
.11250	-.09392	.06392
.12500	-.09392	.06233
.13750	-.09392	.06050
.15000	-.09392	.05767
.16250	-.09392	.05408
.17500	-.09392	.04933
.18750	-.09367	.04300
.20000	-.09100	.03467
.20833	--------	.02733
.21250	-.08517	.02242
.21667	--------	.01683
.22083	-.07842	.00967
.22292	--------	.00525
.22500	-.07367	-.00008
.22708	--------	-.00617
.22917	-.06700	-.01350
.23125	-.06217	-.02258
.23208	-.05908	-------
.23333	--------	-.03558
.23375	--------	-.04042
.23400	-.04850	-.04850

y/l	z/l	z/l
x/l = 0.71354		
0	-0.08775	0.06517
.01250	--------	.06517
.02500	--------	.06508
.03750	--------	.06500
.04167	-.08775	--------
.05000	--------	.06500
.06250	--------	.06492
.07500	--------	.06458
.08333	-.08775	--------
.08750	--------	.06433
.10000	--------	.06367
.11250	--------	.06292
.12500	-.08767	.06183
.13750	--------	.06025
.15000	--------	.05825
.16250	--------	.05558
.16667	-.08775	--------
.17500	--------	.05225
.17917	-.08767	--------
.18750	-.08767	.04742
.19208	-.08750	.04567
x/l = 0.75521		
0	0.06135	-0.07750
.01250	.06135	-.07750
.02500	.06133	-.07750
.03750	.06133	-.07750
.05000	.06133	-.07750
.06250	.06127	-.07750
.07500	.06118	-.07750
.08750	.06098	-.07750
.10000	.06067	-.07750
.11250	.06025	-.07750
.12500	.05971	-.07750
.13750	.05786	-.07750
.15000	.05783	-.07750
.16250	.05631	-.07750
.17500	.05429	-.07750
.18750	.05167	-.07750
.19583	.04927	-.07750
.20000	.04781	-.07750
.20208	.04700	-.07750
.20416	--------	-.07750
.20500	--------	-.07746
.20583	--------	-.07742
.20833	.04425	-.07717
.21458	.04093	-.07621
.22083	.03701	-.07442
.22708	.03255	-.07179
.23333	.02730	-.06808
.23750	.02287	-.06483
.24166	.01748	-.06083
.24583	.01042	-.05792
.24792	.00500	-.05267
.25000	-.00027	-.04883
.25125	-.00552	-.04575
.25208	-.01002	-.04325
.25292	-.01571	-.03979
.25375	-.02575	-.03233
.25378	-.02700	-.02983
x/l = -0.79687		
0	0.05733	-0.06637
.01250	.05733	-.06637
.02500	.05733	-.06637
.03750	.05733	-.06637
.05000	.05733	-.06637
.06250	.05731	-.06637
.07500	.05729	-.06637
.08750	.05728	-.06637
.10000	.05725	-.06637
.11250	.05717	-.06637
.12500	.05697	-.06637
.13750	.05671	-.06637
.15000	.05636	-.06637
.16250	.05585	-.06637
.17500	.05515	-.06637
.18750	.05396	-.06637
.20000	.05170	-.06637
.21250	.04833	-.06637
.21458	.04763	-.06637
.21583	--------	-.06637
.21666	--------	-.06633
.21750	--------	-.06633
.21833	--------	-.06629
.22083	.04525	-.06608
.22708	.04228	-.06510

y/l	z/l	z/l
x/l = -0.79687 – Continued		
0.23333	0.03866	-0.06325
.23750	.03587	-.06150
.24166	.03288	-.05933
.24583	.02966	-.05663
.25000	.02593	-.05329
.25250	.02329	-.05093
.25500	.02025	-.04817
.25750	.01660	-.04508
.26042	.01119	-.04058
.26250	.00607	-.03637
.26416	.00014	-.03150
.26500	-.00531	-.02775
.26542	-.00789	--------
.26575	-.01390	-.01958
x/l = 0.82812		
0.	0.05407	-0.05804
.05000	.05406	-.05804
.06250	.05405	-.05804
.07500	.05404	-.05804
.08750	.05404	-.05804
.10000	.05404	-.05804
.10417	.05404	-.05804
.12708	.05402	-.05804
.13750	.05400	-.05804
.15000	.05395	-.05804
.16250	.05385	-.05804
.17500	.05367	-.05804
.18750	.05341	-.05804
.20000	.05281	-.05804
.21250	.05086	-.05804
.22416	-------	-.05804
.22458	-------	-.05801
.22500	.04706	-.05800
.22542	-------	-.05800
.22583	-------	-.05799
.22625	-------	-.05793
.22708	-------	-.05792
.22792	-------	-.05783
.23333	.04443	-.05718
.24166	.04045	-.05500
.25000	.03531	-.05121
.25416	.03233	-.04858
.25833	.02894	-.04533
.26083	.02662	-.04308
.26333	.02393	-.04043
.26583	.02077	-.03742
.26750	.01830	-.03517
.26916	.01545	-.03250
.27083	.01201	-.02933
.27250	.00767	-.02517
.27375	.00300	-.02033
.27416	.00071	-.01783
.27466	-.00450	-.01179
x/l = 0.86979		
0	0.04948	-0.04692
.04167	.04948	-.04692
.06250	.04947	-.04692
.08333	.04947	-.04692
.10417	.04946	-.04692
.12500	.04946	-.04692
.14583	.04945	-.04692
.16667	.04944	-.04692
.18750	.04942	-.04692
.20833	.04942	-.04692
.21666	.04937	-.04692
.22916	.04857	-.04692
.23625	-------	-.04692
.23666	-------	-.04692
.23708	-------	-.04687
.23750	.04700	-.04683
.24583	.04458	-.04592
.25208	.04222	-.04433
.25833	.03928	-.04192
.26250	.03695	-.03973
.26666	.03427	-.03702
.27083	.03118	-.03374
.27500	.02743	-.02964
.27750	.02467	-.02667
.28000	.02142	-.02317
.28208	.01846	-.01958
.28416	.01363	-.01481
.28542	.00988	-.01054
.28583	.00898	-.00844
.28625	.00579	-.00521
.28656	.00121	-.00108

[redacted]

[redacted]

TABLE I.- ORDINATES FOR HL-10 – Continued

(a) Body ordinates – Concluded

x/l = 0.91145			x/l = 0.95312			x/l = 0.98750		
y/l	z/l	z/l	y/l	z/l	z/l	y/l	z/l	z/l
0	0.04476	-0.03592	0	0.03989	-0.02471	0	0.03572	-0.01533
.04167	.04476	-.03592	.04167	.03988	-.02471	.04167	.03572	-.01533
.06250	.04475	-.03592	.06250	.03987	-.02471	.06250	.03572	-.01533
.08333	.04474	-.03592	.08333	.03987	-.02471	.08333	.03572	-.01533
.10417	.04473	-.03592	.10417	.03987	-.02471	.10417	.03572	-.01533
.12500	.04473	-.03592	.12500	.03987	-.02471	.12500	.03572	-.01533
.14583	.04472	-.03592	.14583	.03987	-.02471	.14583	.03572	-.01533
.16667	.04472	-.03592	.16667	.03987	-.02471	.16667	.03572	-.01533
.18750	.04472	-.03592	.18750	.03987	-.02471	.18750	.03572	-.01533
.20833	.04471	-.03592	.20833	.03986	-.02471	.20833	.03572	-.01533
.22916	.04471	-.03592	.22916	.03985	-.02471	.22916	.03572	-.01533
.24583	.04465	-.03592	.25000	.03985	-.02471	.25000	.03572	-.01533
.24833	.04465	-.03592	.26042	-------	-.02471	.27083	.03572	-.01533
.24875	-------	-.03583	.26250	-------	-.02463	.27458	-------	-.01529
.24916	-------	-.03583	.26458	-------	-.02450	.27708	-------	-.01516
.25000	-------	-.03579	.26666	-------	-.02431	.27916	-------	-.01491
.25416	.04410	-.03546	.27083	.03983	-.02367	.28333	-------	-.01413
.26250	.04246	-.03383	.27916	.03945	-.02117	.28750	-------	-.01292
.27083	.03969	-.03064	.28750	.03760	-.01700	.29166	.03571	-.01127
.27708	.03679	-.02708	.29166	.03609	-.01414	.29792	.03570	-.00800
.28333	.03296	-.02221	.29583	.03404	-.01063	.30000	.03558	-.00667
.28750	.02967	-.01800	.30000	.03135	-.00627	.30416	.03492	-.00352
.29000	.02718	-.01496	.30250	.02922	-.00308	.30833	.03342	.00040
.29250	.02345	-.01125	.30500	.02643	.00069	.31083	.03217	.00317
.29416	.02167	-.00833	.30666	.02444	.00371	.31292	.03060	.00579
.29542	.01942	-.00560						
			.30792	.02163	.00640	.31416	.02948	.00758
.29625	.01758	-.00346	.30833	.02067	.00742	.31542	.02800	.00958
.29708	.01528	-.00079	.30875	.01958	.00858	.31625	.02678	.01104
.29750	.01381	.00086	.30916	.01829	.00983	.31708	.02522	.01273
.29792	.01200	.00293	.30958	.01645	.01133	.31750	.02438	.01343
.29800	.01154	.00350						
.29833	.00817	.00621	.30966	.01593	--------	.31792	.02342	.01427
			.30975	.01548	---------	.31833	.02208	.01525
			.30983	.01452	.01333	.31850	.02118	.01573
						.31875	.01939	.01675
						.31879	.01857	.01700

[redacted]

[redacted]

TABLE I.- ORDINATES FOR HL-10 – Concluded

(b) Tip-fin ordinates

y/l	z/l	z/l
x/l = 0.68750		
0	-0.09398	Out
.1750	-.09380	0.04912
.1792	-.09377	.04721
.1833	-.09365	.04504
.1875	-.09333	.04268
.1917	-.09277	.04010
.1958	-.09200	.03725
.2000	-.09092	.03411
.2042	-.08948	.03050
.2083	-.08762	.02640
.2125	-.08533	.02158
.2167	-.08254	.01588
.2208	-.07902	.00897
.2250	-.07462	-.00017
.2271	-.07193	-.00625
.2292	-.06875	-.01387
.2312	-.06453	-.02345
.2333	-.05746	-.03650
.2341	-.04808	-.04808
x/l = 0.71354		
0	-0.08782	Out
.1875	-.08762	0.04698
.1917	-.08748	.04500
.1958	-.08712	.04289
.2000	-.08654	.04067
.2042	-.08575	.03833
.2083	-.08460	.03567
.2125	-.08317	.03254
.2167	-.08133	.02898
.2208	-.07907	.02475
.2250	-.07622	.01970
.2292	-.07272	.01358
.2312	-.07060	.01000
.2333	-.06817	.00586
.2354	-.06512	.00082
.2375	--------	-.00560
.2396	--------	-.01450
.2420	-.03552	-.03550
x/l = 0.75521		
0	-0.07729	Out
.2000	-.07708	0.04808
.2042	-.07702	.04658
.2083	-.07671	.04498
.2125	-.07611	.04342
.2167	-.07530	.04133
.2208	-.07417	.03918
.2250	-.07275	.03685
.2292	-.07095	.03430
.2333	-.06878	.03119
.2375	-.06617	.02750
.2396	-.06462	-------
.2417	-.06285	.02304
.2437	-.06077	-------
.2458	-.05830	.01746
.2479	-.05511	.01392
.2492	-.05258	.01165
.2500	-.05030	-------
.2512	-.04477	.00650
.2525	-.03878	-------
.2537	-.03287	-.00412
.2550	-.02614	-.01417
.2553	-.01717	-.01717
x/l = 0.79687		
0	-0.06625	Out
.2083	-.06608	0.04873
.2125	-.06604	.04785
.2167	-.06598	.04698
.2208	-.06570	.04602
.2250	-.06505	.04500
.2292	-.06403	.04398
.2333	-.06277	.04308
.2375	-.06120	.04233
.2417	-.05931	.04165
.2458	-.05712	.04092
.2500	-.05455	.03992
.2521	-.05297	-------
.2542	-.05112	.03847
.2562	-.04892	-------

y/l	z/l	z/l
x/l = 0.79687 – Continued		
0.2583	-0.04604	0.03619
.2592	-.04433	-------
.2604	-.03957	.03475
.2617	-.03367	-------
.2629	-.02767	.03282
.2642	-.02176	-------
.2654	-.01573	.03058
.2667	-.00972	-------
.2679	-.00386	.02764
.2692	.00213	.02542
.2704	.00807	.02185
.2712	.01392	.01392
x/l = 0.82812		
0	-0.05790	Out
.2208	-.05775	0.04733
.2250	-.05768	.04704
.2292	-.05742	.04700
.2333	-.05684	.04742
.2375	-.05587	.04835
.2417	-.05457	.04980
.2458	-.05300	.05183
.2500	-.05108	.05452
.2542	-.04883	.05752
.2583	-.04643	.06050
.2625	-.04324	.06309
.2646	-.04097	.06410
.2658	-.03916	.06457
.2671	-.03628	.06490
.2683	--------	.06515
.2696	--------	.06526
.2700	--------	.06527
.2704	.06525	.06527
.2708	-.01875	-------
.2708	.06517	-------
.2717	.06504	-------
.2733	.06446	-------
.2750	.00121	-------
.2750	.06367	-------
.2771	.06217	-------
.2792	.02096	-------
.2792	.06021	-------
.2812	.05737	-------
.2833	.04081	-------
.2833	.05262	-------
.2840	.04578	-------
x/l = 0.86979		
0	-0.04692	Out
.2333	-.04692	0.04800
.2375	-.04672	.04876
.2417	-.04636	.05035
.2458	-.04578	.05265
.2479	--------	.05417
.2500	-.04492	.05587
.2542	-.04377	.06056
.2583	-.04240	.06664
.2625	-.04066	.07356
.2667	-.03849	.08073
.2708	-.03567	.08757
.2729	-.03380	-------
.2750	-.03137	.09400
.2767	-.02822	-------
.2775	-.02552	-------
.2792	-.01768	.09912
.2812	--------	.10111
.2833	.00229	.10270
.2854	--------	.10383
.2875	.02210	.10458
.2896	--------	.10492
.2904	--------	.10496
.2907	.10492	.10496
.2912	.10492	-------
.2917	.04192	-------
.2921	.10475	-------
.2937	.10400	-------
.2958	.06182	-------
.2958	.10257	-------
.2979	.10037	-------
.3000	.08165	-------
.3000	.09633	-------
.3012	.08840	-------

y/l	z/l	z/l
x/l = 0.91146		
0	-0.03577	Out
.2292	--------	0.04498
.2333	--------	.04568
.2375	--------	.04615
.2417	--------	.04698
.2458	-.03568	.04856
.2500	-.03558	.05078
.2542	-.03537	.05408
.2583	-.03500	.05902
.2625	-.03457	.06548
.2667	-.03378	.07267
.2708	-.03252	.08024
.2750	-.03074	.08825
.2792	-.02832	.09655
.2812	-.02671	-------
.2833	-.02467	.10527
.2854	-.02194	-------
.2862	-.02031	-------
.2875	-.01637	.11431
.2917	.00350	.12346
.2958	.02333	.13197
.3000	.04315	.13835
.3021	--------	.14075
.3042	.06314	.14260
.3054	--------	.14345
.3067	--------	.14403
.3075	--------	.14428
.3079	--------	.14437
.3083	.08296	.14446
.3087	--------	.14450
.3092	--------	.14453
.3095	.14458	.14457
.3112	.14425	-------
.3125	.10282	-------
.3129	.14367	-------
.3146	.14218	-------
.3162	.13955	-------
.3167	.12260	-------
.3175	.13667	-------
.3183	.13271	-------
x/l = 0.95312		
0	-0.02458	0.04000
.2333	--------	.04095
.2375	--------	.04137
.2417	--------	.04186
.2458	--------	.04269
.2500	--------	.04427
.2542	--------	.04637
.2562	--------	.04777
.2583	--------	.04957
.2604	--------	.05182
.2625	--------	.05462
.2646	--------	.05782
.2667	-.02458	.06125
.2708	-.02446	.06862
.2750	-.02417	.07636
.2792	-.02361	.08449
.2833	-.02257	.09291
.2875	-.02079	.10159
.2917	-.01786	.11062
.2937	-.01573	-------
.2958	-.01258	.12000
.2967	-.01046	-------
.2971	-.00908	-------
.2975	-.00073	-------
.3000	--------	.12984
.3021	.01462	-------
.3042	--------	.14007
.3083	.04435	.15032
.3125	--------	.15805
.3146	.07415	.15991
.3167	--------	.16108
.3179	--------	.16154
.3192	--------	.16186
.3204	--------	.16205
.3208	.10389	.16206
.3215	.16212	.16207
.3229	.16196	-------

y/l	z/l	z/l
x/l = 0.95312 – Continued		
0.3250	0.16133	-------
.3271	.13371	-------
.3271	.16014	-------
.3292	.15817	-------
.3312	.15325	-------
.3312	.15367	-------
x/l = 0.98750		
0	-0.01527	0.03567
.2333	--------	.03607
.2375	--------	.03650
.2417	--------	.03688
.2458	--------	.03746
.2500	--------	.03851
.2542	--------	.04016
.2583	--------	.04242
.2625	--------	.04617
.2667	--------	.05147
.2708	--------	.05850
.2750	--------	.06592
.2792	--------	.07382
.2833	-.01571	.08202
.2875	-.01542	.09045
.2917	-.01479	.09910
.2937	-.01421	-------
.2958	-.01337	.10815
.2979	-.01223	-------
.3000	-.01067	.11752
.3021	-.00860	-------
.3033	-.00692	-------
.3042	--------	.12729
.3046	-.00442	-------
.3048	-.00300	-------
.3083	.01258	.13759
.3125	--------	.14840
.3167	--------	.15942
.3208	.07212	.16903
.3229	--------	.17167
.3250	--------	.17323
.3262	--------	.17389
.3275	--------	.17438
.3287	--------	.17437
.3292	.11183	-------
.3296	--------	.17486
.3304	--------	.17492
.3307	.17492	.17492
.3312	.17483	-------
.3333	.17442	-------
.3354	.17350	-------
.3375	.15150	-------
.3375	.17183	-------
.3396	.16929	-------
.3409	.16717	-------
x/l = 1.00375		
0	Out	-------
.2375	0.03415	-------
.2417	.03442	-------
.2458	.03502	-------
.2500	.03600	-------
.2542	.03745	-------
.2583	.03948	-------
.2625	.04258	-------
.2667	.04712	-------
.2708	.05340	-------
.2750	.06074	-------
.2792	.06850	-------
.2833	.07662	-------
.2875	.08494	-------
.2917	.09352	-------
.2958	.10236	-------
.3000	.11150	-------
.3042	.12111	-------
.3083	.13125	-------
.3117	--------	0.01333
.3125	.14186	-------
.3167	.15300	-------
.3208	.16427	-------
.3250	.17433	-------
.3271	.17734	-------
.3292	.17905	.09687

y/l	z/l	z/l
x/l = 1.00375 – Continued		
0.3304	0.17979	-------
.3317	.18036	-------
.3329	.18077	-------
.3342	.18100	-------
.3350	.18107	-------
.3359	.18107	0.18104
.3375	-------	.13650
.3375	-------	.18062
.3396	-------	.17992
.3417	-------	.17817
.3437	-------	.17583
.3450	-------	.17283
x/l = 1.02100		
0	Out	-------
.2857	0.07442	-------
.2875	.07865	-------
.2917	.08733	-------
.2958	.09611	-------
.3000	.10510	-------
.3042	.11453	-------
.3083	.12437	-------
.3125	.13477	-------
.3167	.14575	-------
.3208	.15719	-------
.3250	.16858	-------
.3286	-------	0.07805
.3292	.17925	-------
.3312	.18303	-------
.3329	.18477	-------
.3350	.18621	-------
.3367	.18700	-------
.3379	.18739	-------
.3392	.18758	-------
.3400	.18767	-------
.3408	.18767	-------
.3411	.18767	.18767
.3417	-------	.18740
.3437	-------	.18662
.3458	-------	.18521
.3479	-------	.18304
.3497	-------	.17917
x/l = 1.03400		
0	Out	-------
.3103	0.12362	-------
.3146	.13485	-------
.3208	.15164	-------
.3250	.16317	-------
.3292	.17454	-------
.3333	.18519	-------
.3354	.18860	-------
.3375	.19050	-------
.3392	.19153	-------
.3408	.19221	-------
.3412	-------	0.12596
.3421	.19252	-------
.3433	.19267	-------
.3437	.19269	-------
.3440	.19269	.19267
.3458	-------	.19225
.3479	-------	.19142
.3500	-------	.18975
.3521	-------	.18717
.3532	-------	.18400
x/l = 1.0510		
0.3374	0.18967	-------

[redacted]

[redacted]

TABLE II.- STABILITY DERIVATIVES

Tip fin	Center fin	δ_e, deg	Sting	α, deg	C_{l_β}	C_{n_β}	C_{Y_β}
Off	Off	0	Straight	-0.1	0.00102	0	-0.01193
				5.0	.00061	-.00046	-.01051
				10.1	.00046	-.00067	-.00974
				15.2	.00026	-.00073	-.00854
				20.2	-.00005	-.00075	-.00813
				25.3	-.00044	-.00072	-.00796
				30.4	-.00080	-.00069	-.00741
Off	Off	0	Bent	25.7	-0.00050	-0.00070	-0.00970
				29.2	-.00075	-.00065	-.00965
				34.2	-.00108	-.00054	-.00911
				39.2	-.00148	-.00066	-.00872
				42.2	-.00175	-.00066	-.00863
				49.2	-.00203	-.00066	-.00791
				54.1	-.00212	-.00069	-.00725
				59.1	-.00225	-.00073	-.00701
I_4	Off	0	Bent	-1.0	0.00075	0.00098	-0.01109
				4.0	.00118	.00091	-.01091
				9.0	.00069	.00190	-.01143
				14.0	-.00005	.00184	-.01116
				19.0	-.00039	.00143	-.01138
				24.0	-.00080	.00120	-.01140
				29.1	-.00115	.00120	-.01200
				32.6	-.00144	.00119	-.01035
I_4	Off	0	Straight	-0.1	0.00112	0.00102	-0.01284
				4.9	.00116	.00111	-.01172
				10.0	.00041	.00188	-.01188
				15.0	-.00005	.00161	-.01109
				20.1	-.00045	.00126	-.01020
				25.2	-.00082	.00121	-.01000
				30.3	-.00126	.00114	-.00960
I_4	Off	0	Bent	25.7	-0.00090	0.00118	-0.01152
				29.2	-.00120	.00131	-.01094
				29.3	-.00109	.00129	-.01104
				34.3	-.00153	.00121	-.01132
				39.2	-.00188	.00115	-.01091
				39.3	-.00172	.00131	-.01081
				44.2	-.00221	.00108	-.01020
				49.2	-.00232	.00098	-.00964
				49.3	-.00228	.00101	-.00984
				54.2	-.00242	.00093	-.00912
				57.7	-.00237	.00085	-.00831
				59.1	-.00258	.00090	-.00865
I_4	E_2	0	Straight	-0.1	0.00066	0.00192	-0.01424
				5.0	.00076	.00162	-.01232
				10.0	.00020	.00218	-.01218
				15.1	-.00026	.00181	-.01119
				20.2	-.00059	.00149	-.01064
				25.2	-.00082	.00121	-.00962
				30.3	-.00126	.00120	-.00937
I_4	Off	-45	Bent	25.8	-0.00085	0.00134	-0.01144
				54.3	-.00225	.00115	-.00937
				59.3	-.00236	.00115	-.00885
I_4	Off	-30	Bent	25.7	-0.00090	0.00129	-0.01174
				29.4	-.00104	.00134	-.01109
				39.4	-.00166	.00135	-.01109
				49.4	-.00197	.00112	-.00963
				51.5	-.00226	.00124	-.00968
				57.8	-.00222	.00114	-.00875
				59.4	-.00241	.00126	-.00920
I_4	Off	-15	Bent	25.7	-0.00084	0.00126	-0.01199
				48.2	-.00210	.00113	-.00990
				59.1	-.00243	.00101	-.00864
I_4	E_2	15	Straight	-0.1	0.00076	0.00197	-0.01460
				10.0	.00015	.00224	-.01260
				20.2	-.00069	.00149	-.01090
				30.3	-.00154	.00131	-.00977
I_4	Off	15	Bent	25.7	-0.00107	0.00136	-0.01146
				37.2	-.00196	.00139	-.01108
				59.0	-.00279	.00115	-.00885
I_4	E_2	30	Straight	-0.1	0.00070	0.00197	-0.01414
				10.0	.00010	.00213	-.01193
				20.1	-.00096	.00154	-.01043
				30.2	-.00206	.00137	-.00920
I_4	Off	30	Bent	25.7	-0.00146	0.00136	-0.01141
				29.2	-.00189	.00139	-.01125
				59.0	-.00356	.00172	-.00983
I_4	E_2	45	Straight	0	0.00078	0.00202	-0.01446
				10.1	-.00010	.00229	-.01235
				20.2	-.00138	.00167	-.01019
				30.3	-.00347	.00153	-.00682

[redacted]

[redacted]

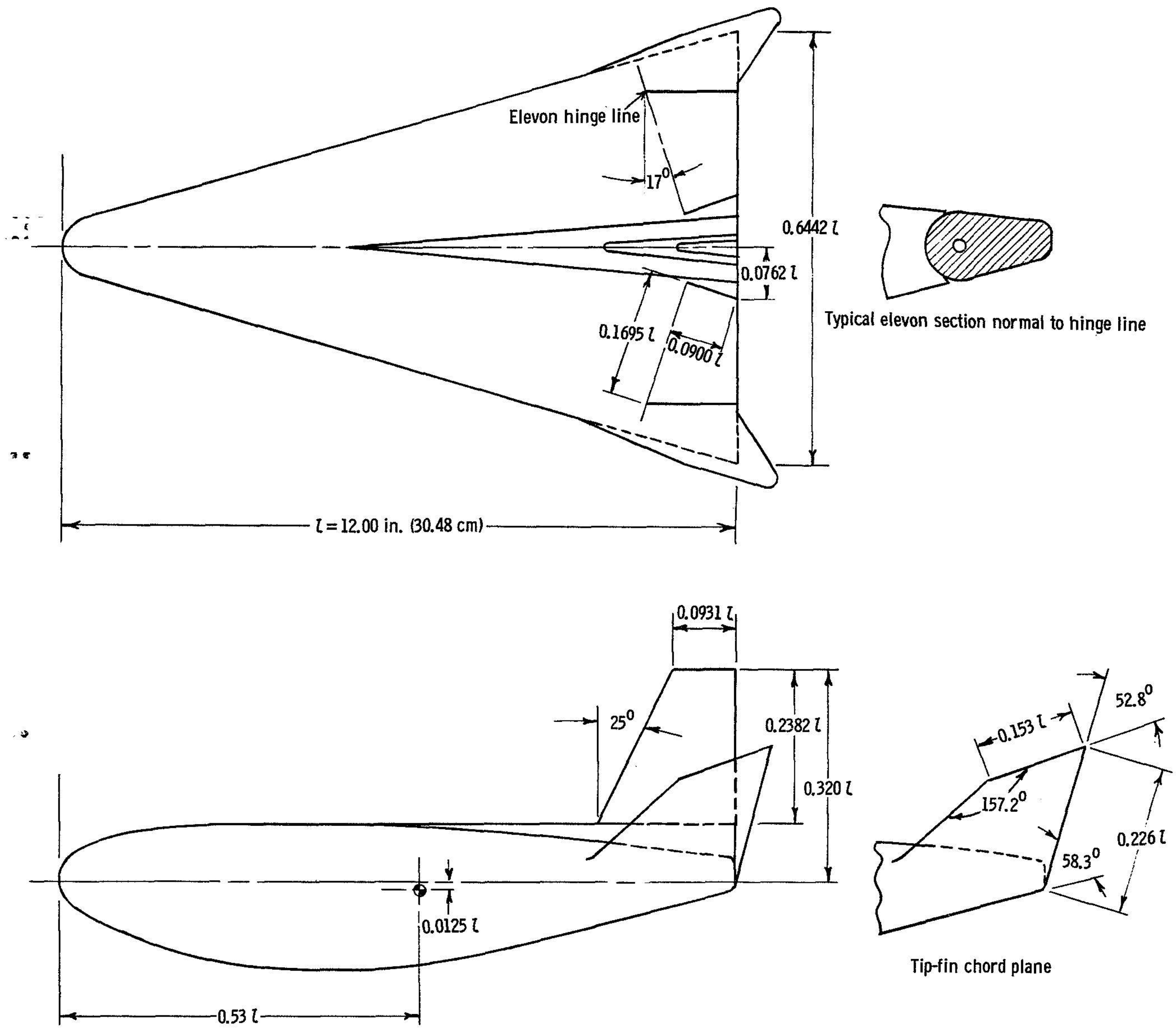

(a) Two-view drawing of model with tip fin l_4 and center fin E_2.

Figure 1.- Details of model.

[redacted]

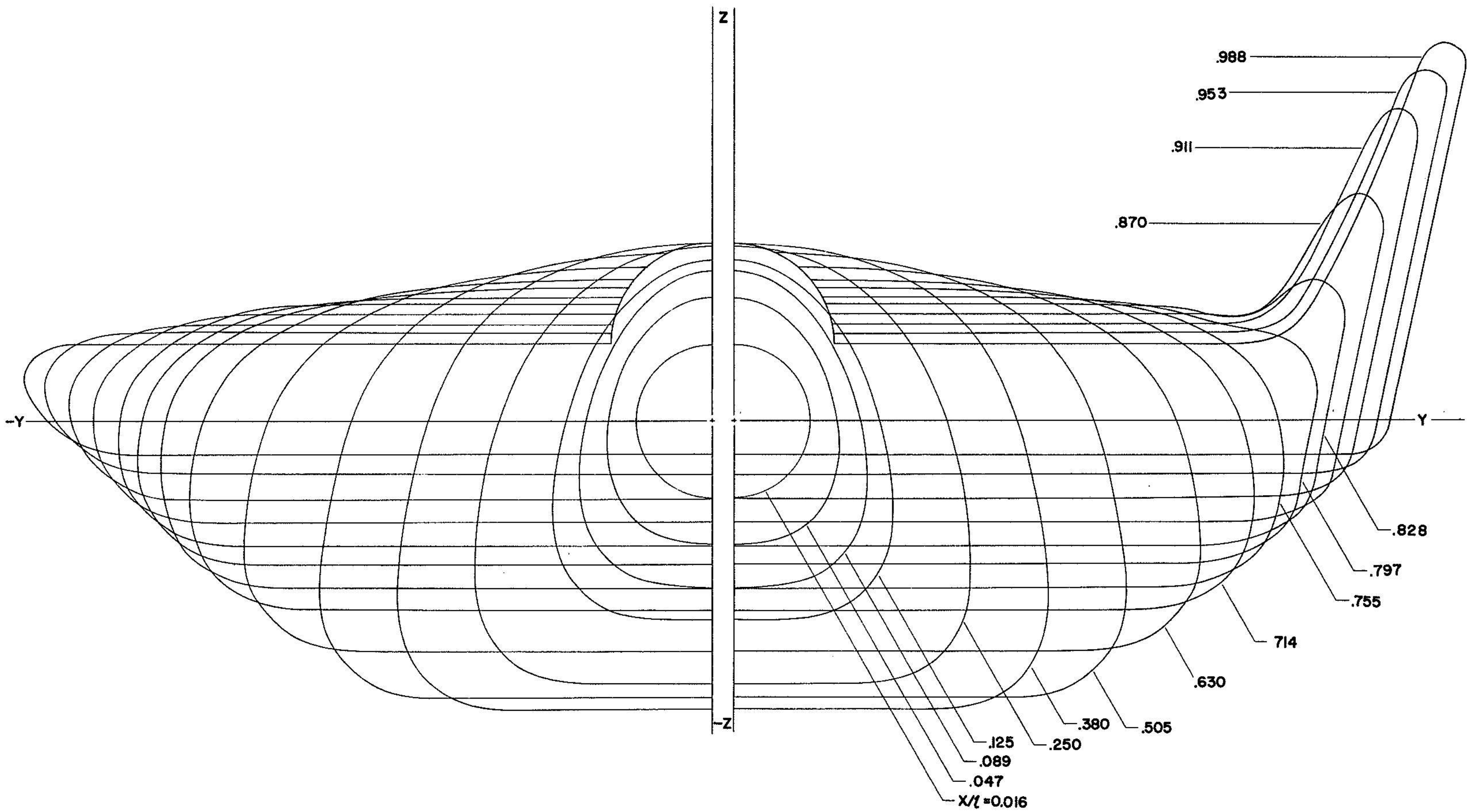

(b) Model cross section with and without tip fins.

Figure 1.- Continued.

[redacted]

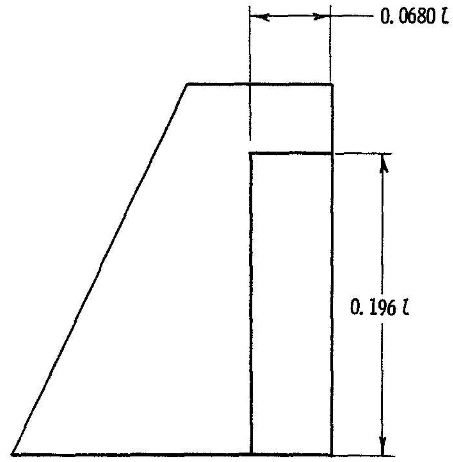

Rudder R_1

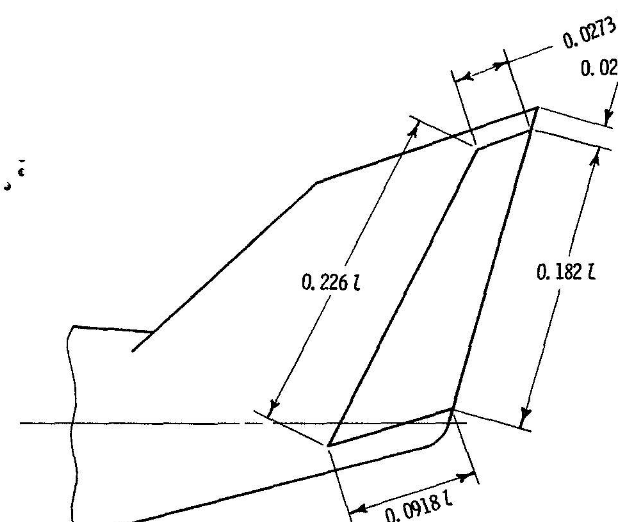

Rudder R_4

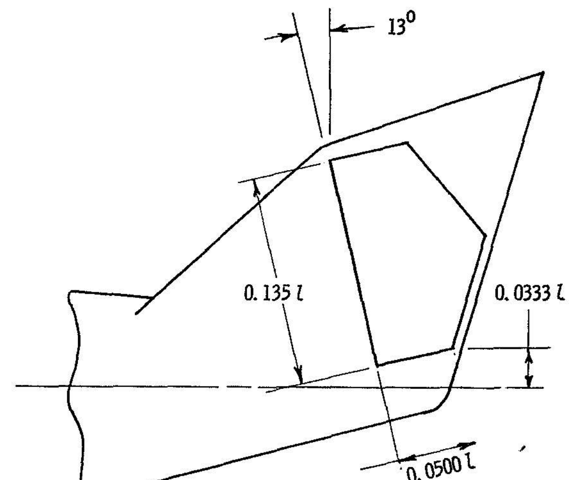

Rudder R_5

(c) Rudder details.

Figure 1.- Concluded.

[redacted]

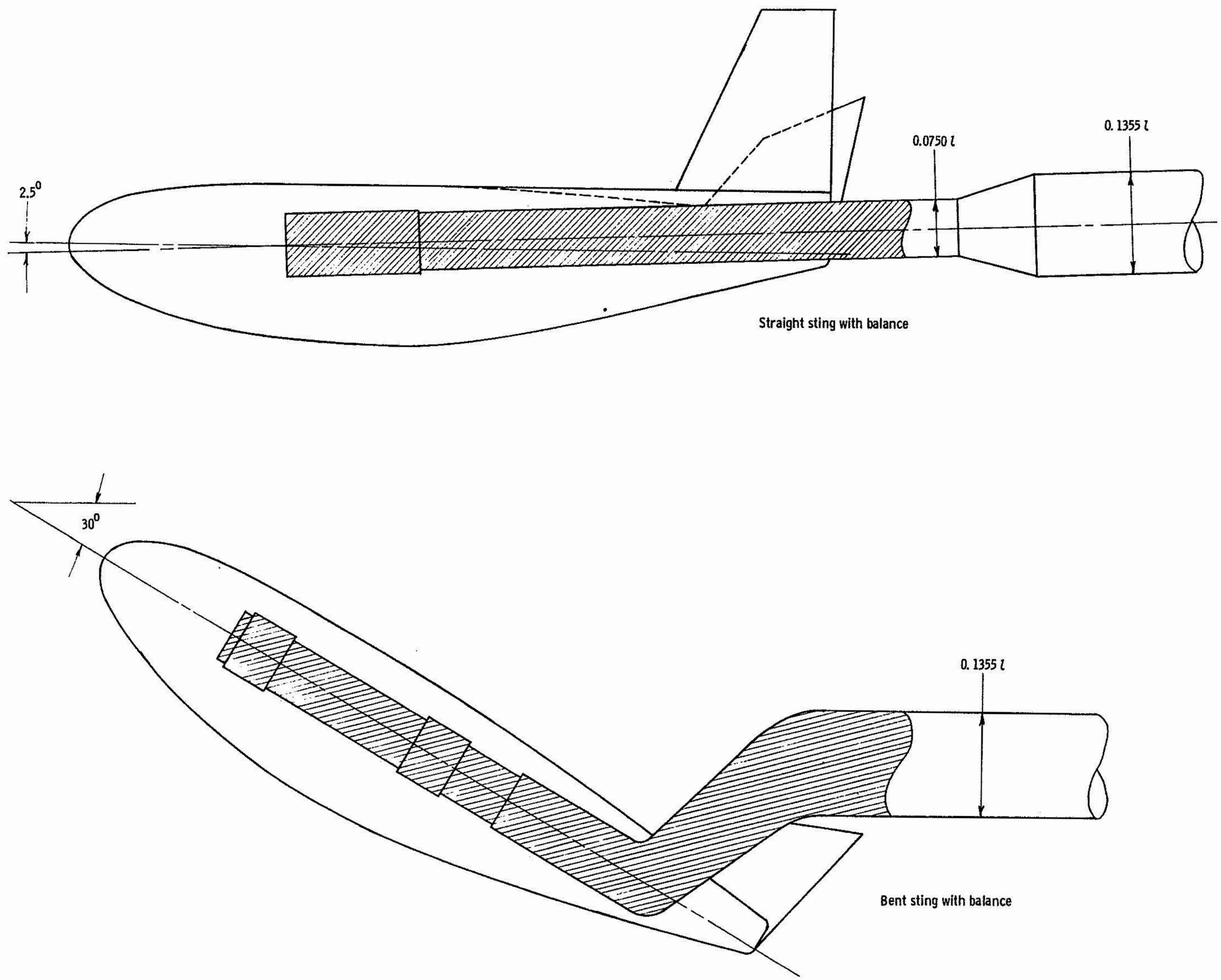

(a) Side view of stings.

Figure 2.- Sting geometry used with model.

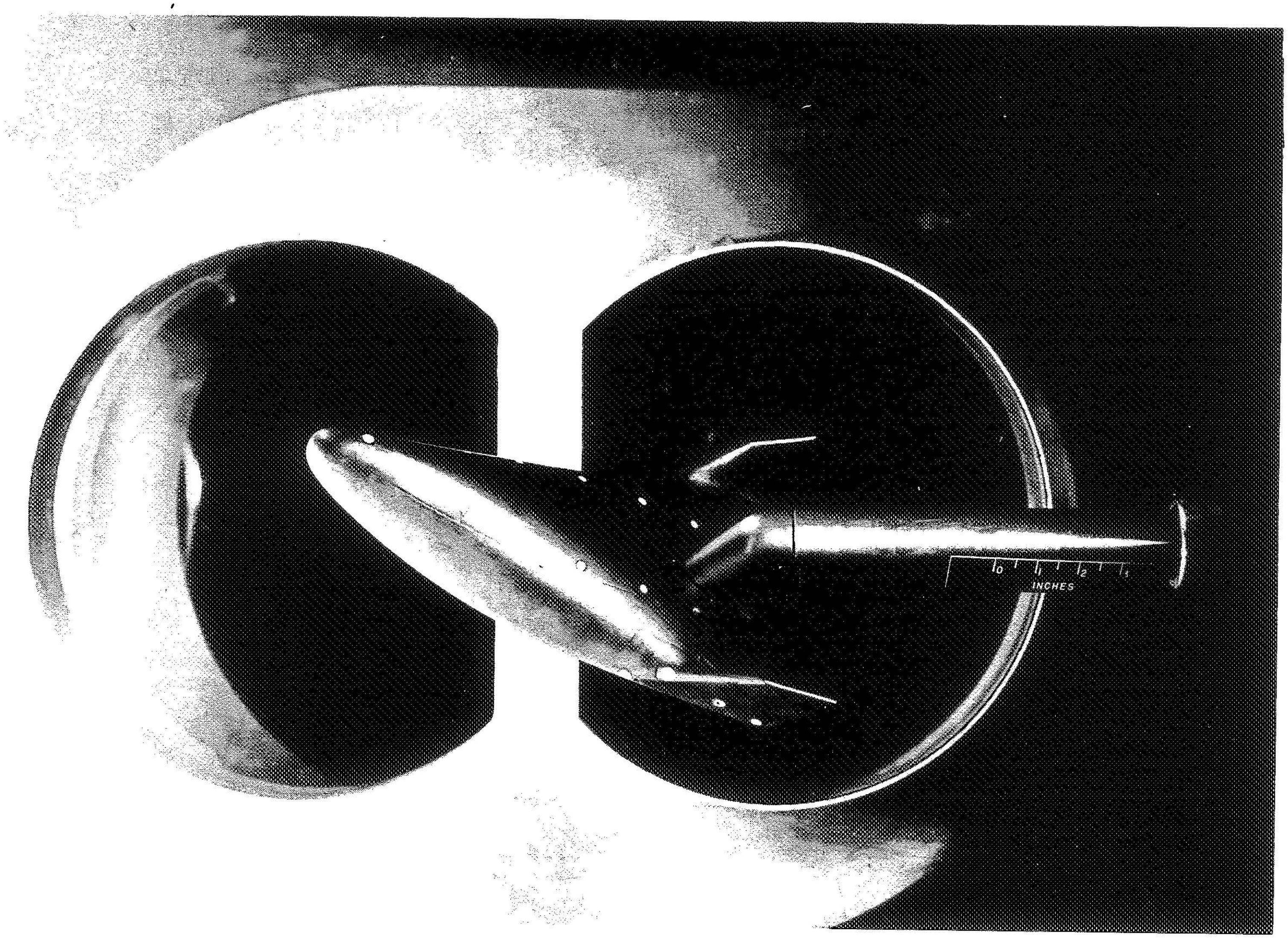

(b) Photograph of model in tunnel with bent sting.

L-65-5064

Figure 2.- Concluded.

[redacted]

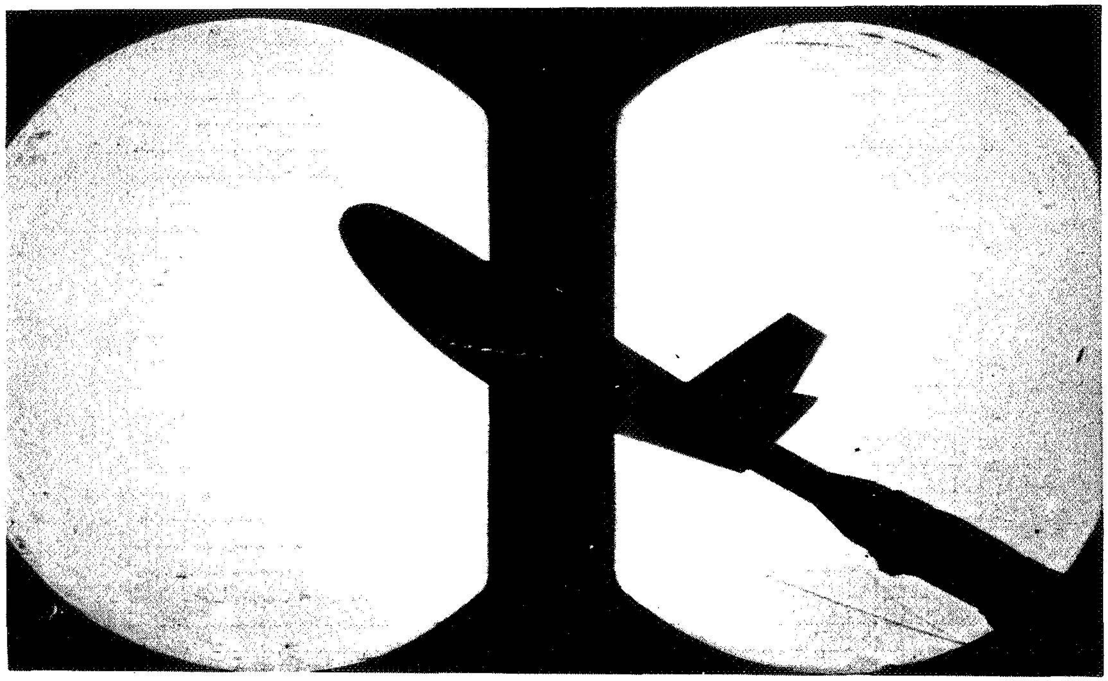

(a) Straight sting.

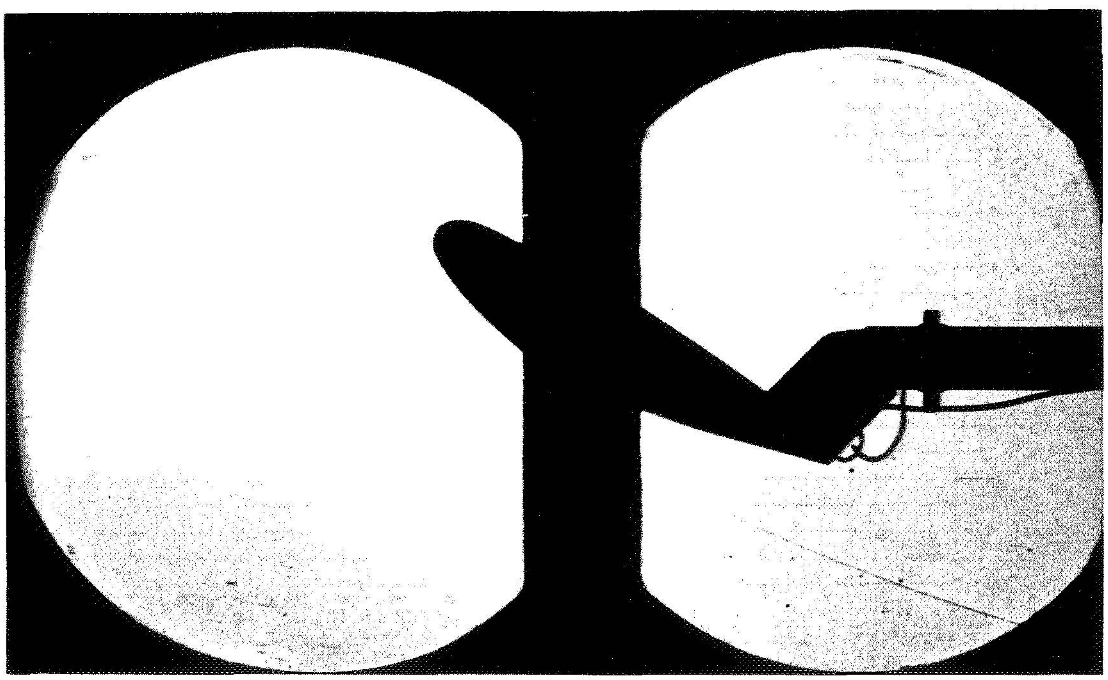

(b) Bent sting.

Figure 3.- Shadowgraphs of model at $\alpha \approx 30^{\circ}$.

L-67-6669

[redacted]

[redacted]

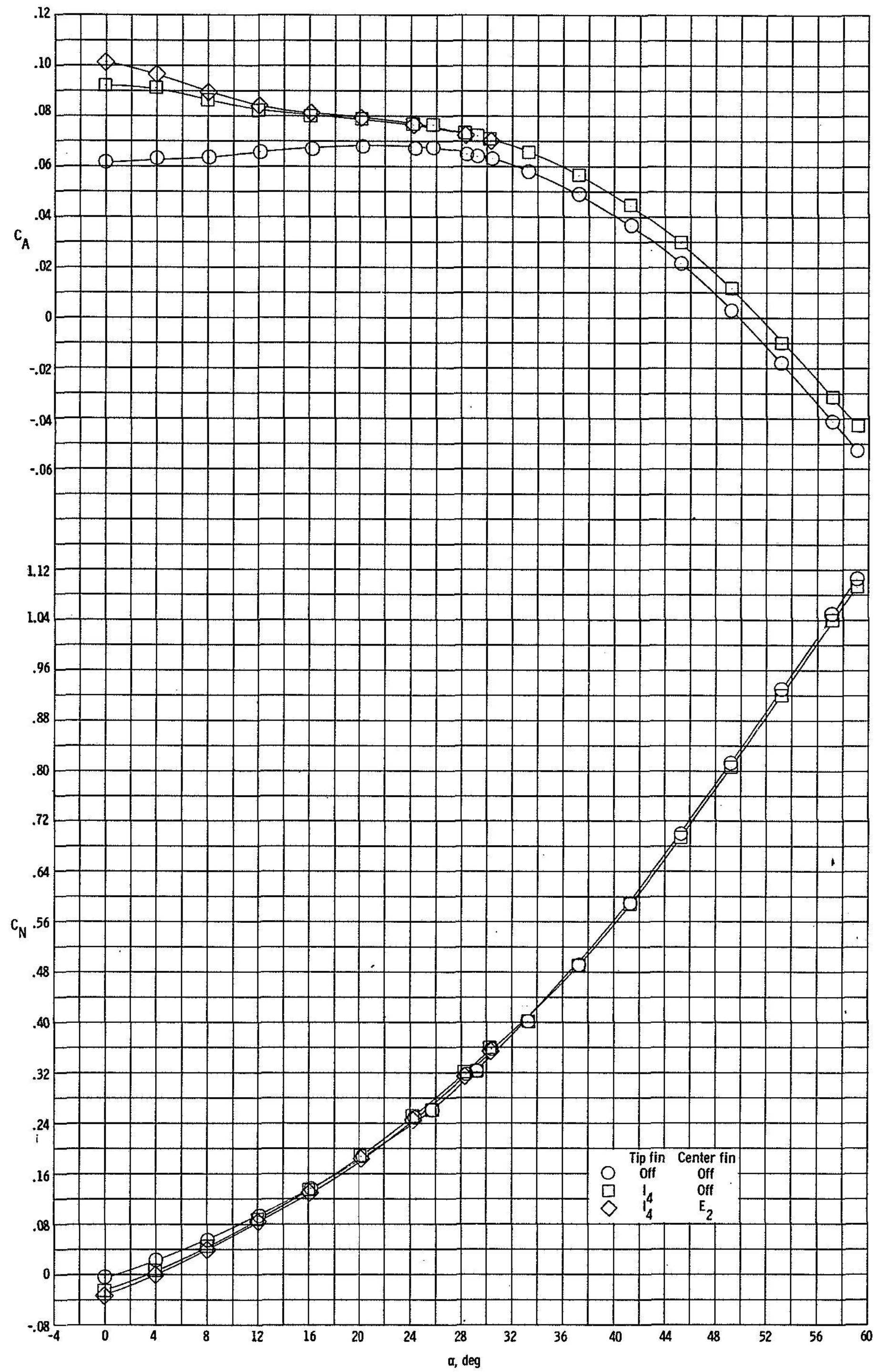

(a) Body-axis data.

Figure 4.- Effects of tip and center fins on the longitudinal aerodynamic characteristics. $\delta_e = 0^{\circ}$.

[redacted]

[redacted]

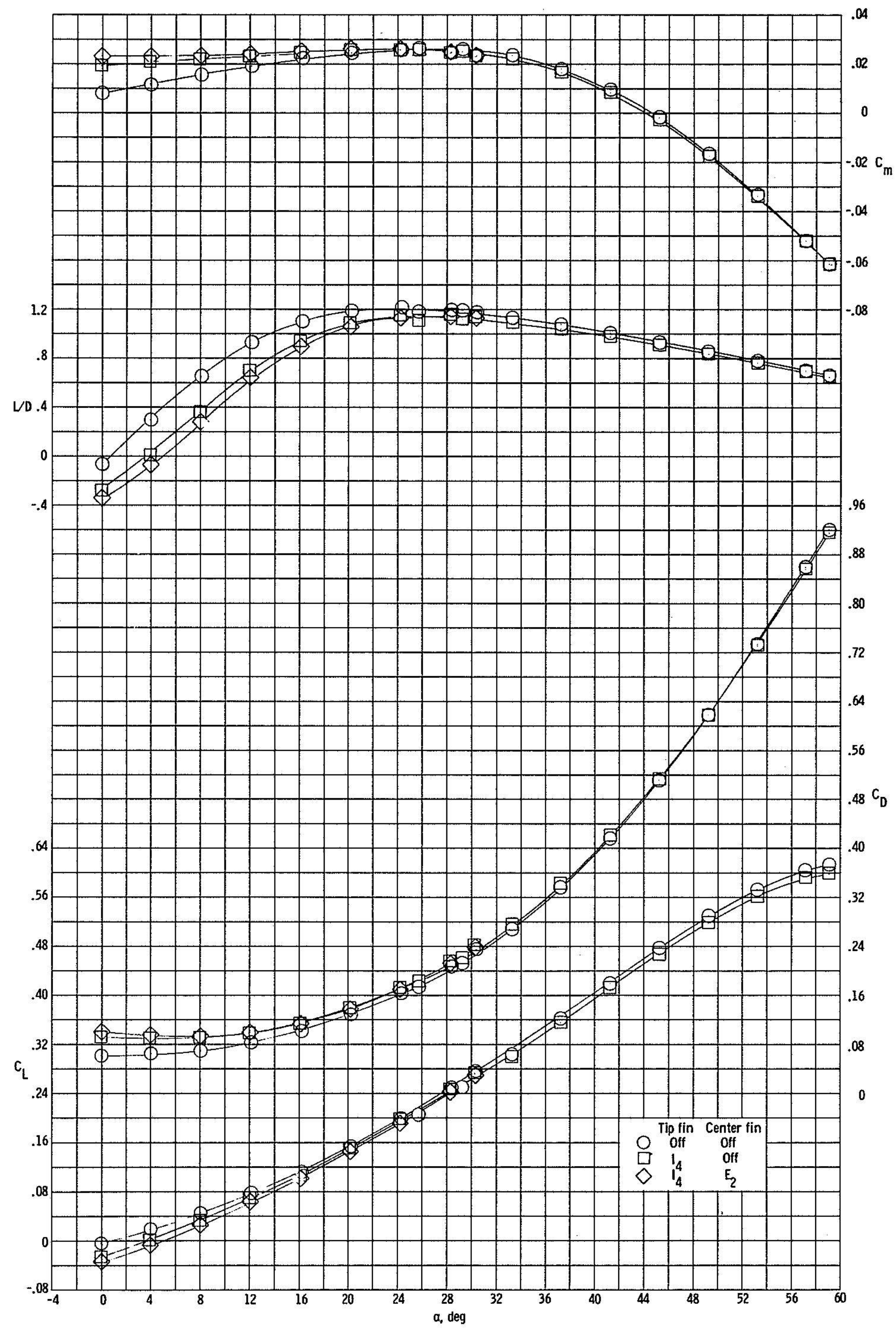

(b) Stability-axis data.

Figure 4.- Concluded.

[redacted]

[redacted]

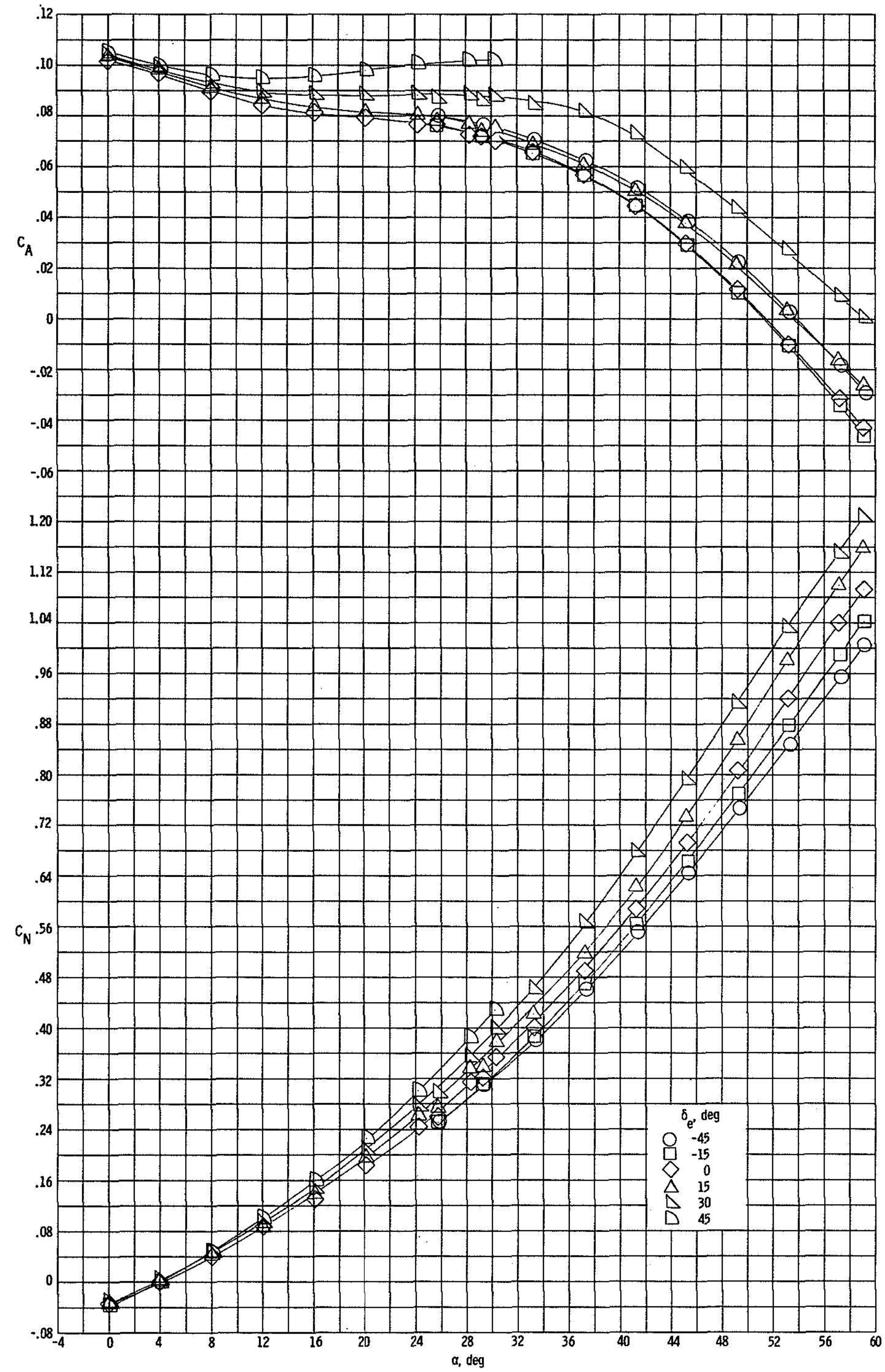

(a) Body-axis data.

Figure 5.- Effects of elevon deflection on the longitudinal aerodynamic characteristics of the complete configuration.

[redacted]

[redacted]

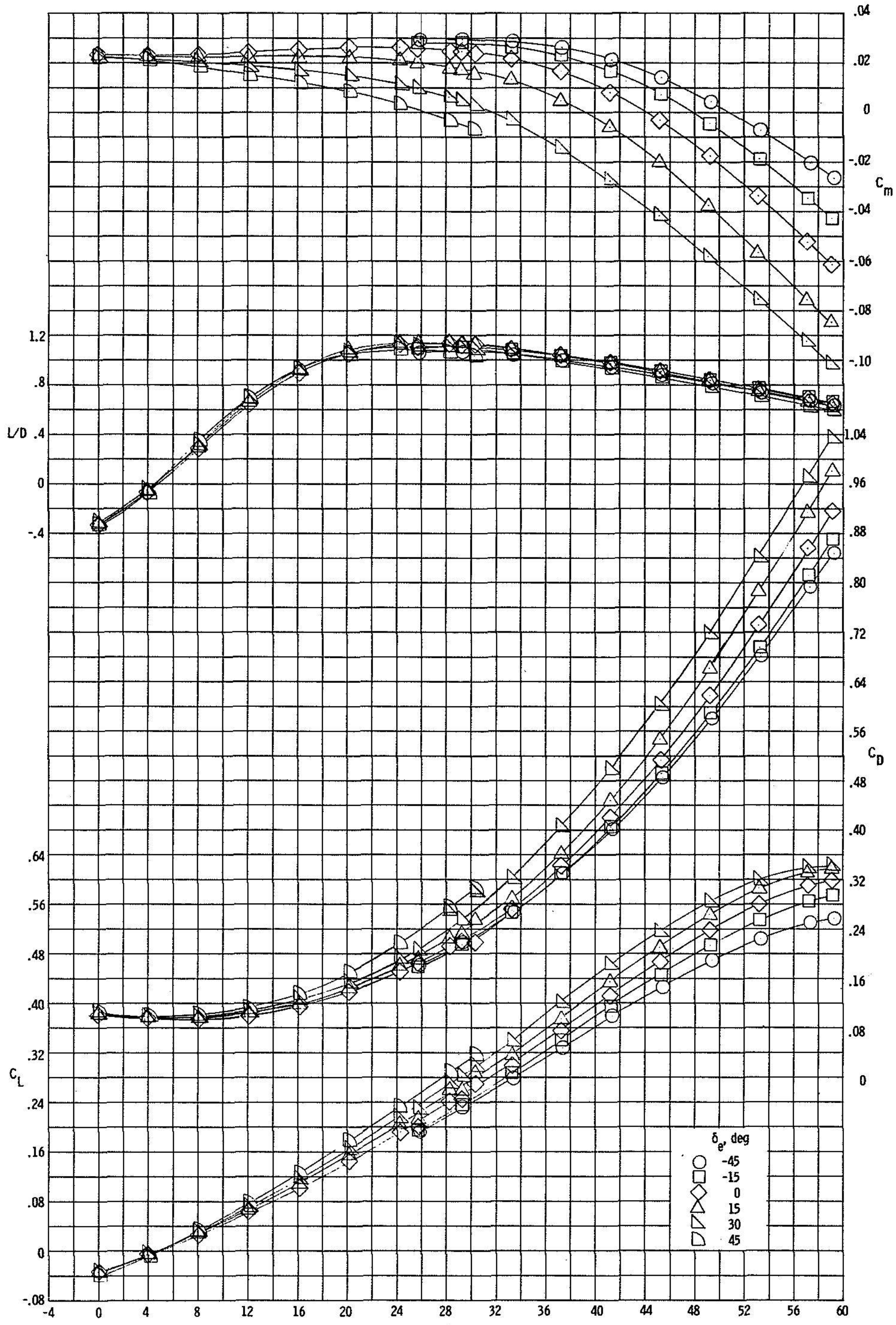

(b) Stability-axis data.

Figure 5.- Concluded.

[redacted]

[redacted]

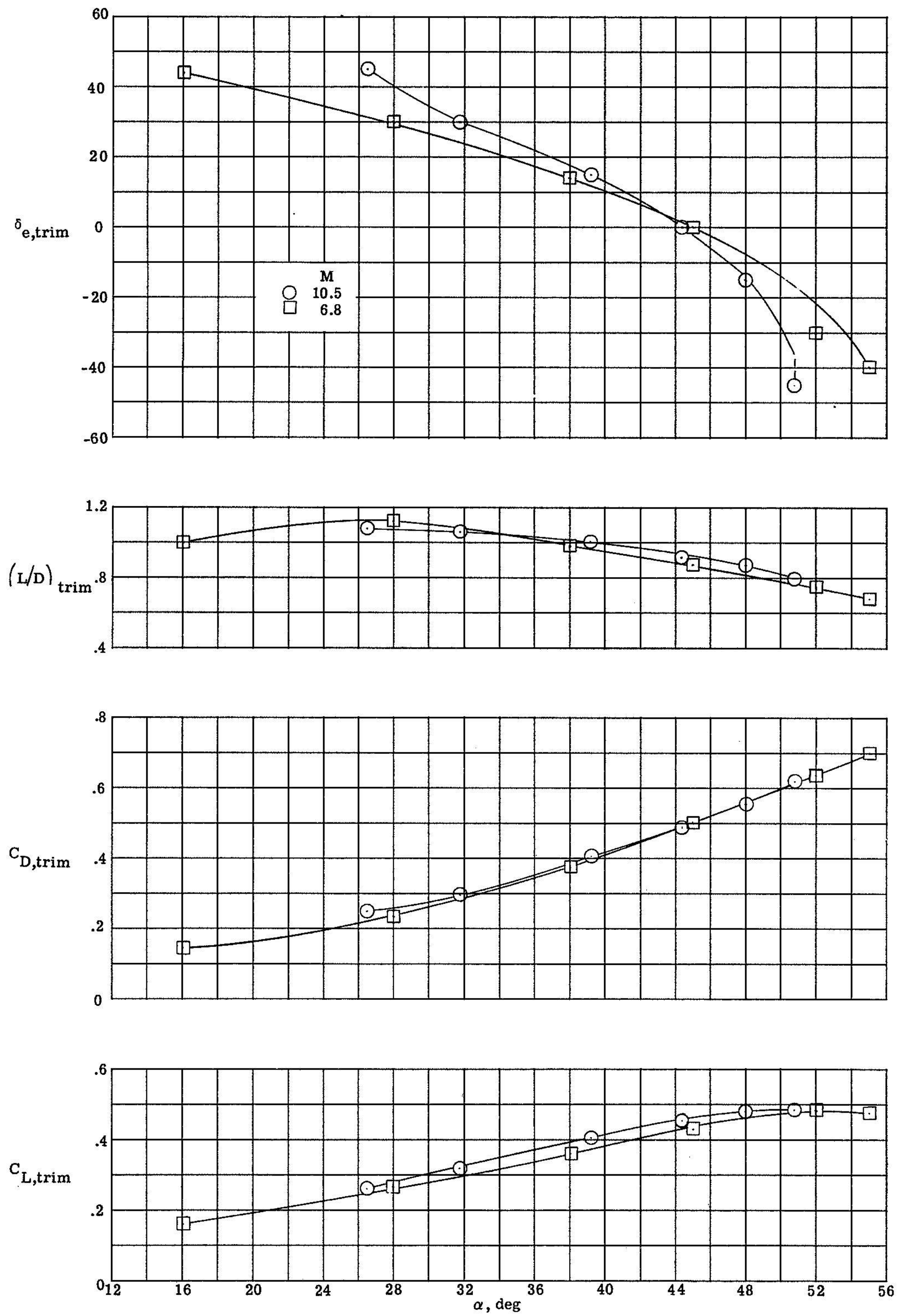

Figure 6.- Comparison of trim characteristics at M = 10.5 with data at M = 6.8 from reference 15.

[redacted]

[redacted]

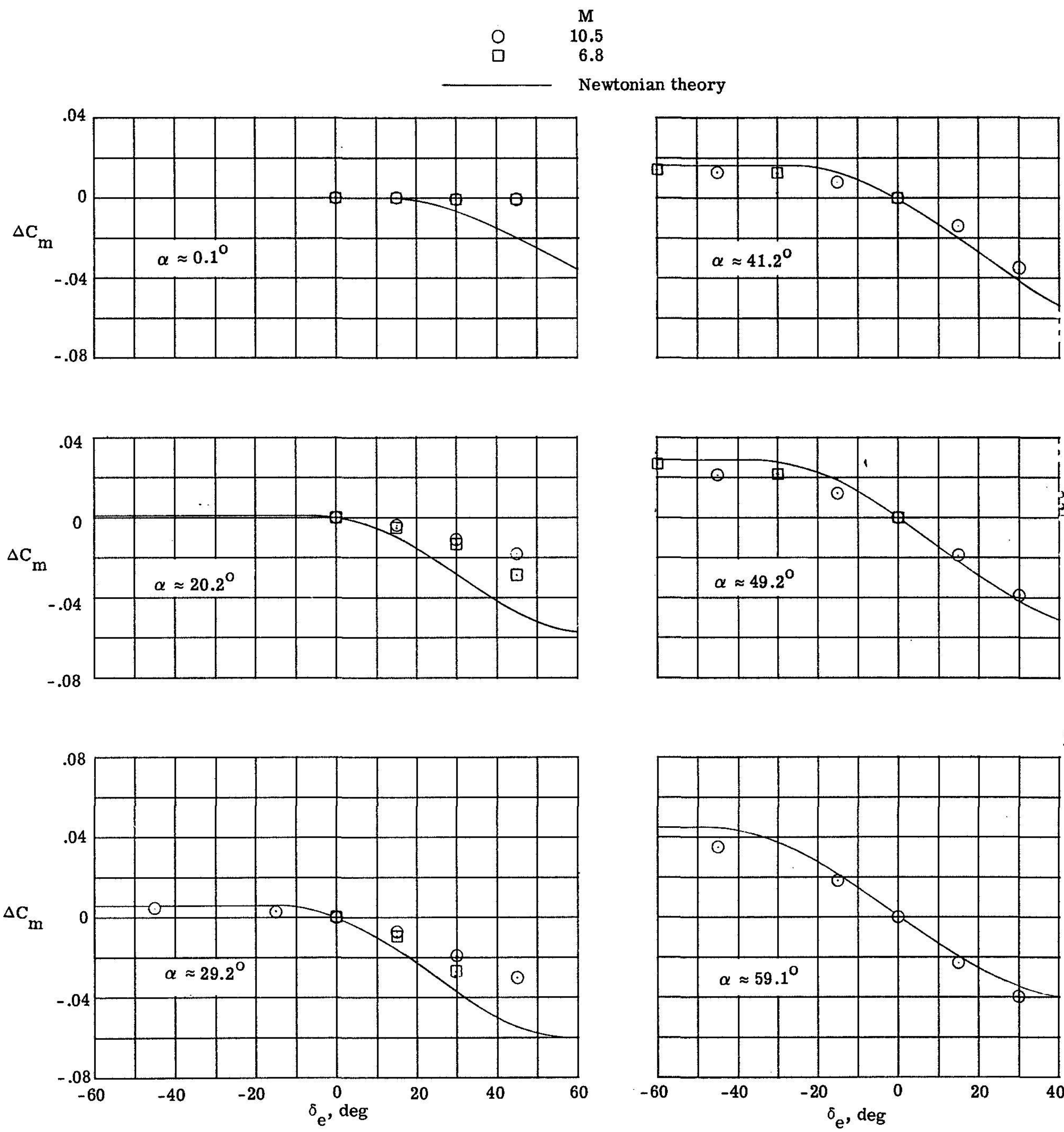

Figure 7.- Comparison of experimental and theoretical elevon effectiveness at various angles of attack.

[redacted]

[redacted]

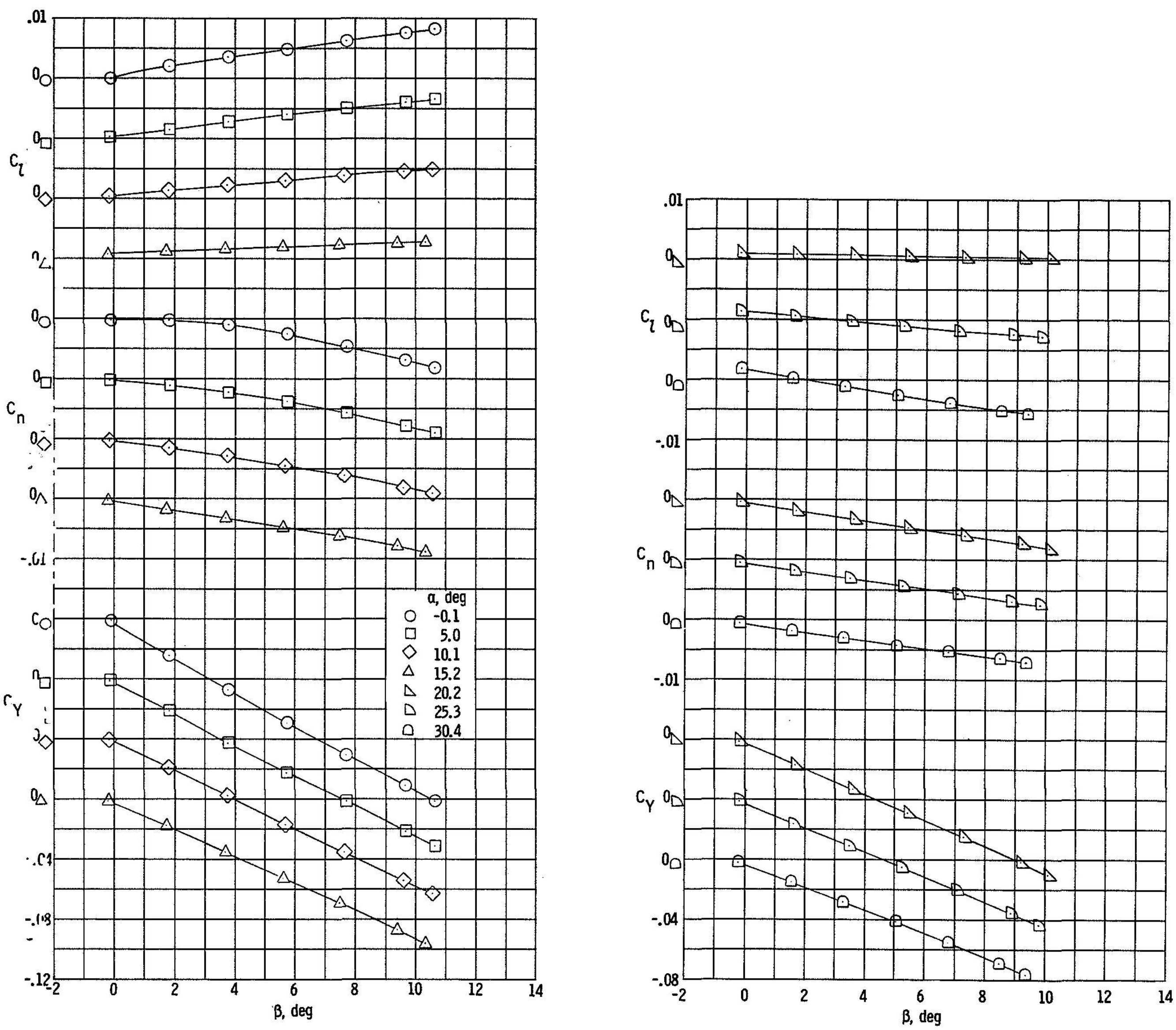

(a) Low angles of attack, straight sting.

Figure 8.- Variation of directional and lateral characteristics with sideslip angle for configuration with fins off at $\delta_e = 0^0$.

[redacted]

[redacted]

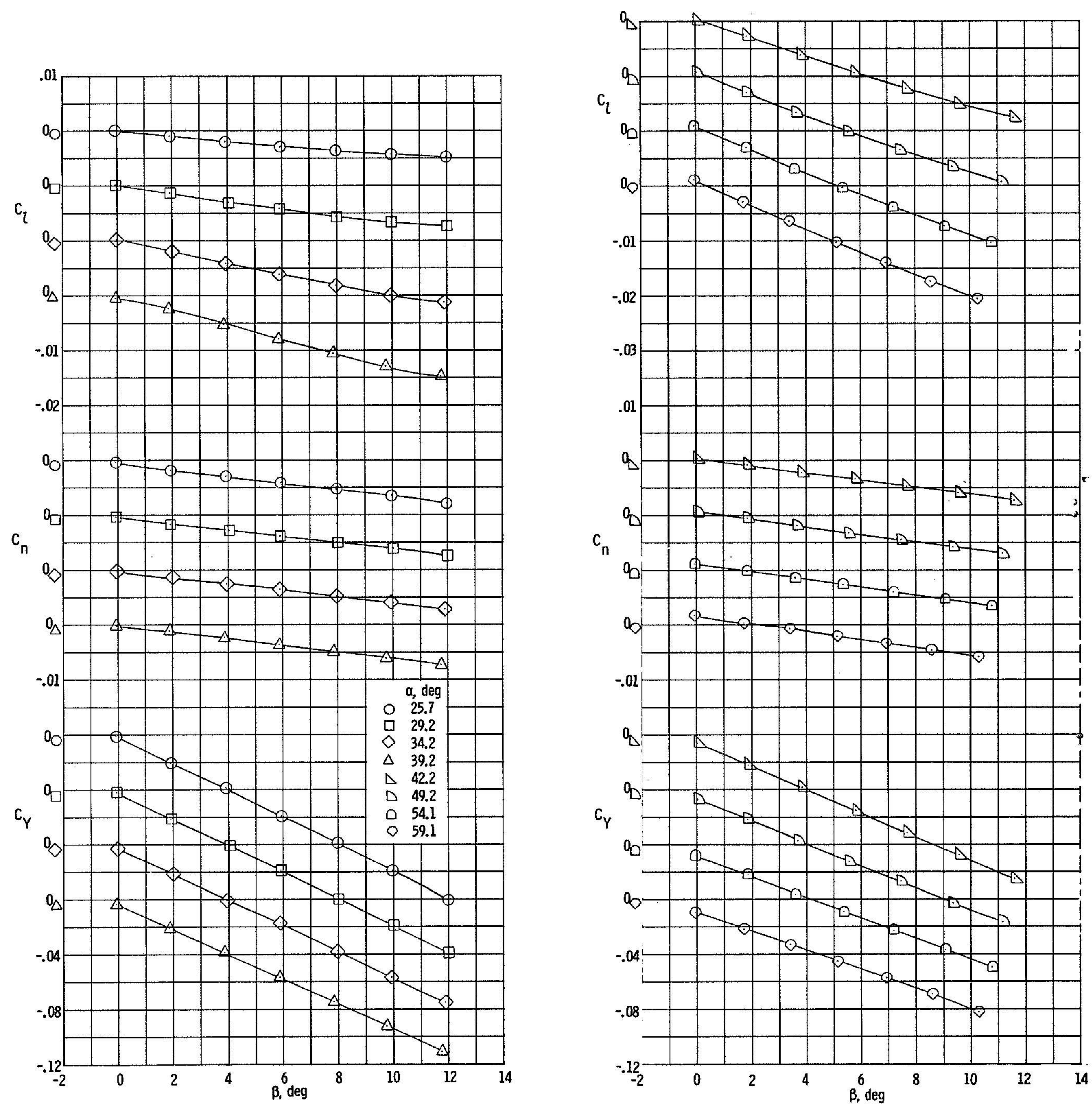

(b) High angles of attack, bent sting.

Figure 8.- Concluded.

[redacted]

[redacted]

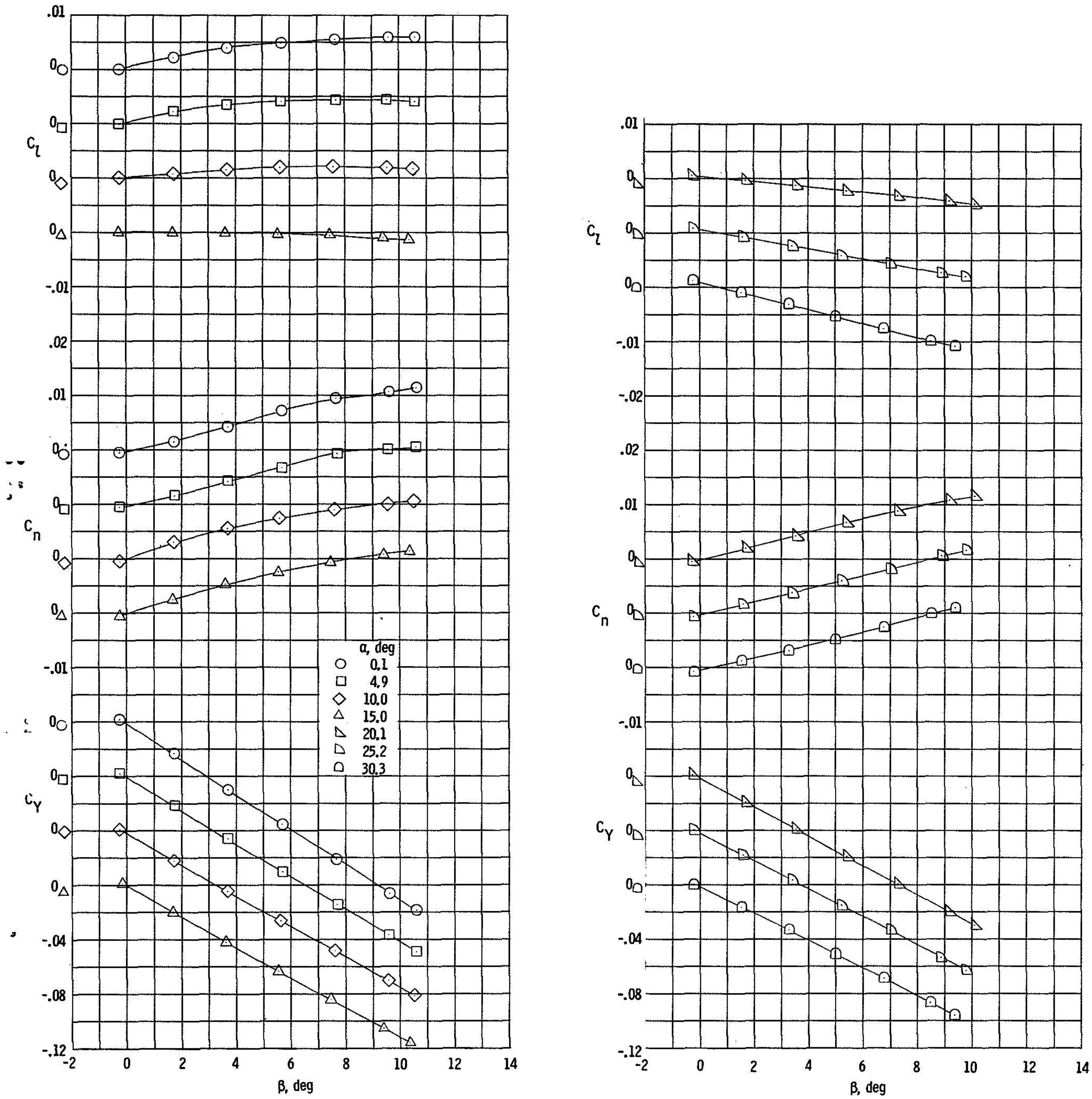

(a) $\delta_e = 0^0$, straight sting.

Figure 9.- Variation of directional and lateral characteristics with sideslip angle for configuration with tip fins on.

[redacted]

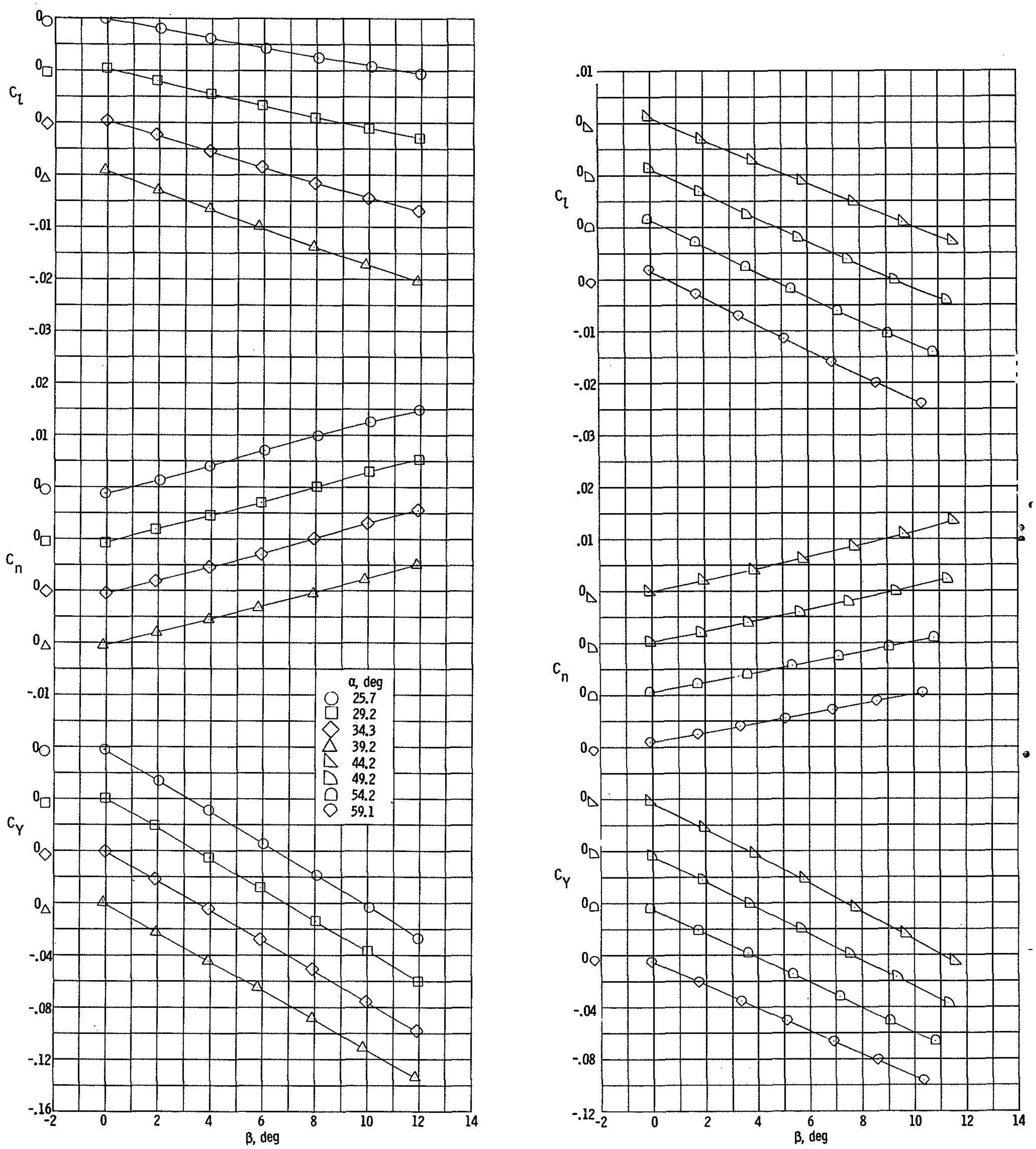

(b) $\delta_e = 0^0$, bent sting.

Figure 9.- Continued.

[redacted]

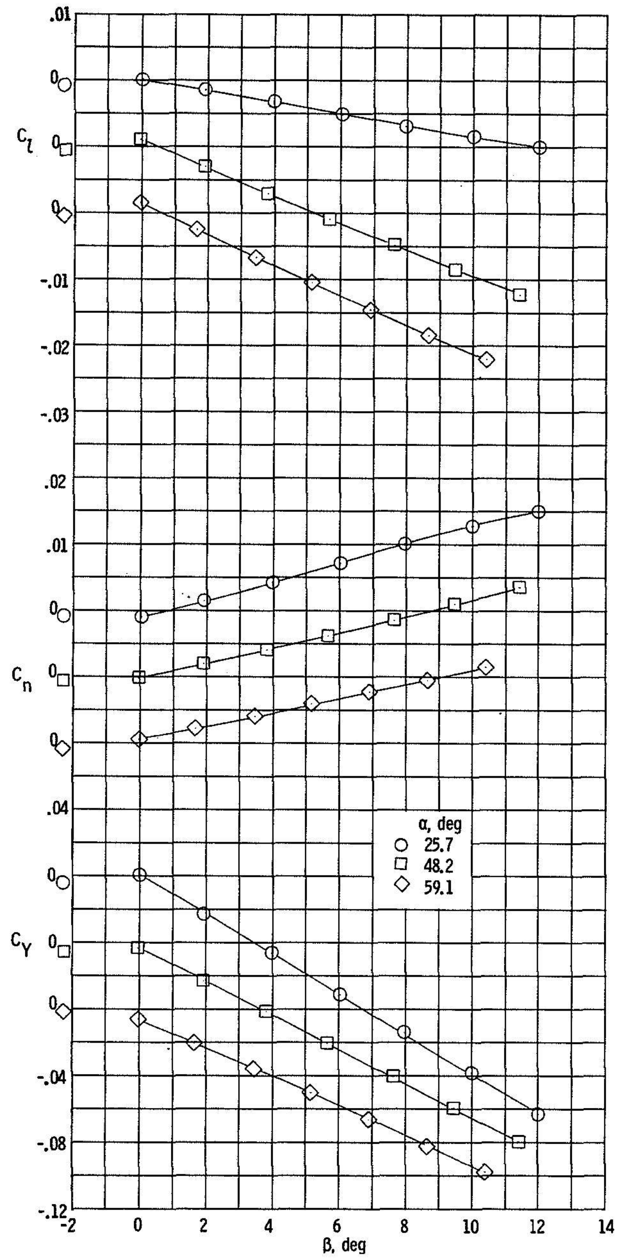

(c) $\delta_e = -15^0$, bent sting.

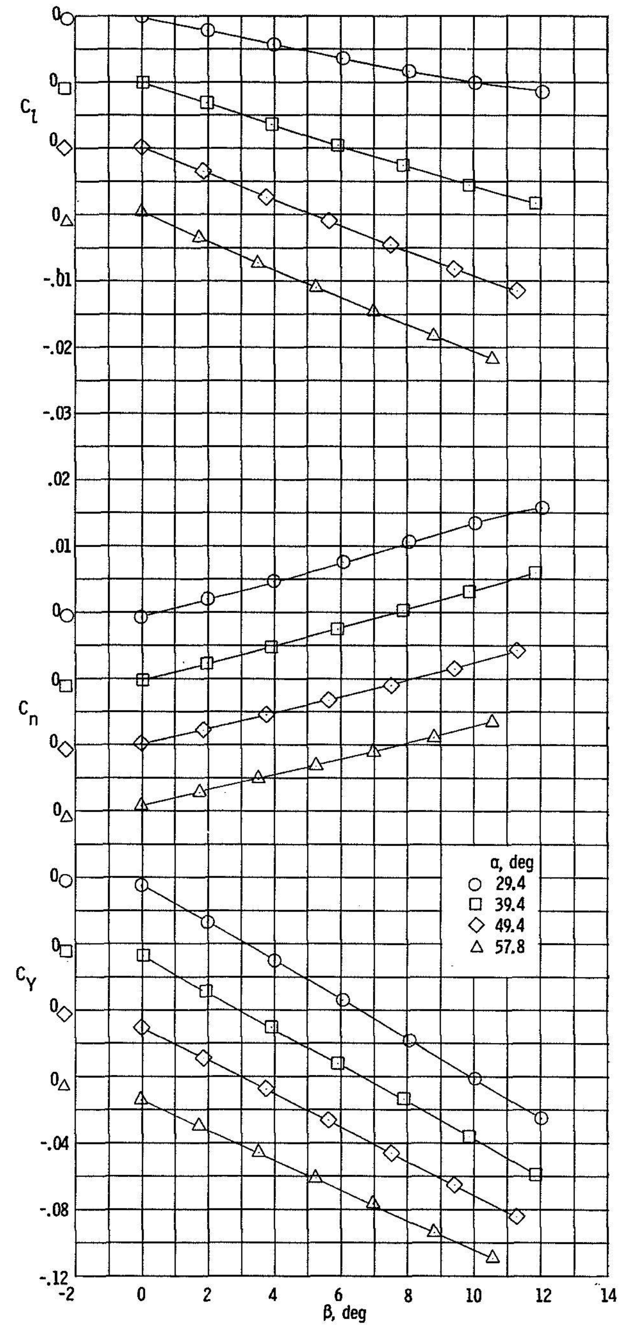

(d) $\delta_e = -30^0$, bent sting.

Figure 9.- Continued.

[redacted]

[redacted]

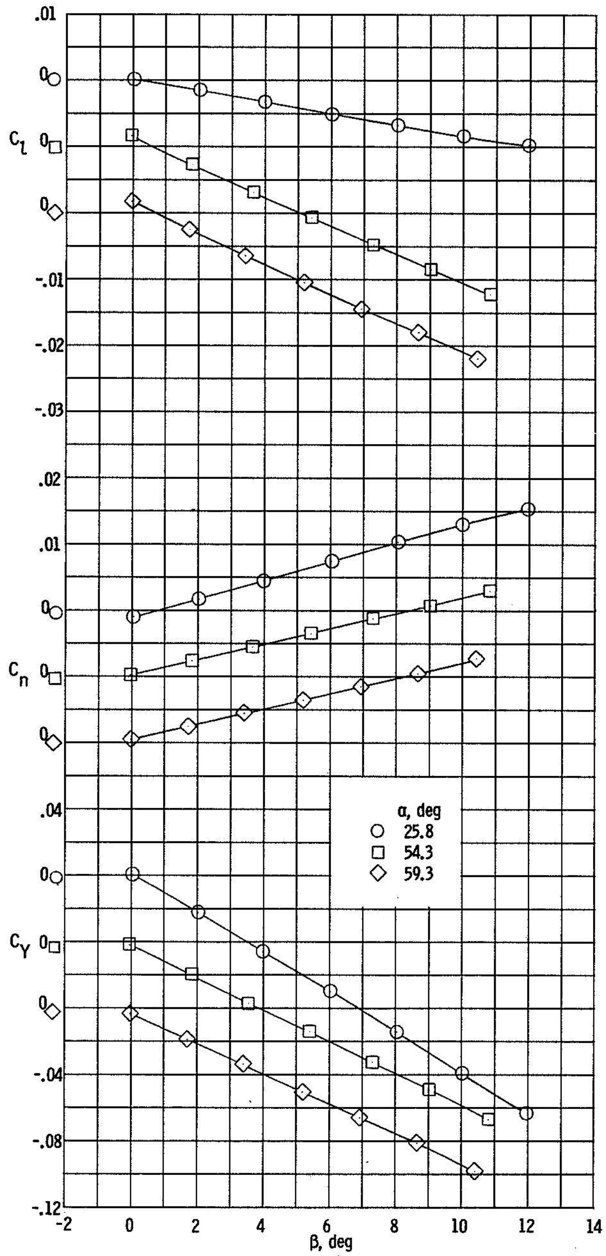

(e) $\delta_e = -45^{\circ}$, bent sting.

Figure 9.- Concluded.

[redacted]

[redacted]

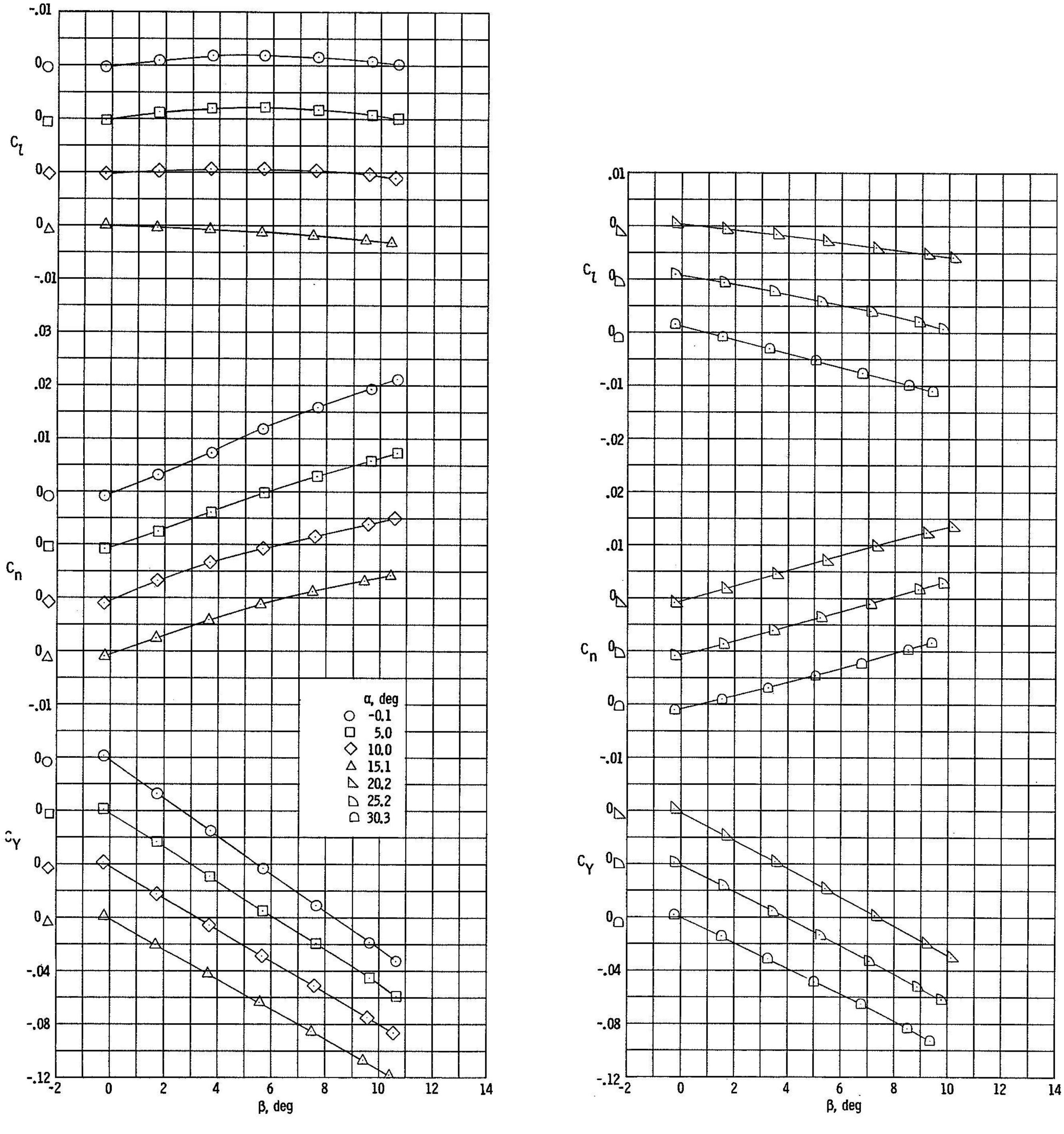

(a) $\delta_e = 0^{\circ}$, straight sting.

Figure 10.- Variation of directional and lateral characteristics with sideslip angle for complete configuration.

[redacted]

[redacted]

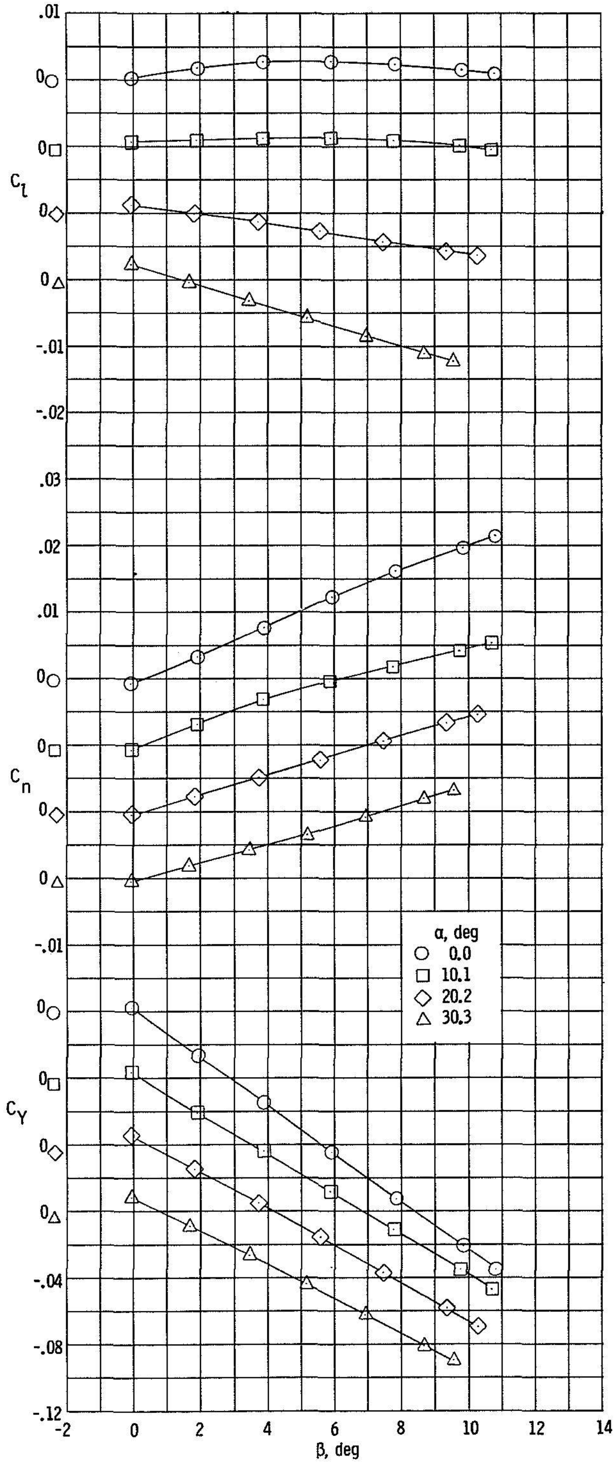

(b) $\delta_e = 15^0$, straight sting.

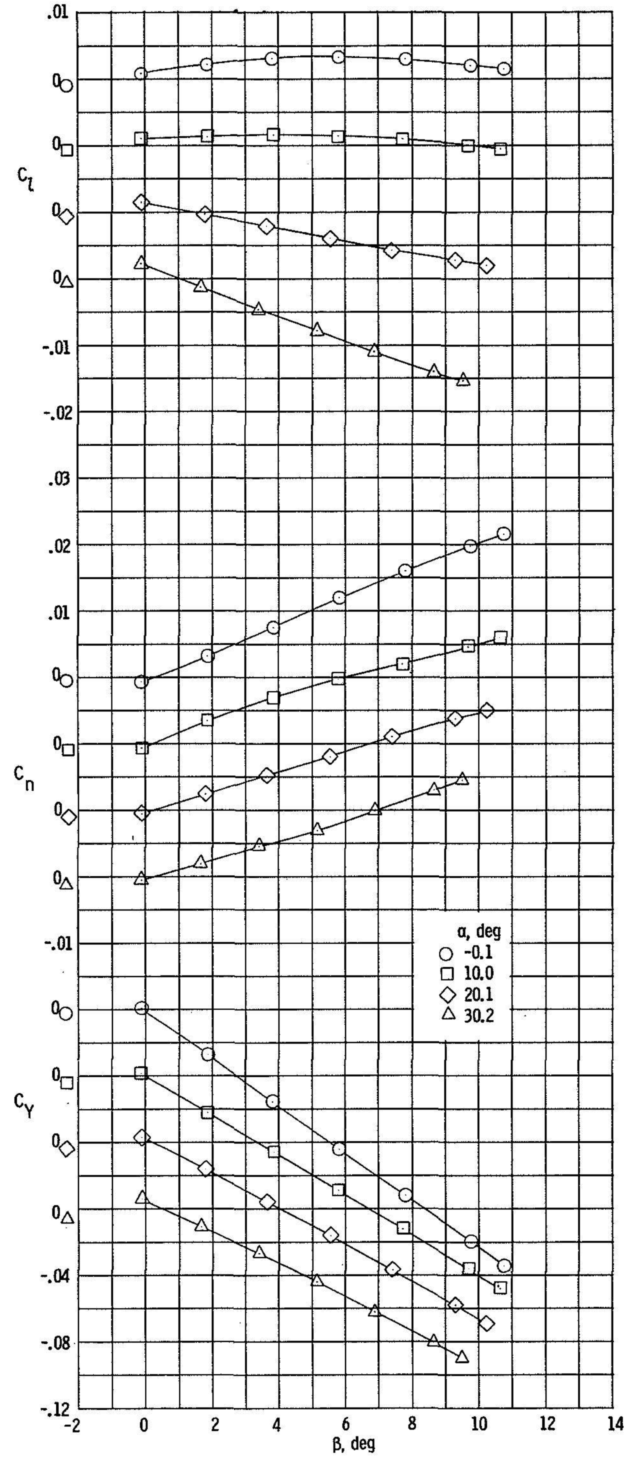

(c) $\delta_e = 30^0$, straight sting.

Figure 10.- Continued.

[redacted]

[redacted]

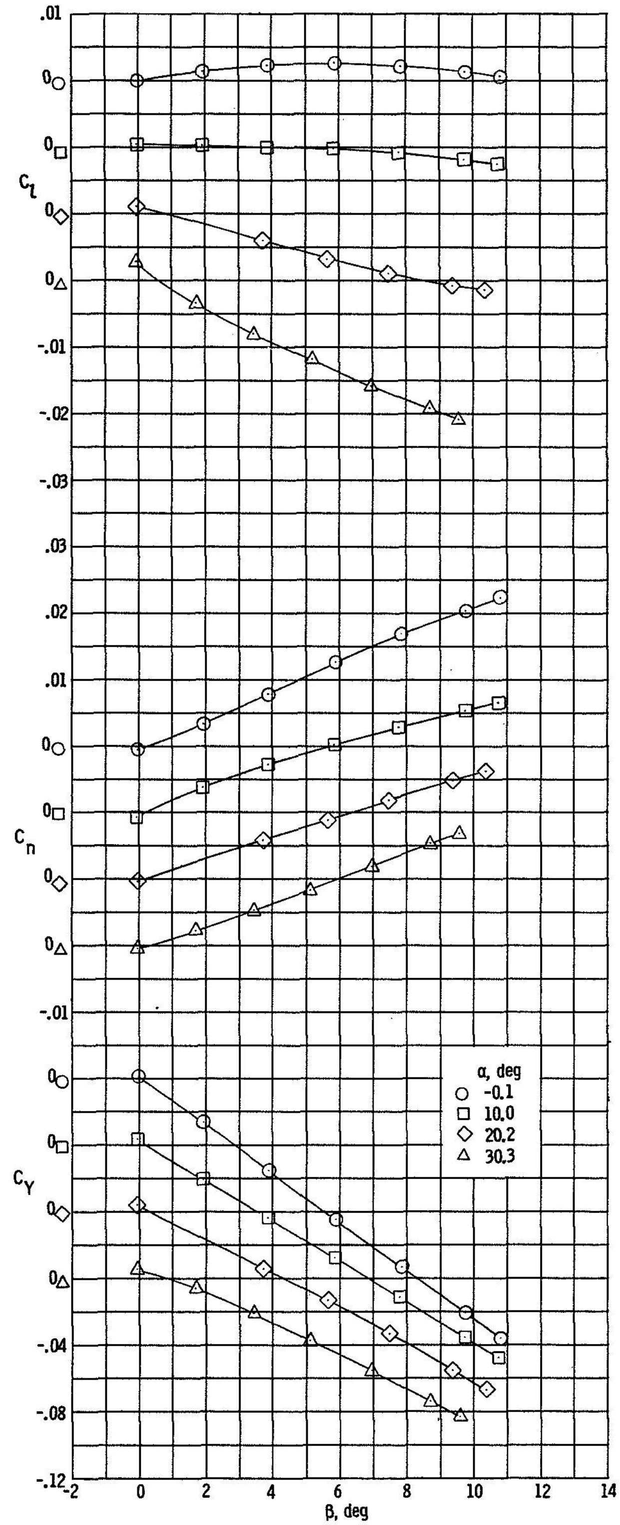

(d) $\delta_e = 45^{\circ}$, straight sting.

Figure 10.- Concluded.

[redacted]

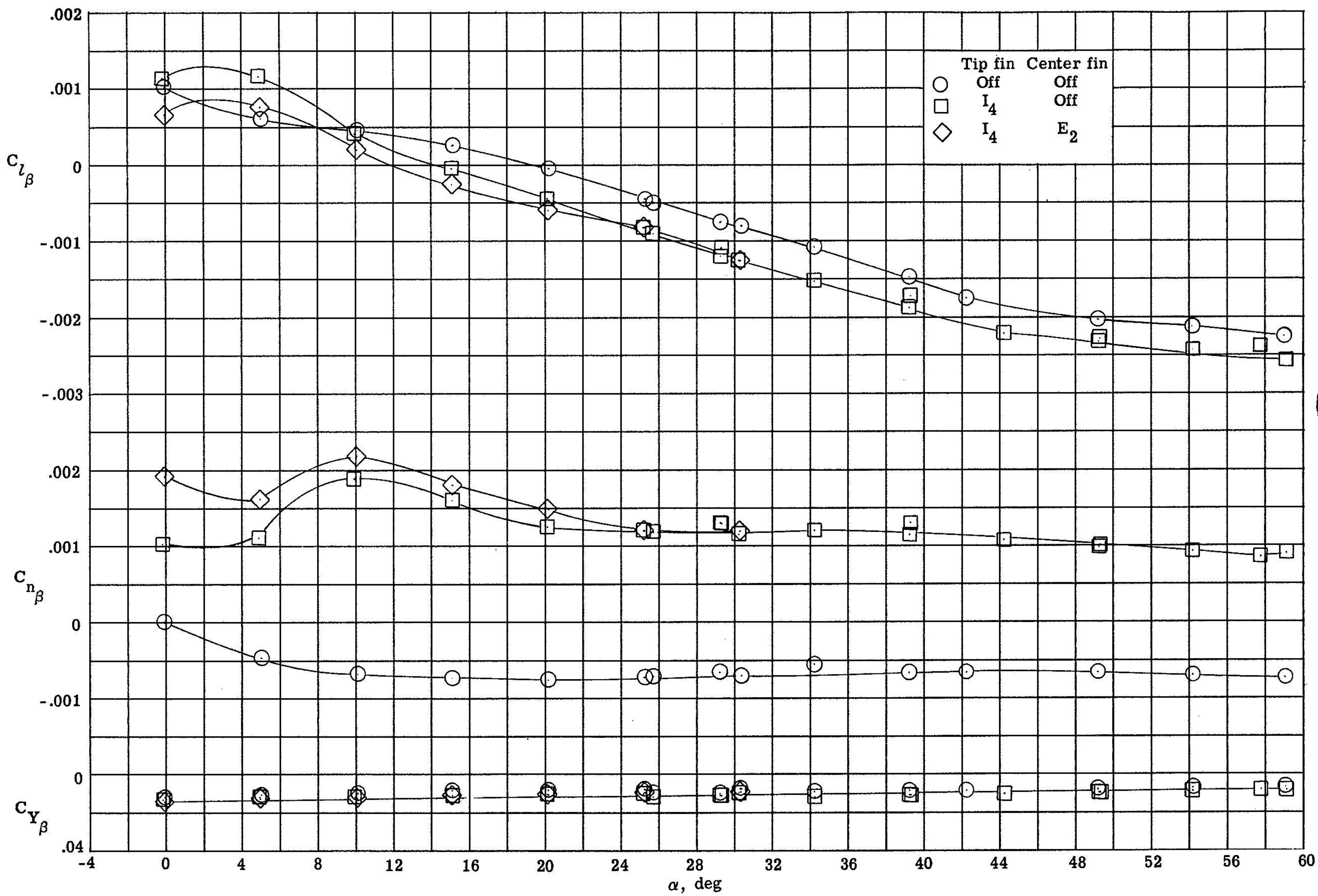

Figure 11.- Effects of tip and center fins on the directional and lateral stability characteristics.

[redacted]

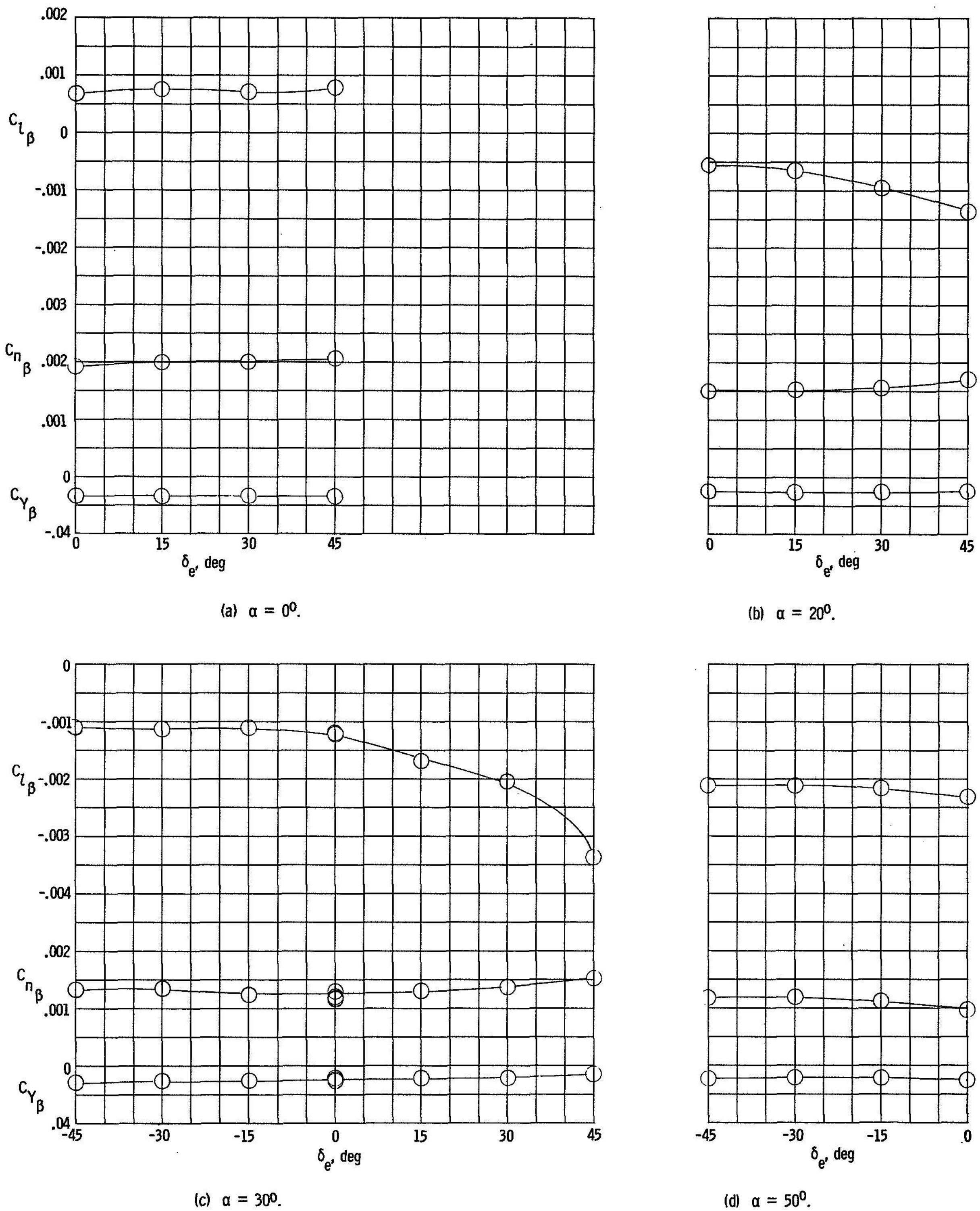

Figure 12.- Effects of elevon deflection angle on the directional and lateral stability characteristics of the complete configuration selected angles of attack.

[redacted]

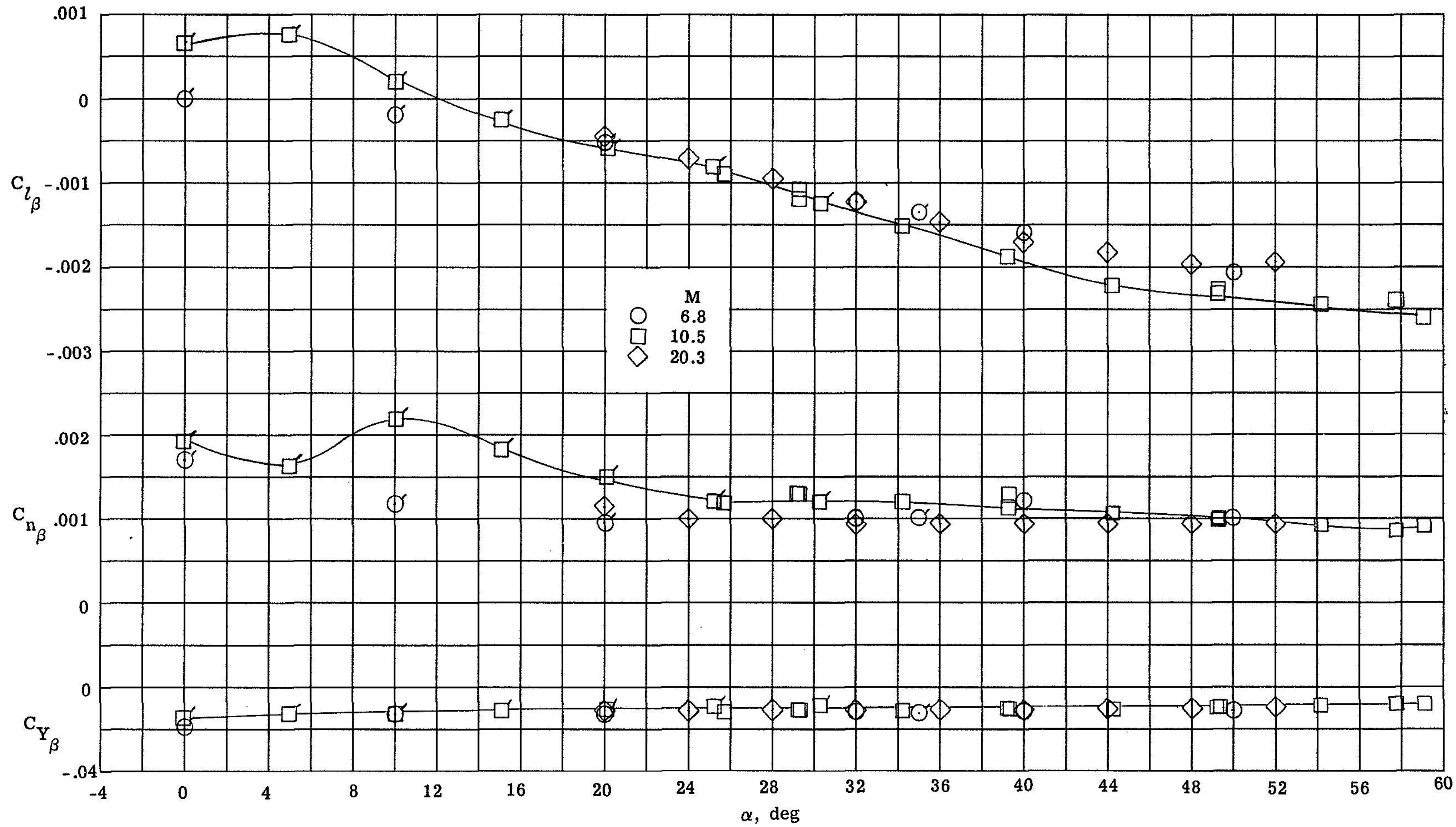

Figure 13.- Comparison of the directional and lateral stability characteristics at M = 10.5 with data at M = 6.8 from reference 15 and data at M = 20.3 from reference 13. (Flags indicate center fin on.)

[redacted]

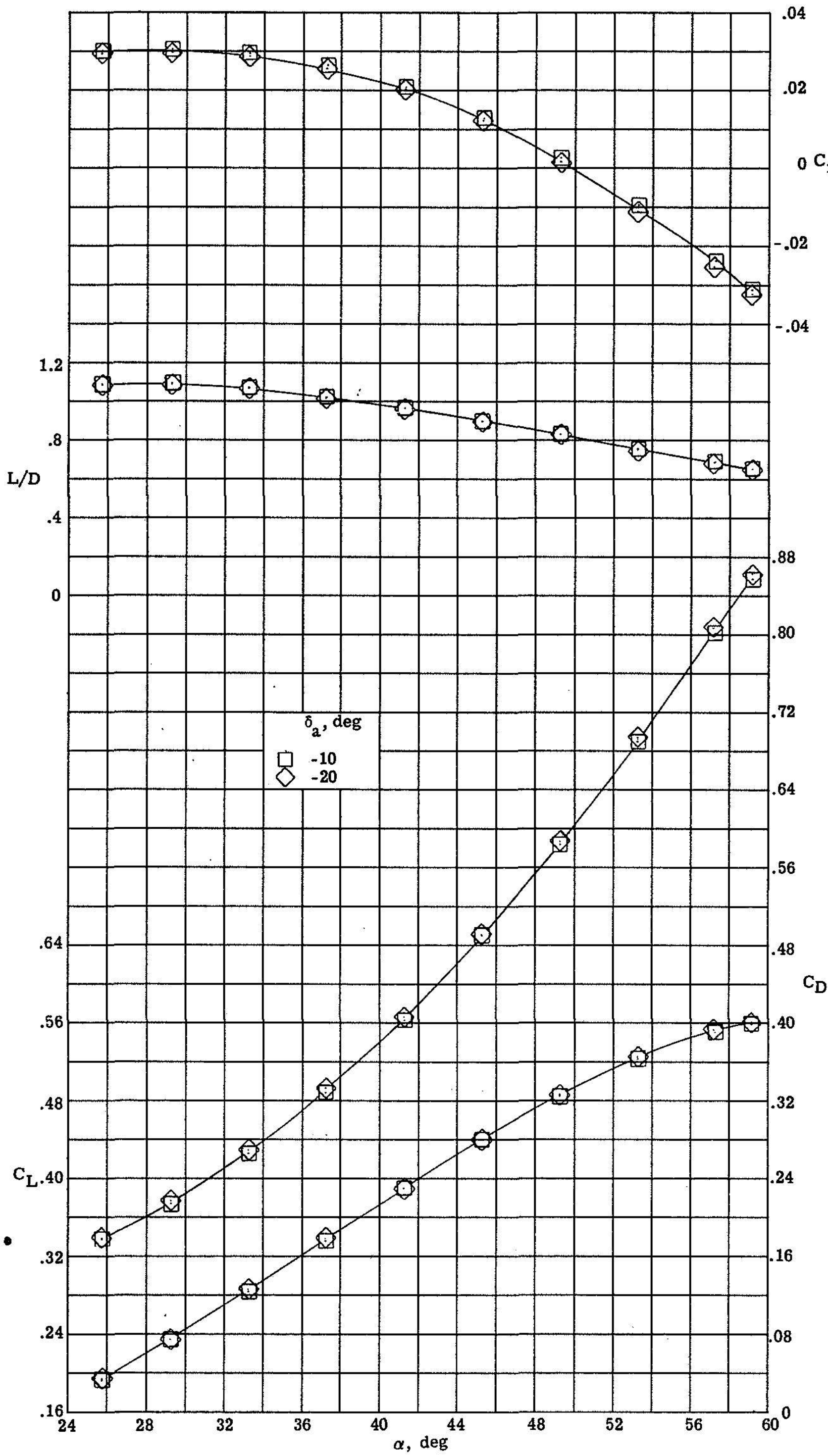

(a) $\delta_e = -30^0$.

Figure 14.- Effects of aileron deflections on the longitudinal aerodynamic characteristics for various elevon deflection angles.

[redacted]

[redacted]

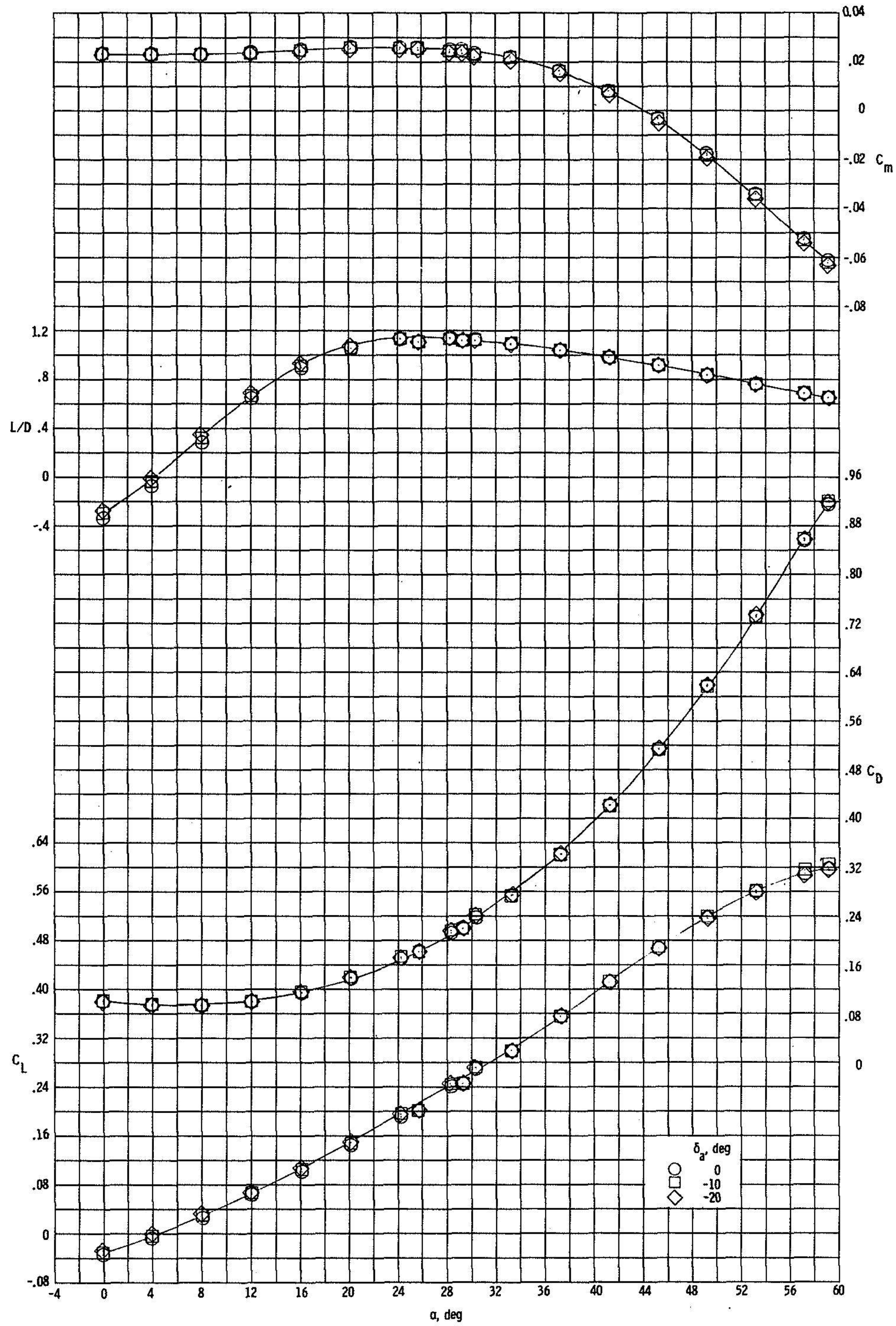

(b) $\delta_e = 0^{\circ}$.

Figure 14.- Continued.

[redacted]

[redacted]

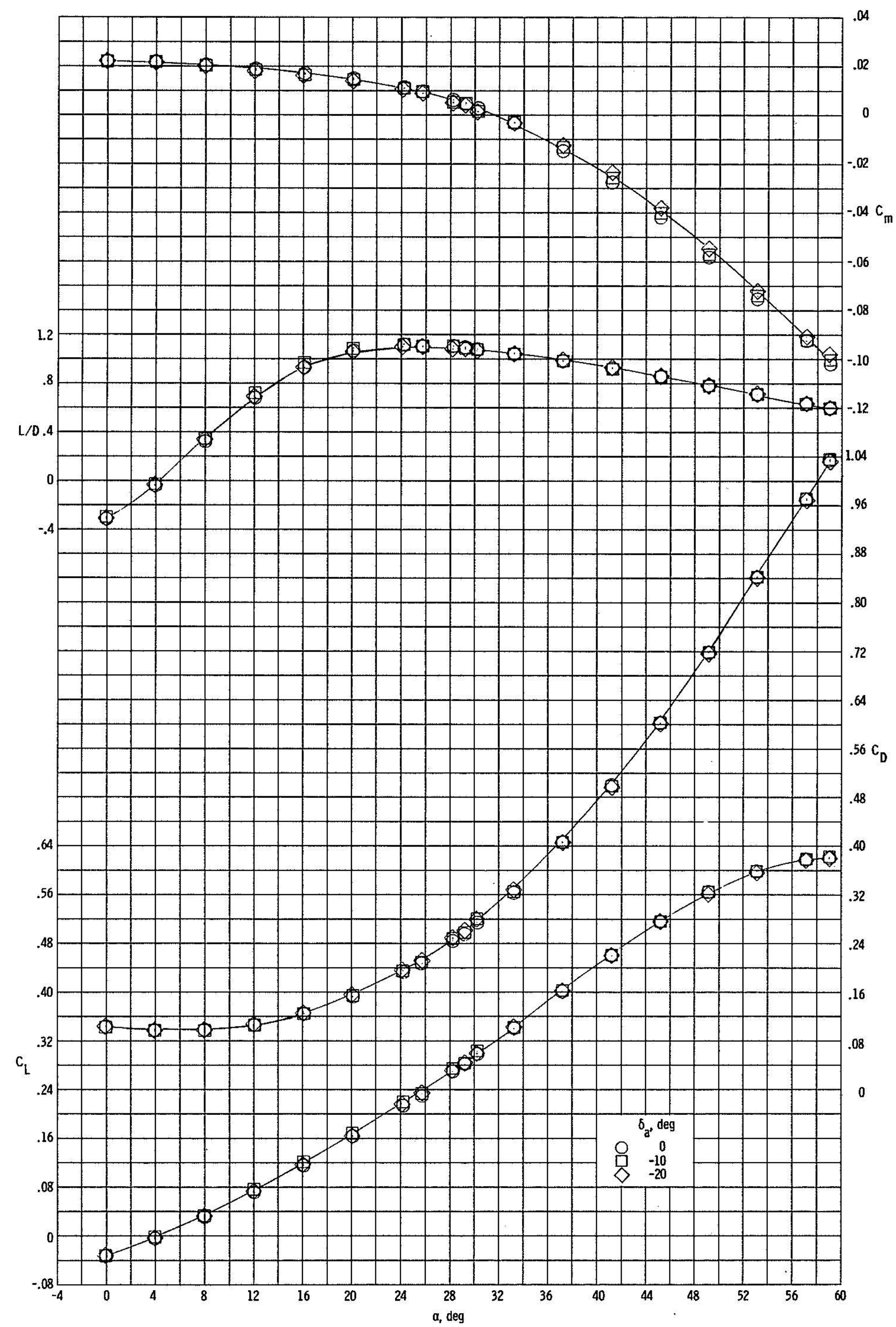

(c) $\delta_e = 30^0$.

Figure 14.- Concluded.

[redacted]

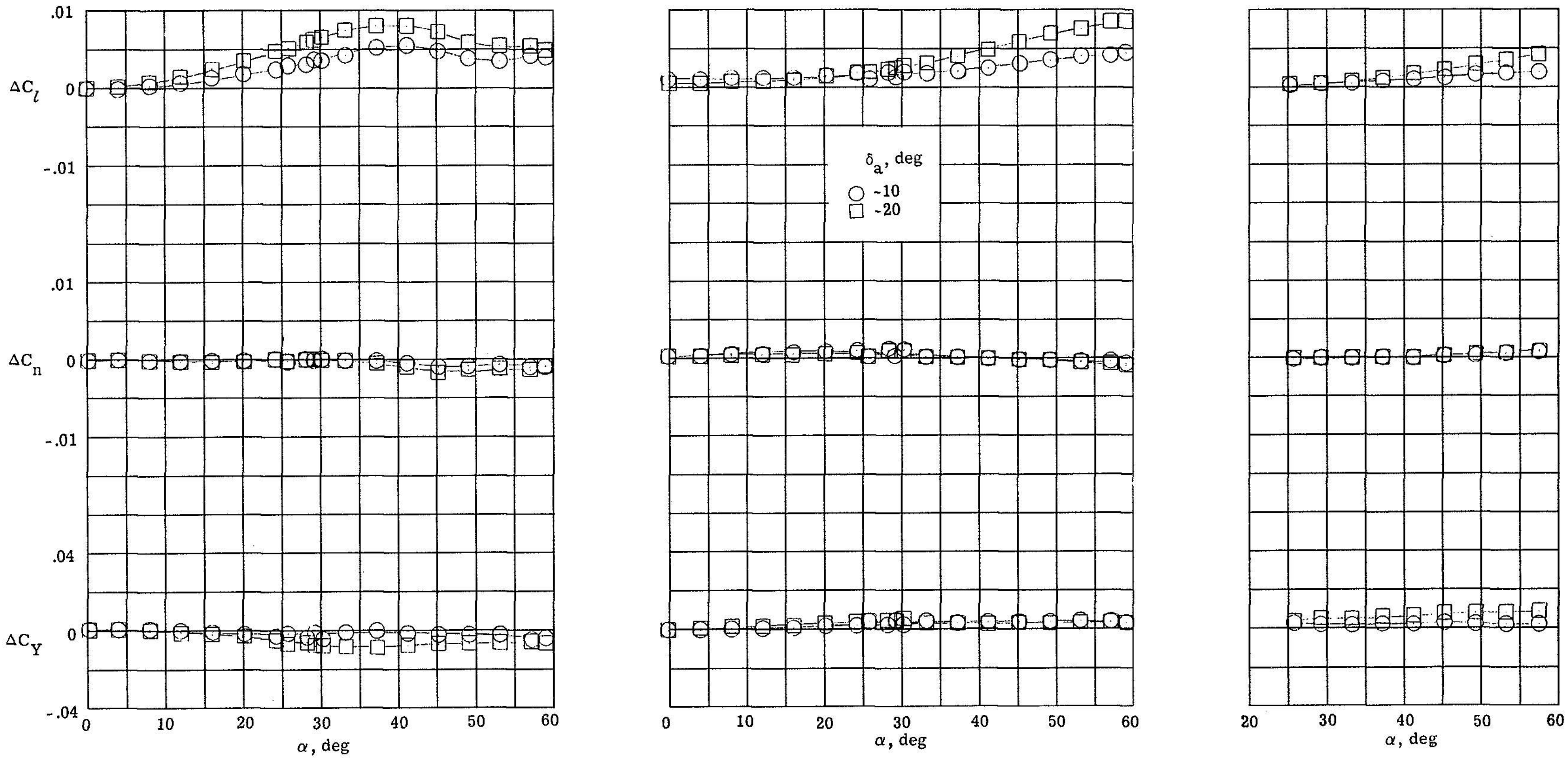

(a) $\delta_e = 30^0$.

(b) $\delta_e = 0^0$.

(c) $\delta_e = -30^0$.

Figure 15.- Lateral control characteristics for various elevon deflection angles.

[redacted]

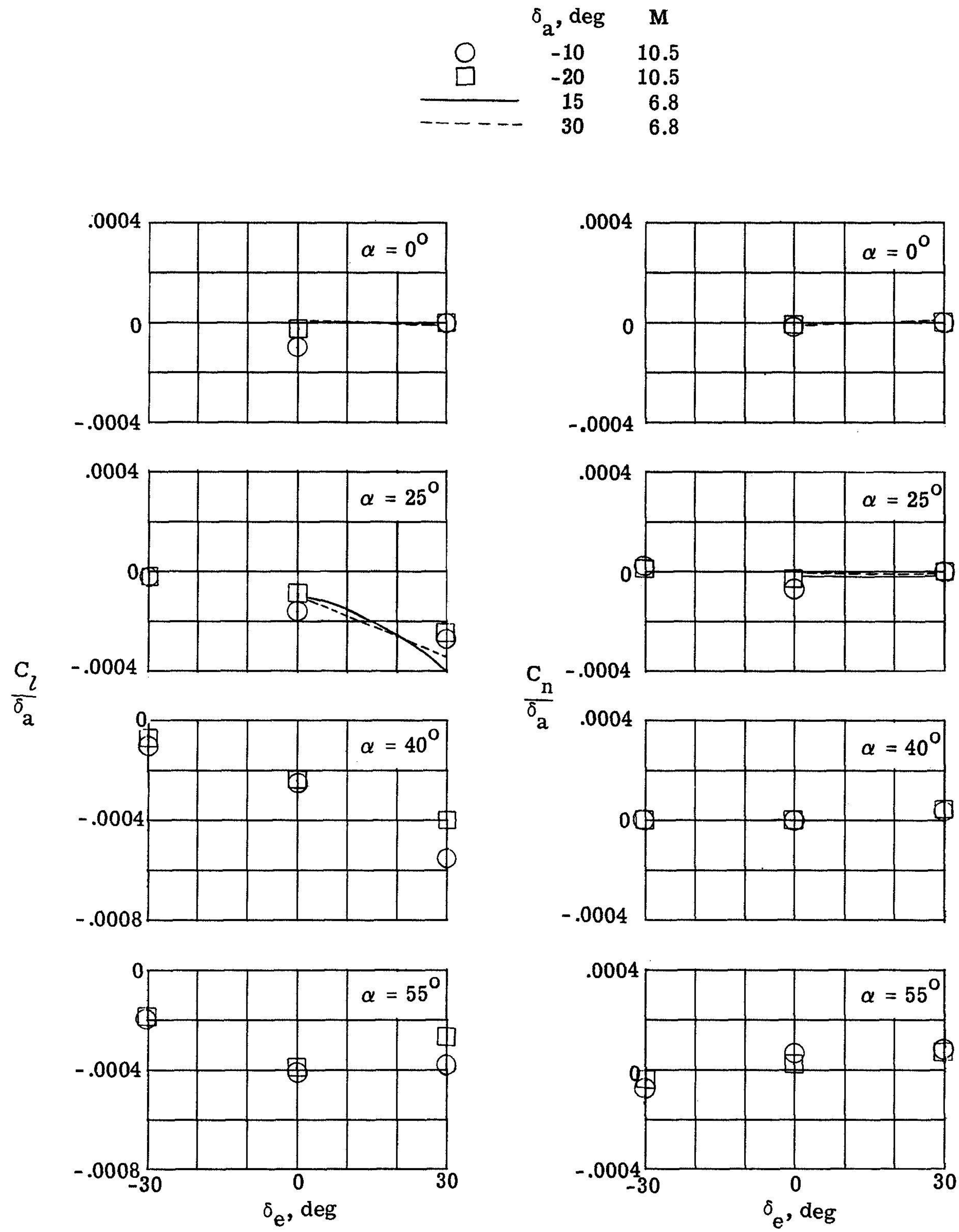

Figure 16.- Comparison of lateral control effectiveness at M = 10.5 with data at M = 6.8 from reference 15.

[redacted]

[redacted]

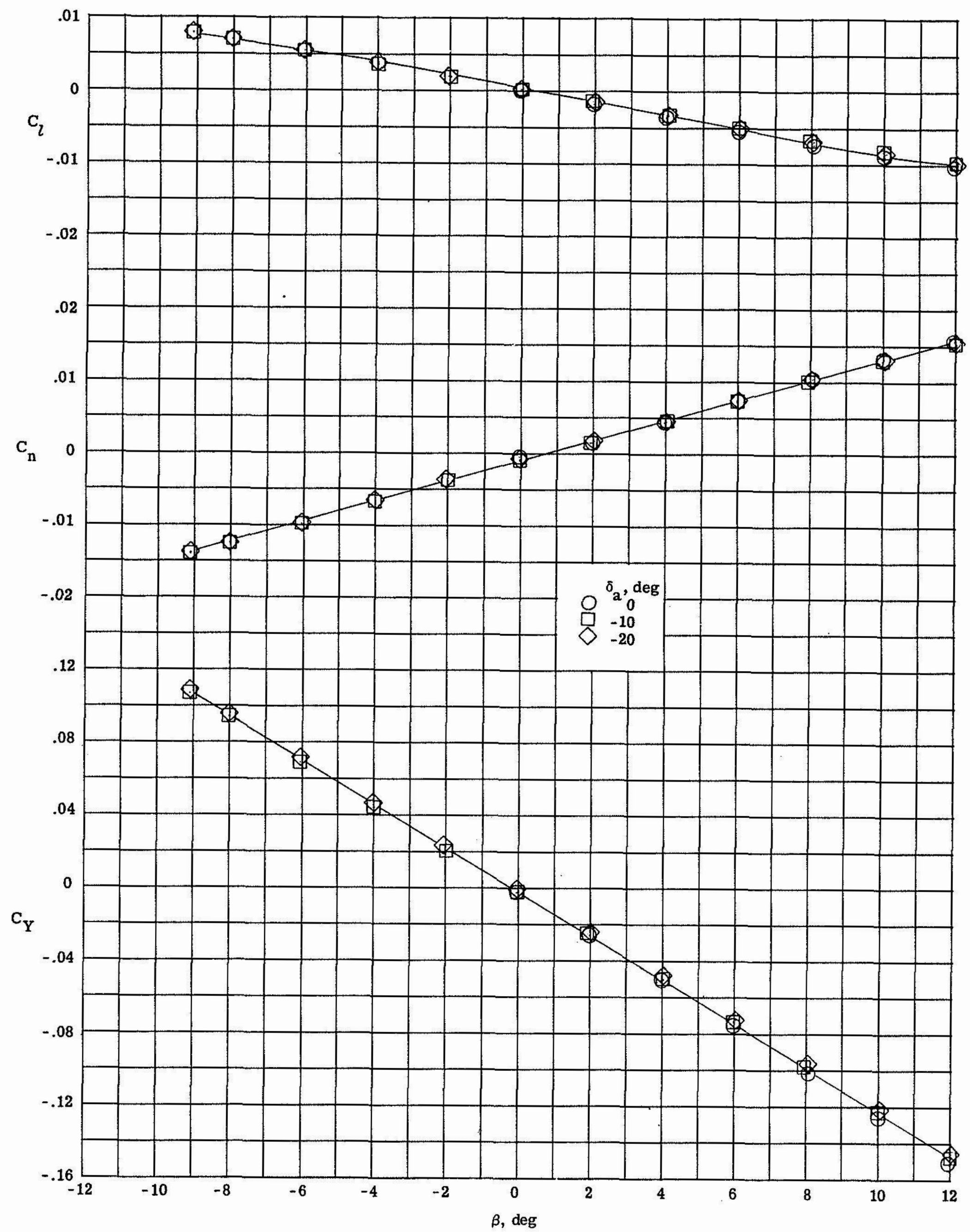

(a) $\alpha = 25.7^{\circ}$, bent sting.

Figure 17.- Variation of directional and lateral characteristics with sideslip angle for various aileron deflections at $\delta_e = -30^{\circ}$.

[redacted]

[redacted]

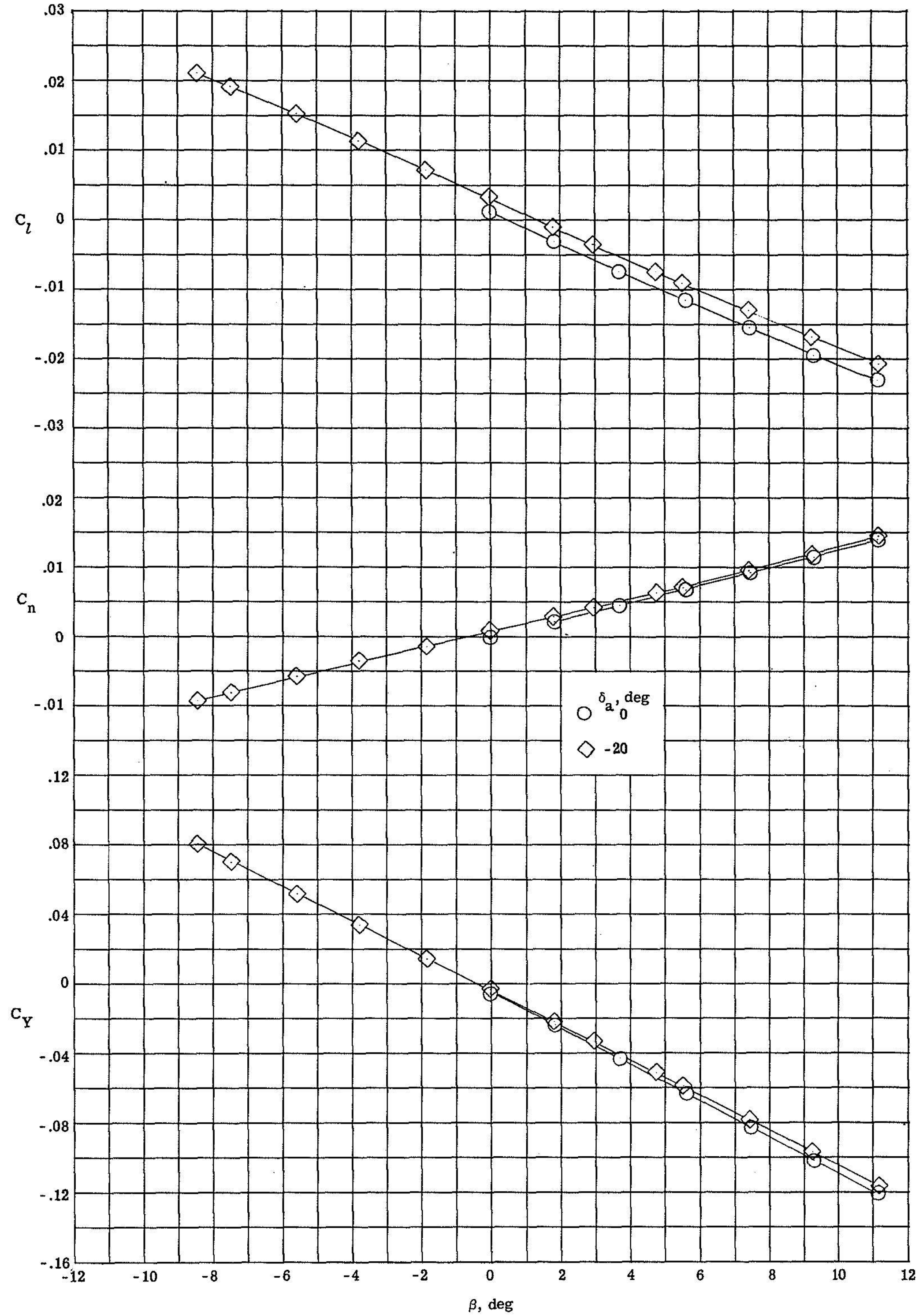

(b) $\alpha = 51.5^{\circ}$, bent sting.

Figure 17.- Continued.

[redacted]

[redacted]

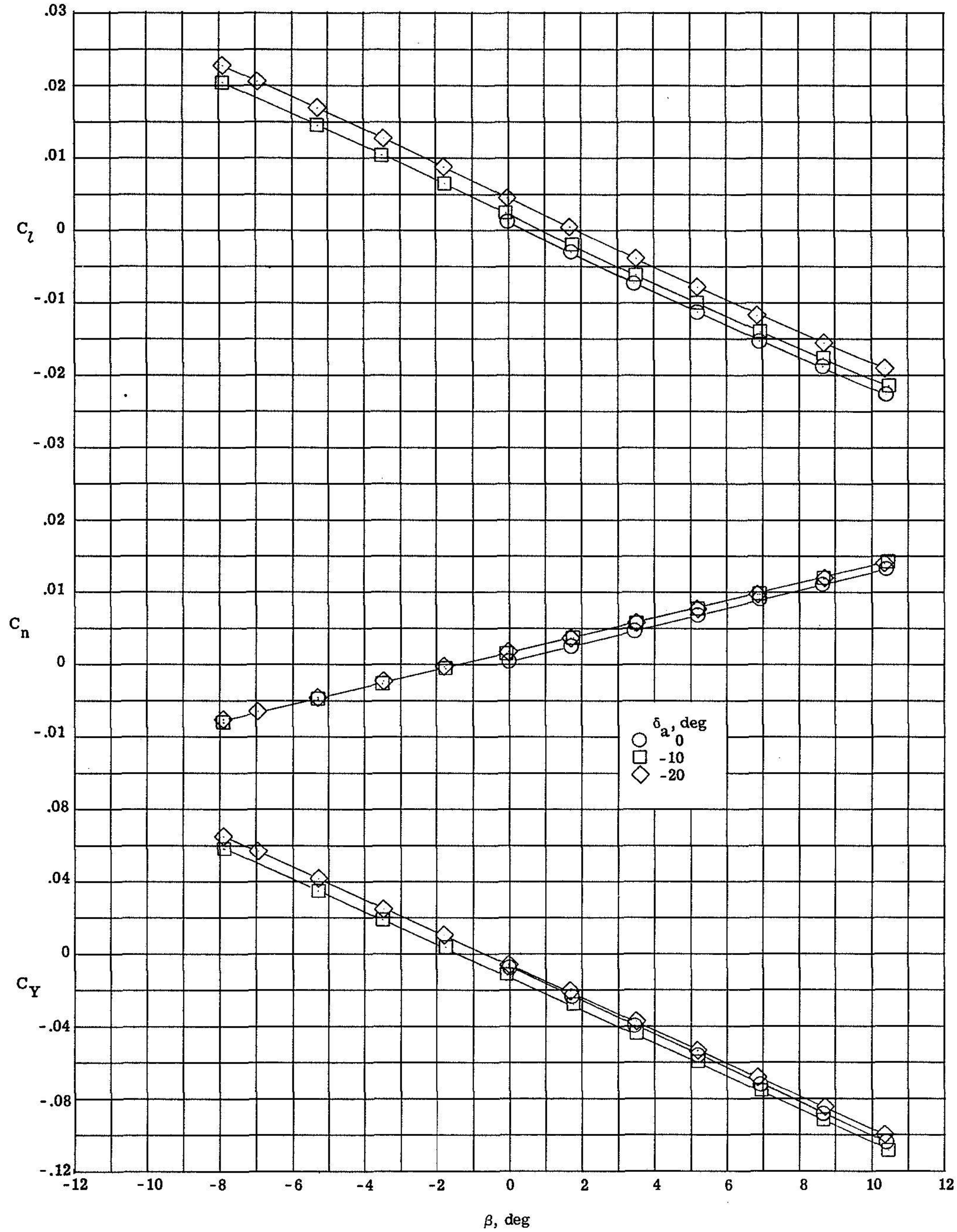

(c) $\alpha = 59.4^{0}$, bent sting.

Figure 17.- Concluded.

[redacted]

[redacted]

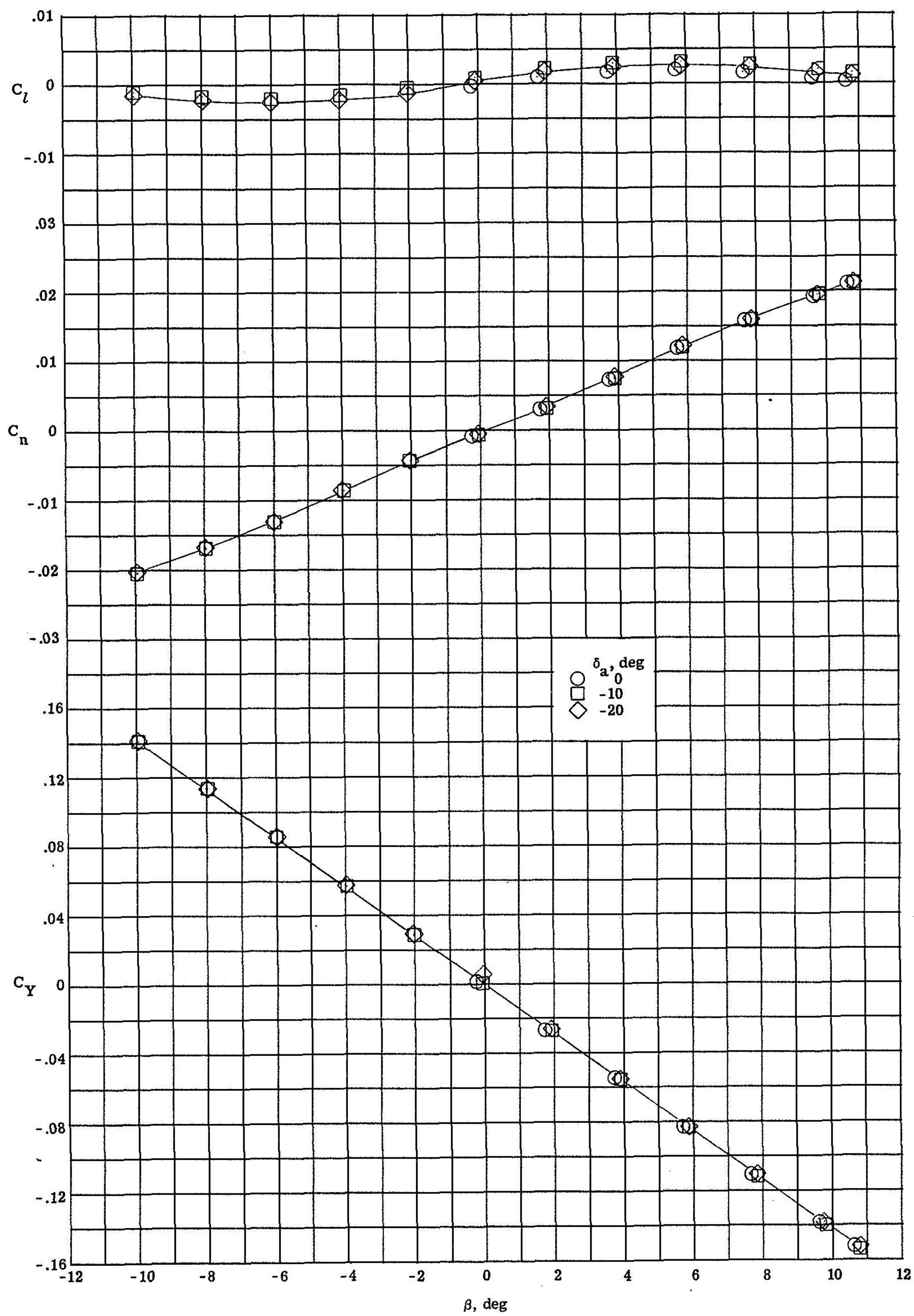

(a) $\alpha = -0.1^0$, straight sting.

Figure 18.- Variation of directional and lateral characteristics with sideslip angle for various aileron deflections at $\delta_e = 0^0$.

[redacted]

[redacted]

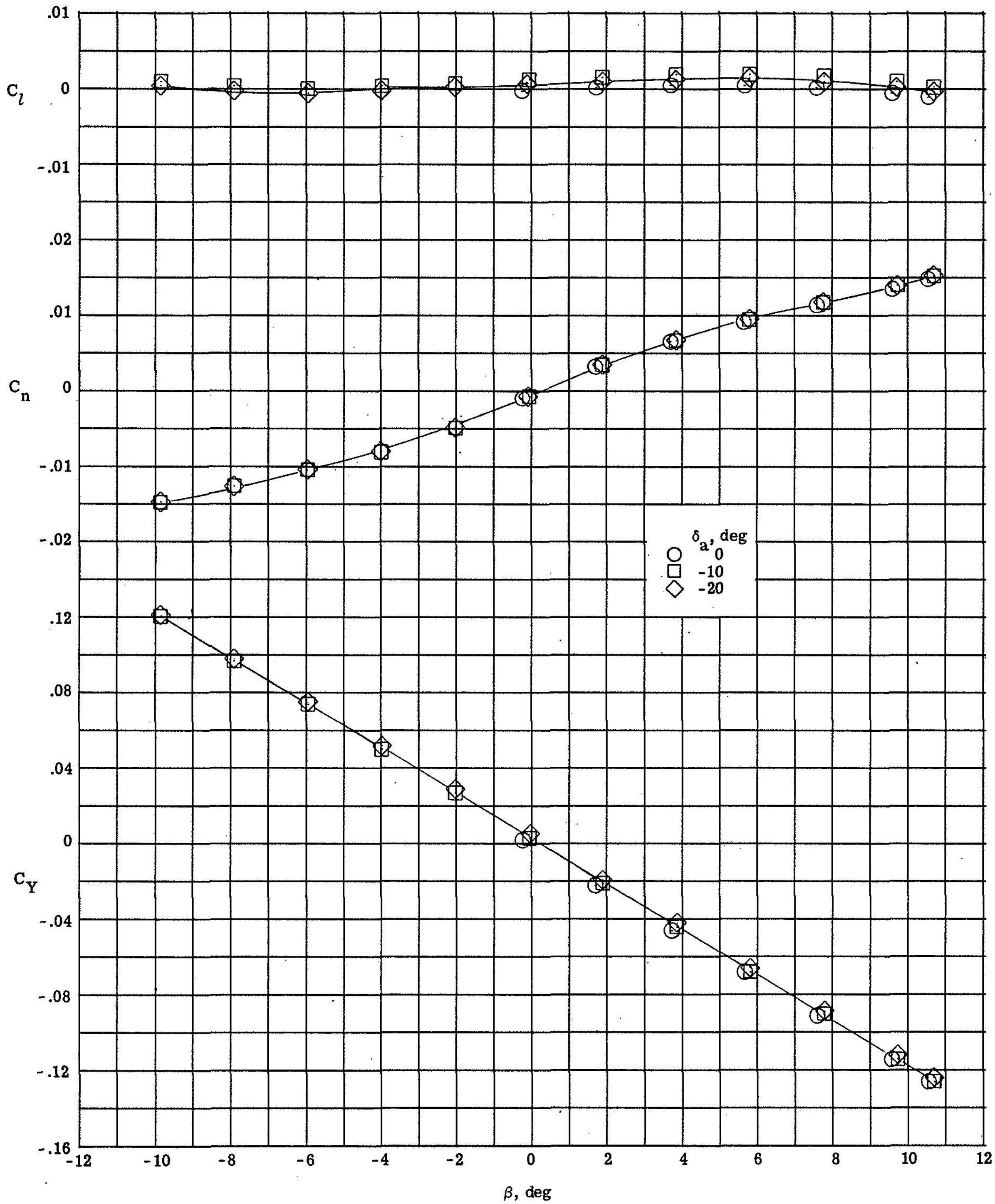

(b) $\alpha = 10.0^{\circ}$, straight sting.

Figure 18.- Continued.

[redacted]

[redacted]

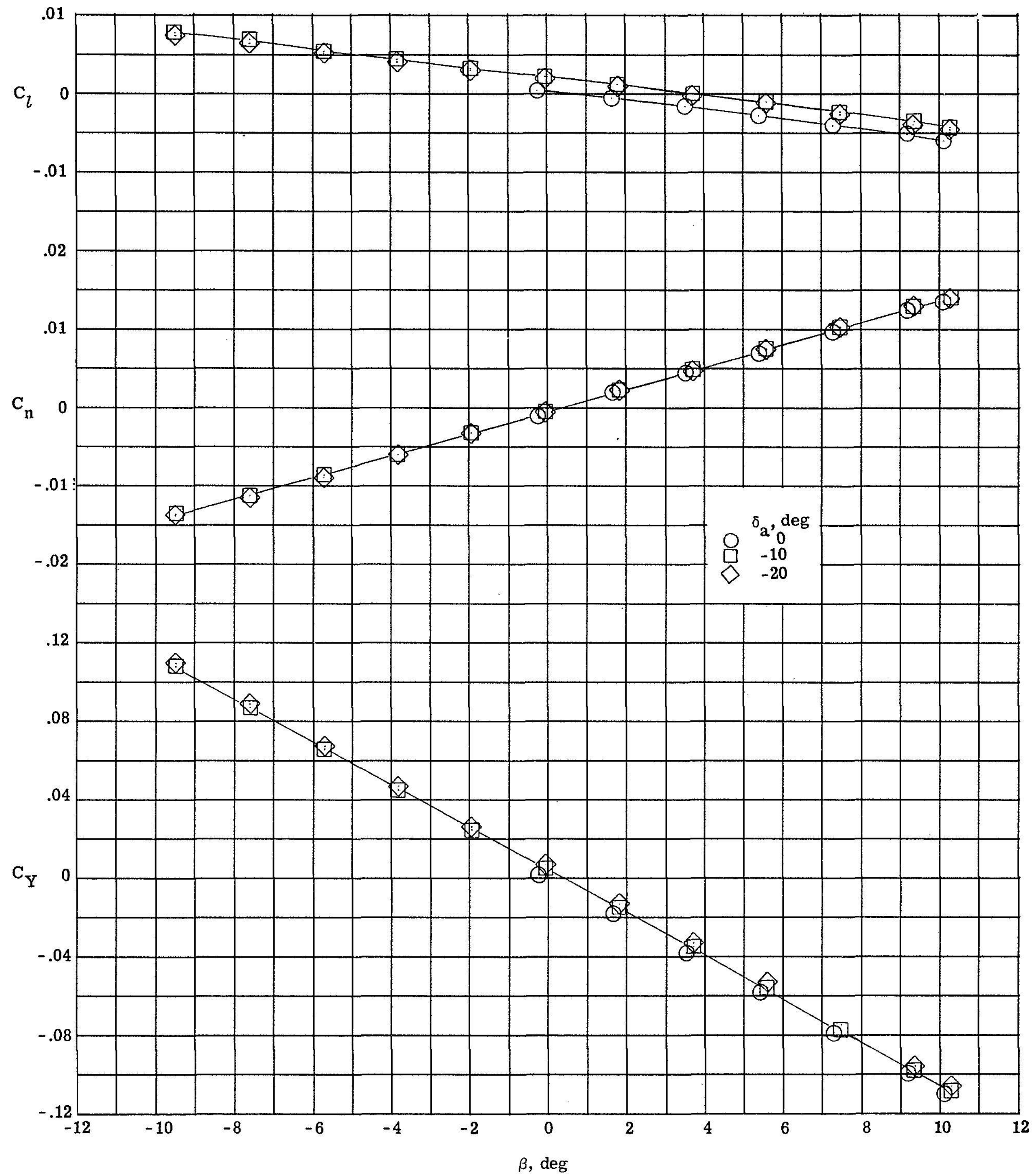

(c) $\alpha = 20.2^0$, straight sting.

Figure 18.- Continued.

[redacted]

[redacted]

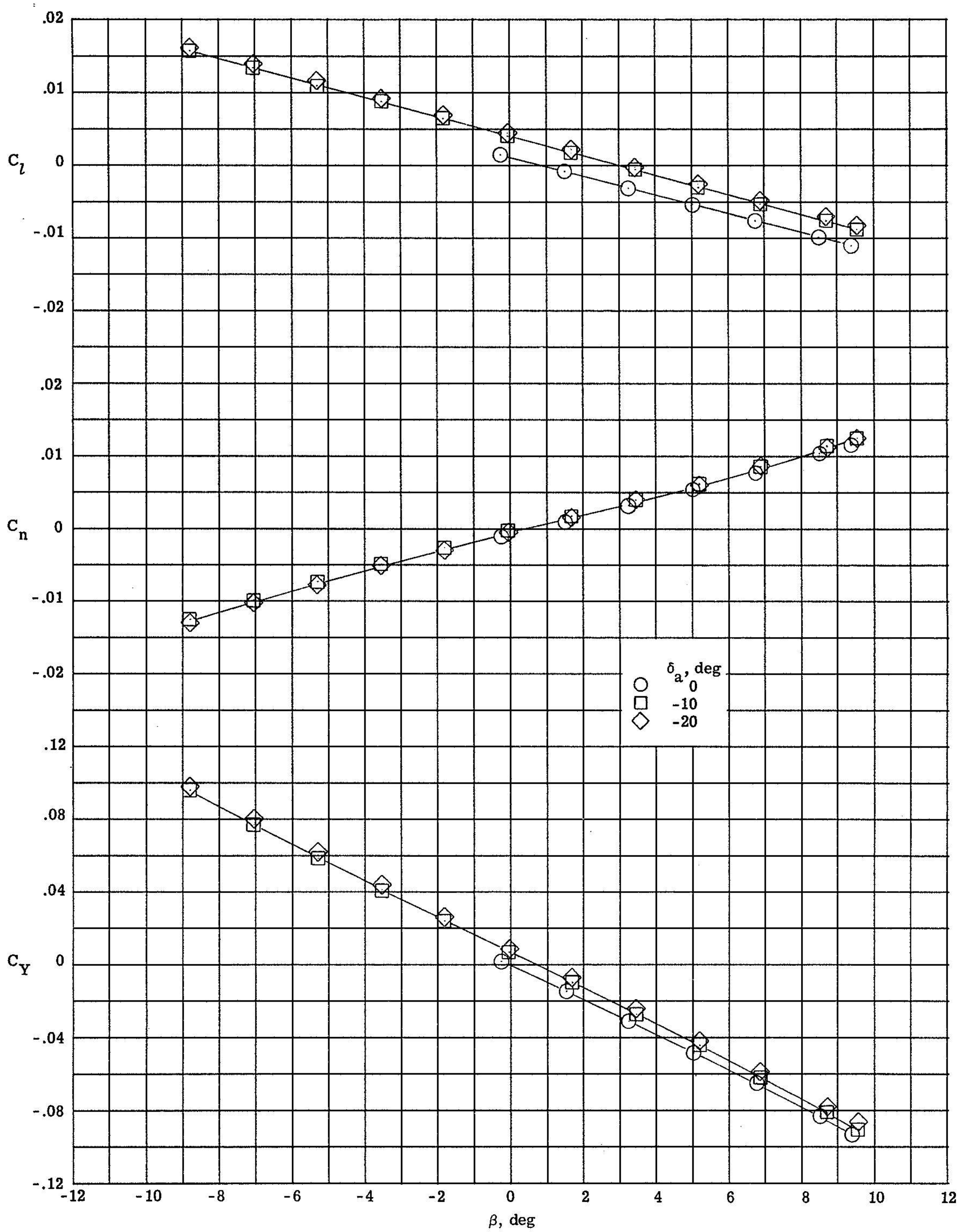

(d) $\alpha = 30.3^0$, straight sting.

Figure 18.- Continued.

[redacted]

[redacted]

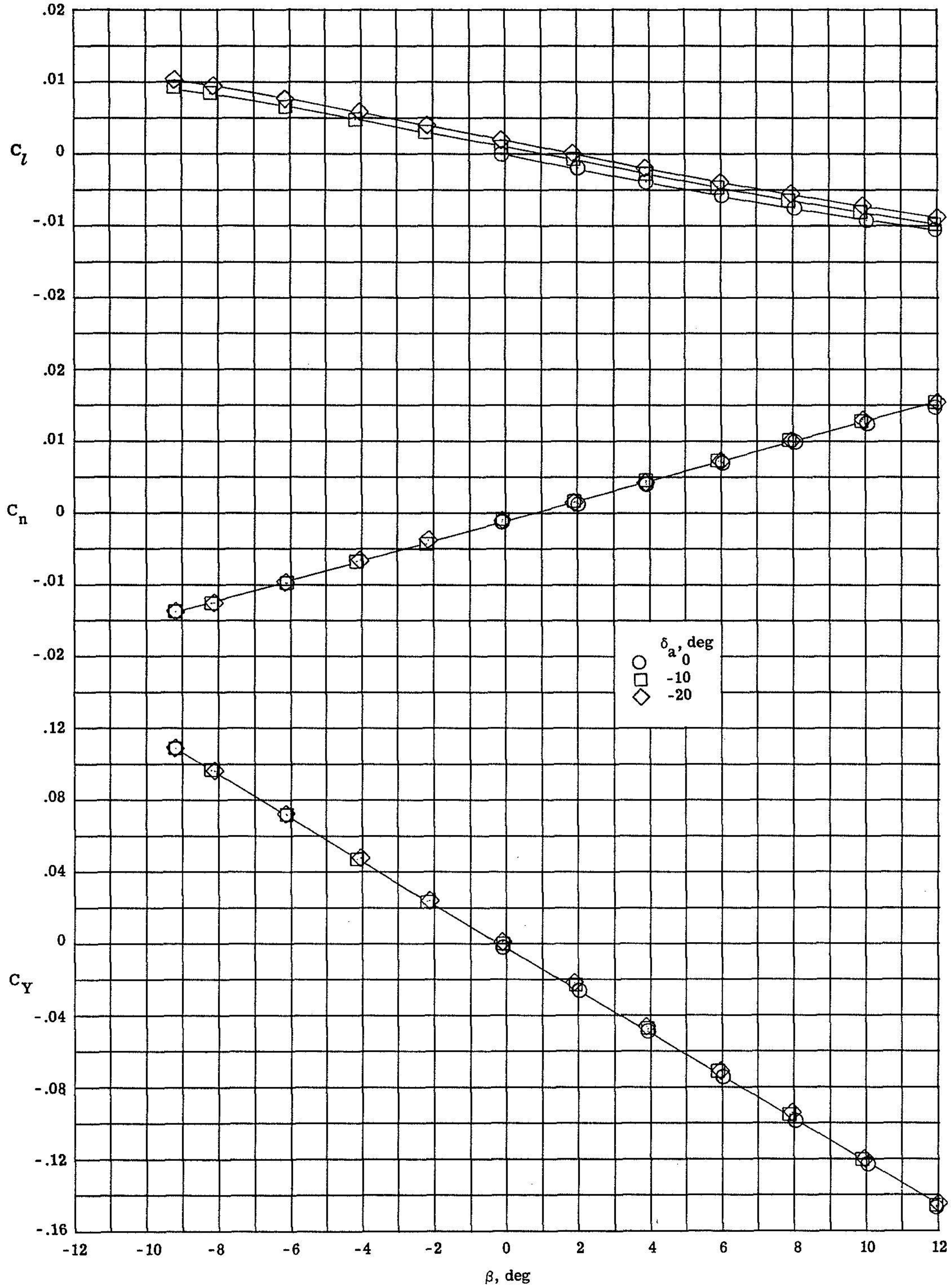

(e) $\alpha = 25.7^{0}$, bent sting.

Figure 18.- Continued.

[redacted]

[redacted]

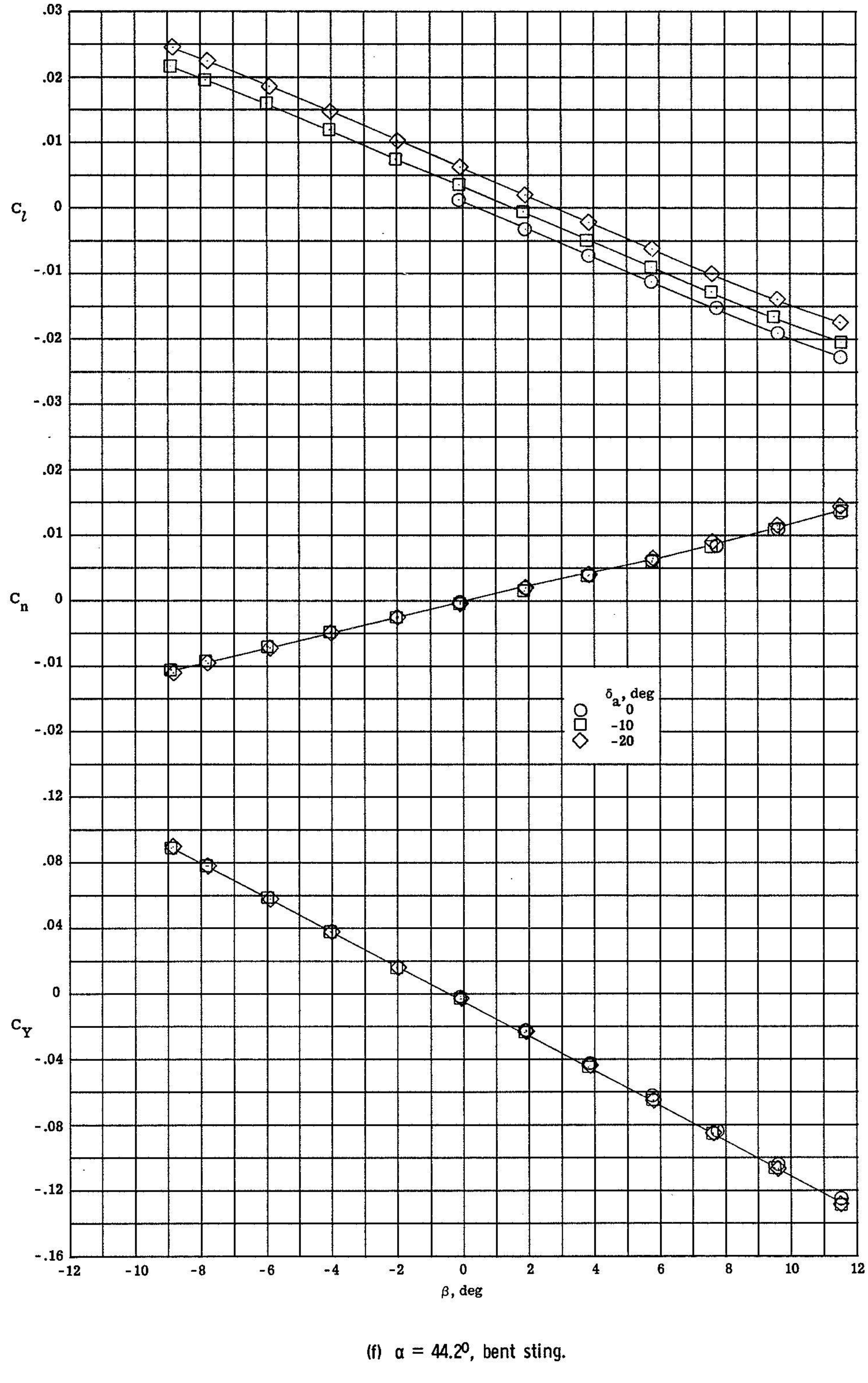

(f) $\alpha = 44.2^{0}$, bent sting.

Figure 18.- Continued.

[redacted]

[redacted]

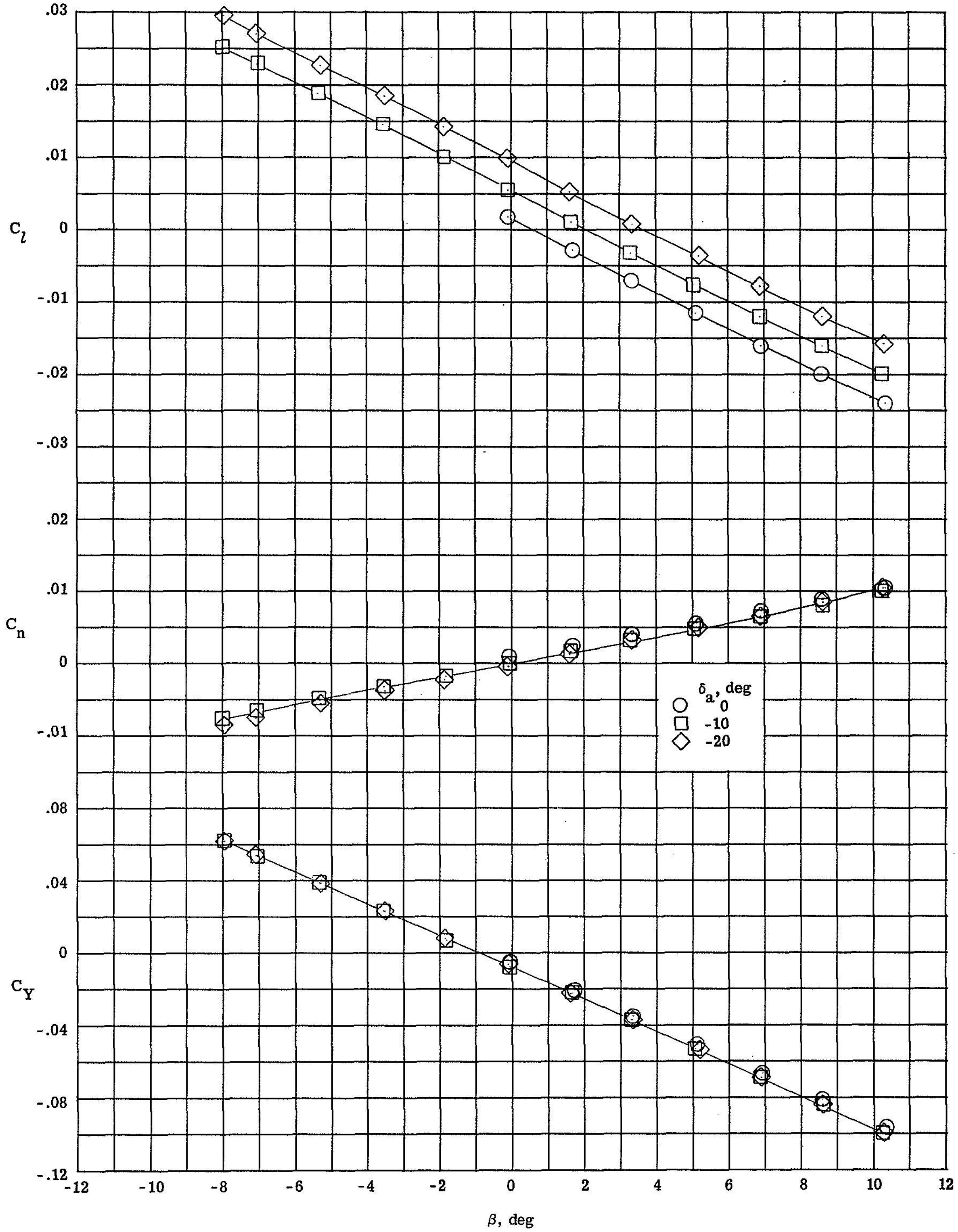

(g) $\alpha = 59.1^{0}$, bent sting.

Figure 18.- Concluded.

[redacted]

[redacted]

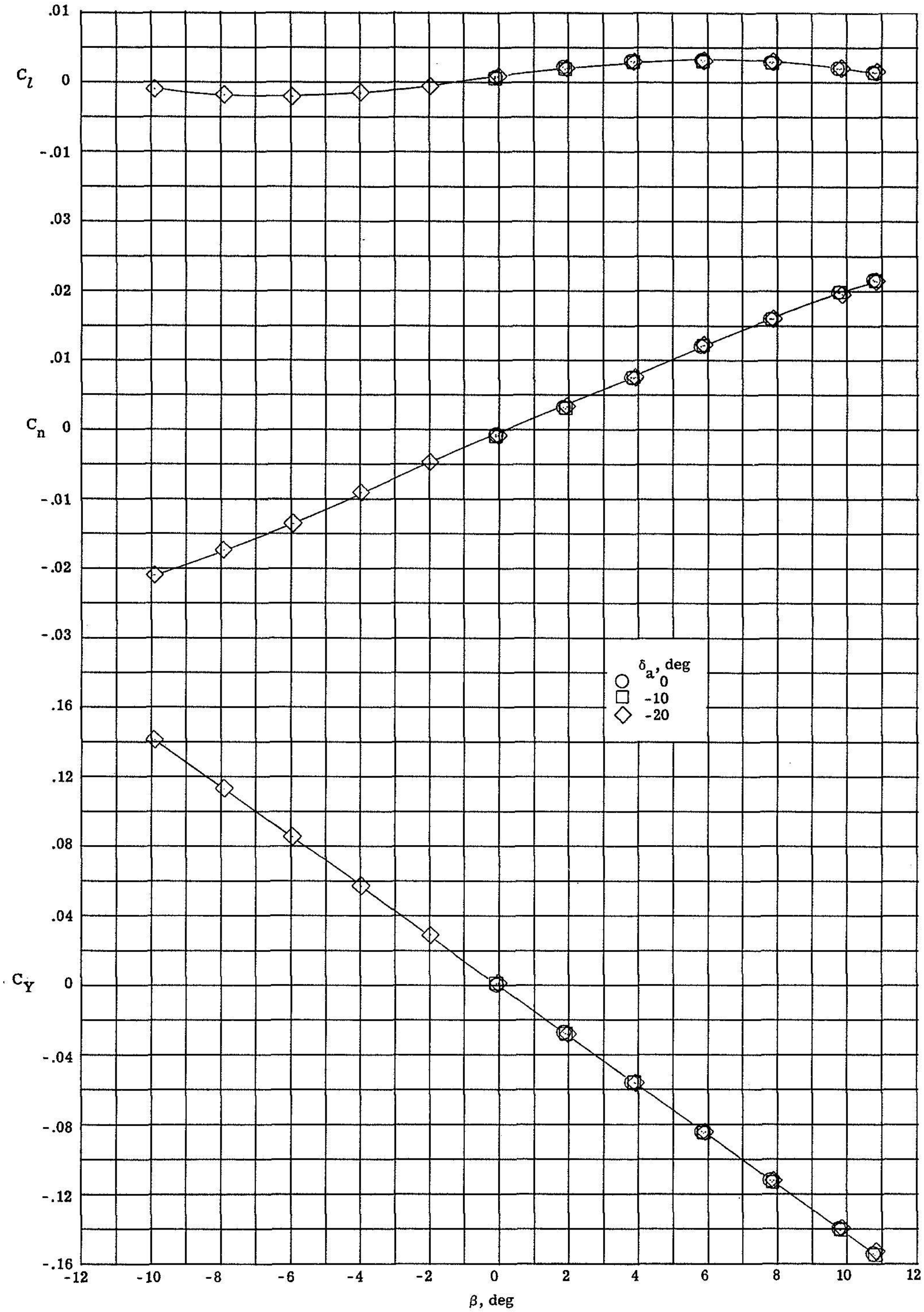

(a) $\alpha = -0.1^{\circ}$, straight sting.

Figure 19.- Variation of directional and lateral characteristics with sideslip angle for various aileron deflections at $\delta_e = 30^{\circ}$.

[redacted]

[redacted]

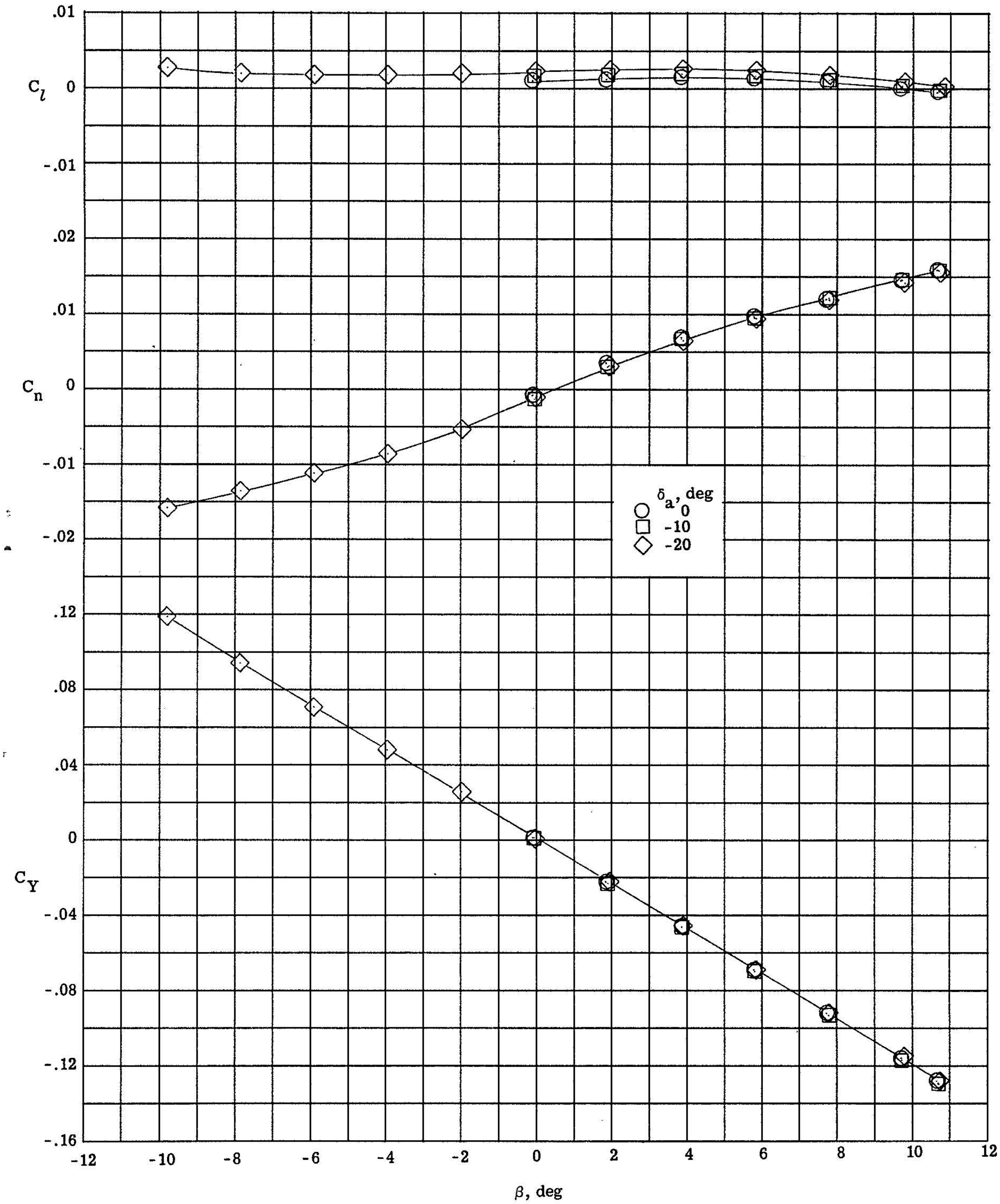

(b) $\alpha = 10.0^{\circ}$, straight sting.

Figure 19.- Continued.

[redacted]

[redacted]

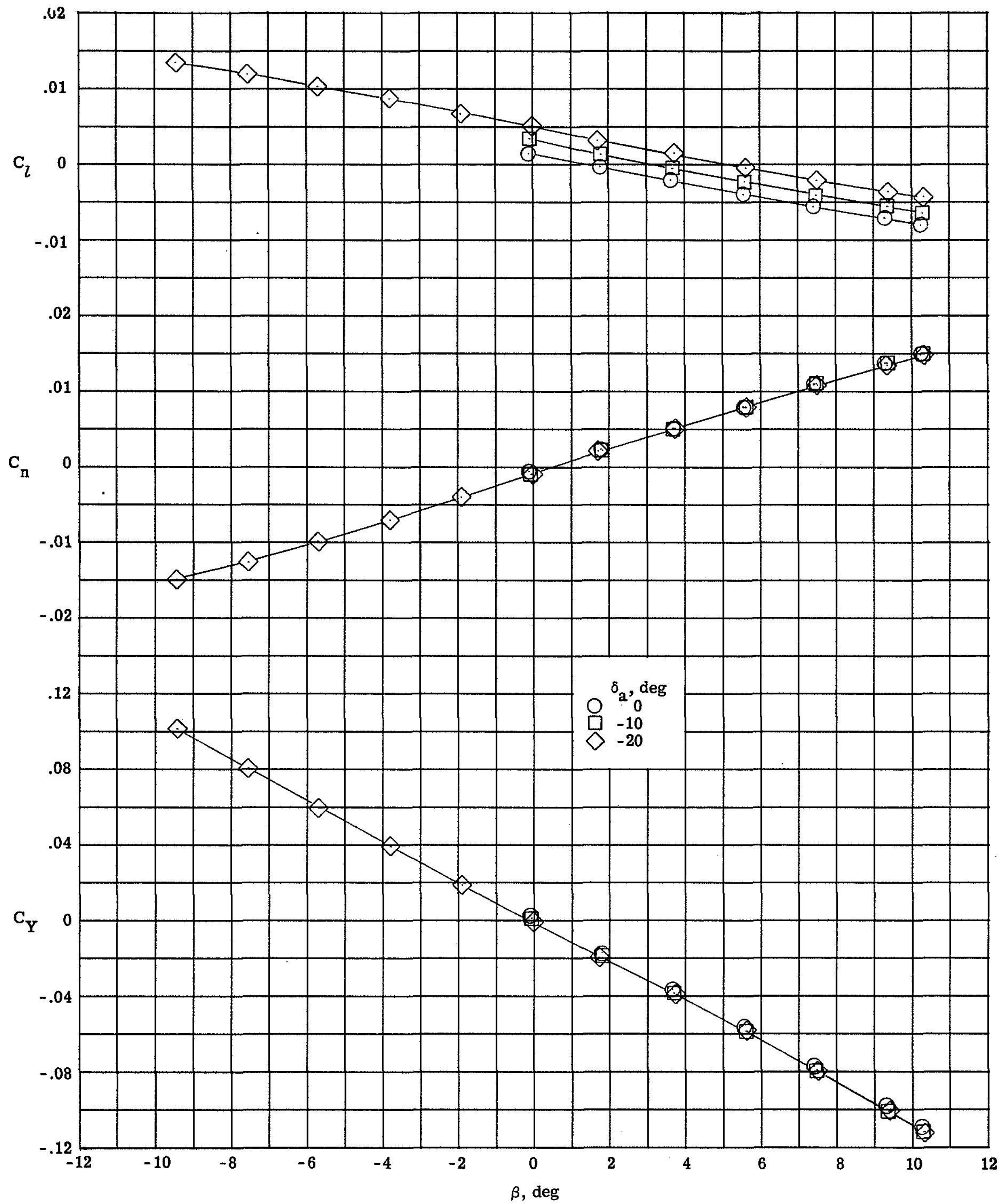

(c) $\alpha = 20.1^0$, straight sting.

Figure 19.- Continued.

[redacted]

[redacted]

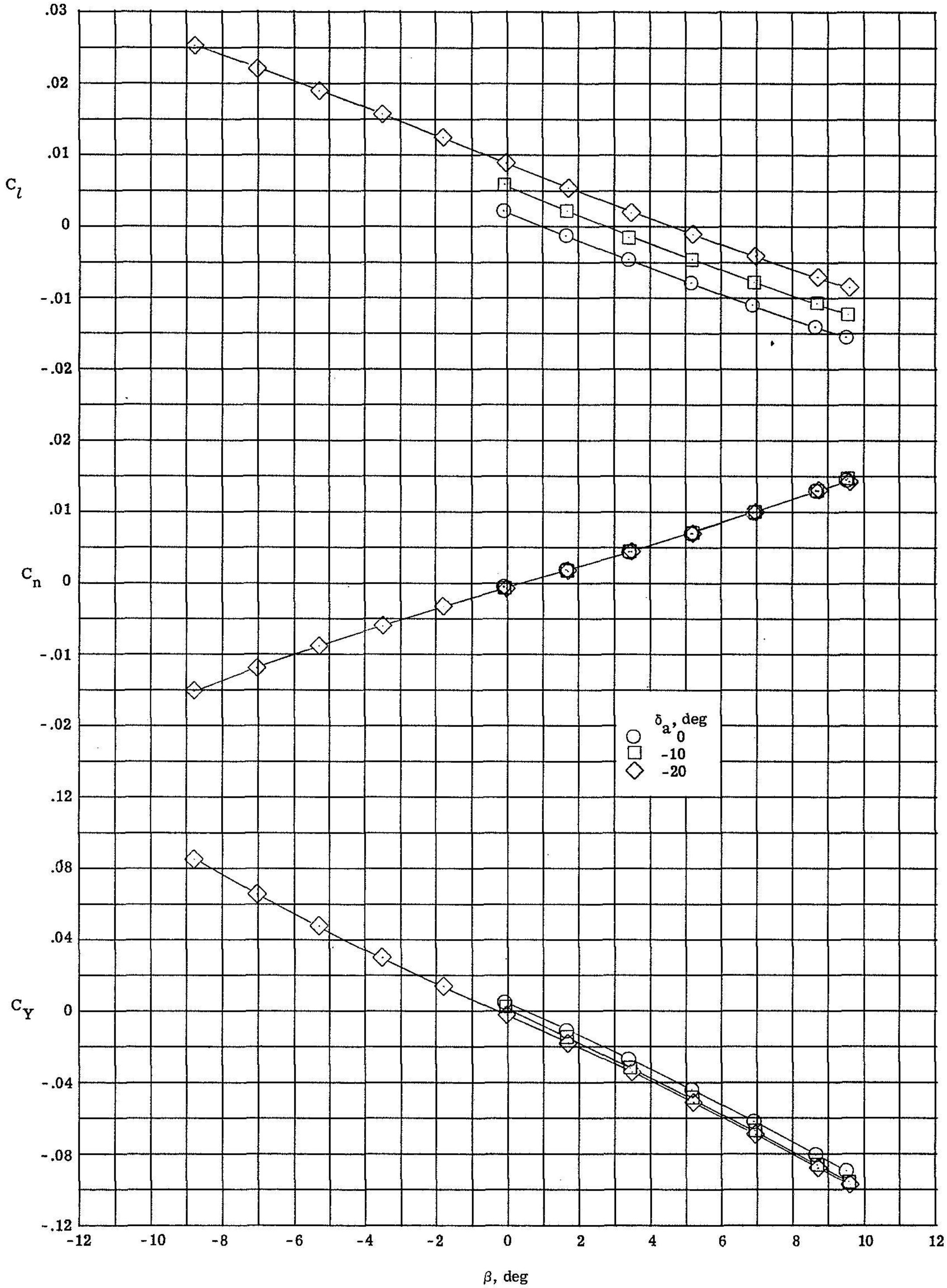

(d) $\alpha = 30.2^0$, straight sting.

Figure 19.- Concluded.

[redacted]

[redacted]

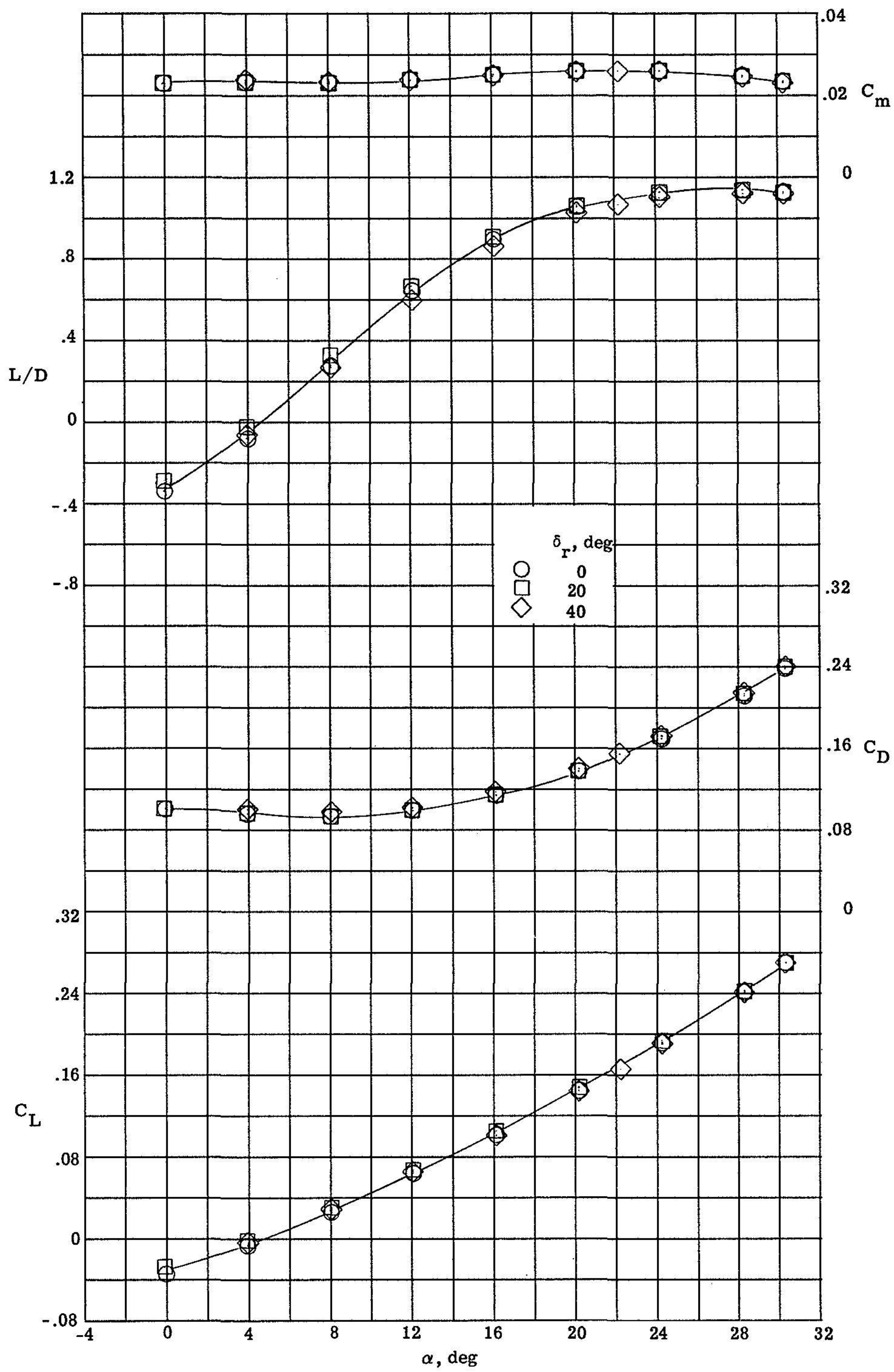

(a) Rudder R_1.

Figure 20.- Effects of rudder deflection on the longitudinal aerodynamic characteristics.

[redacted]

[redacted]

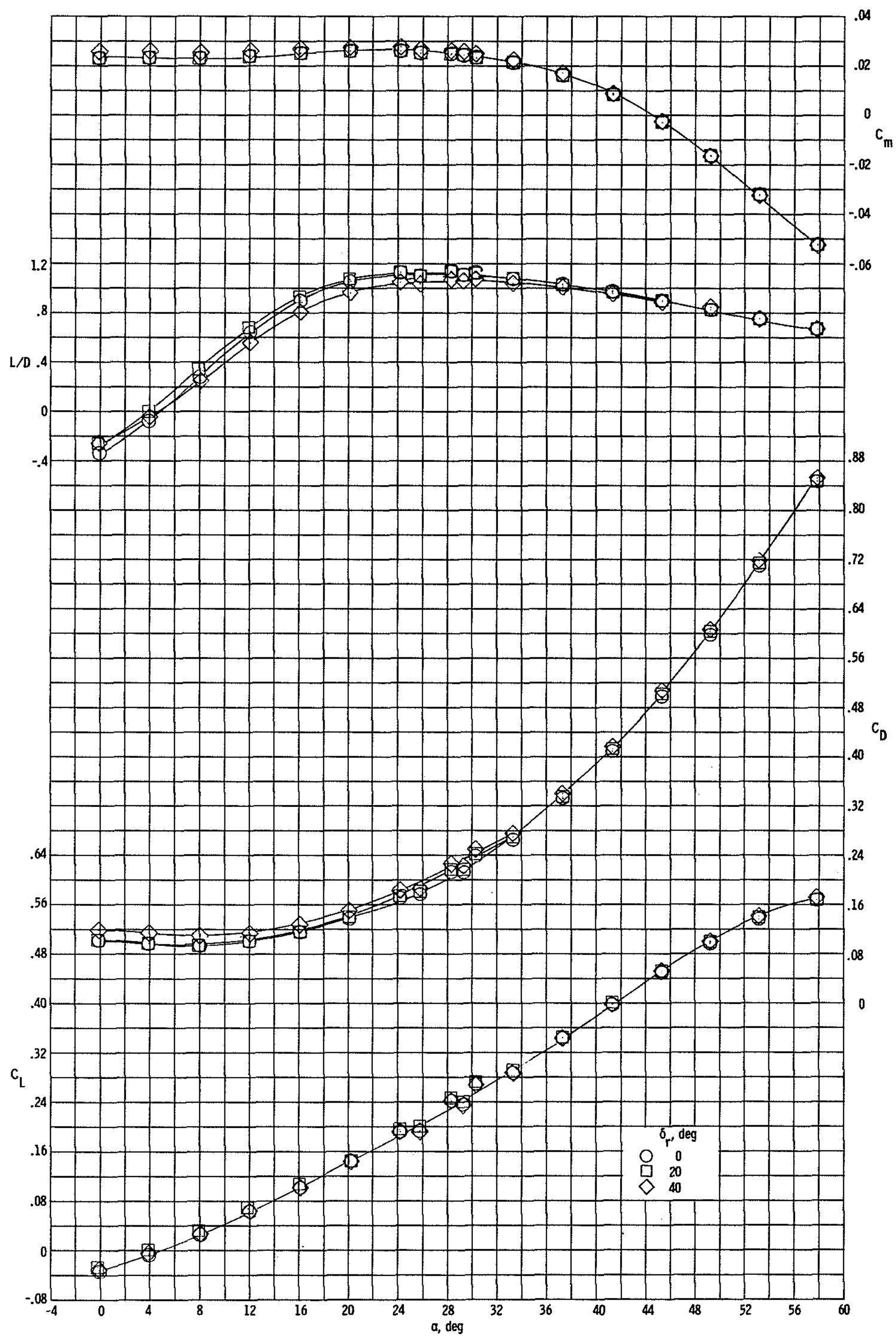

(b) Rudder R_4.

Figure 20.- Continued.

[redacted]

[redacted]

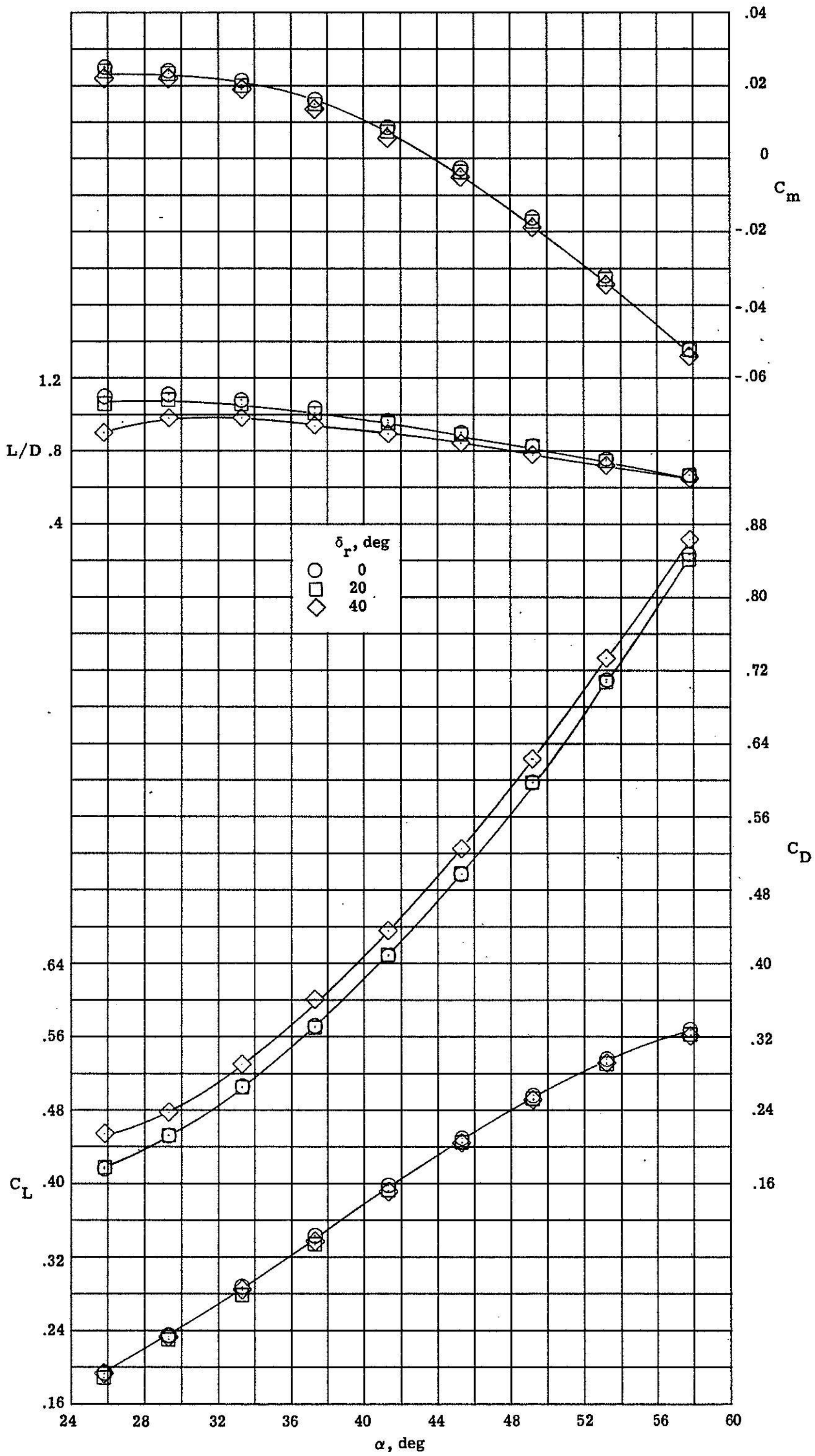

(c) Rudder R_5.

Figure 20.- Concluded.

[redacted]

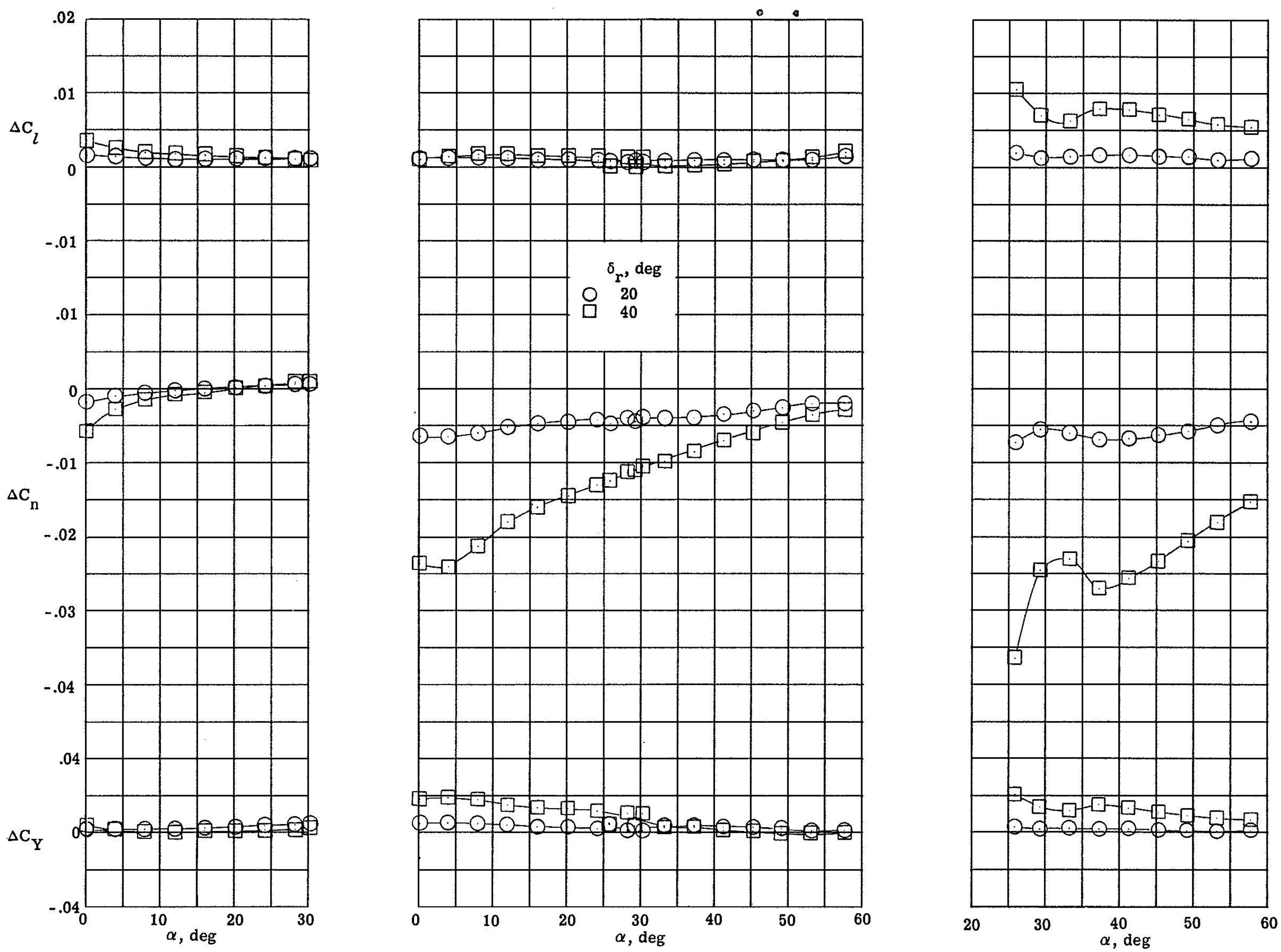

(a) Rudder R_1.

(b) Rudder R_4.

(c) Rudder R_5.

Figure 21.- Directional control characteristics of the rudders tested.

[redacted]

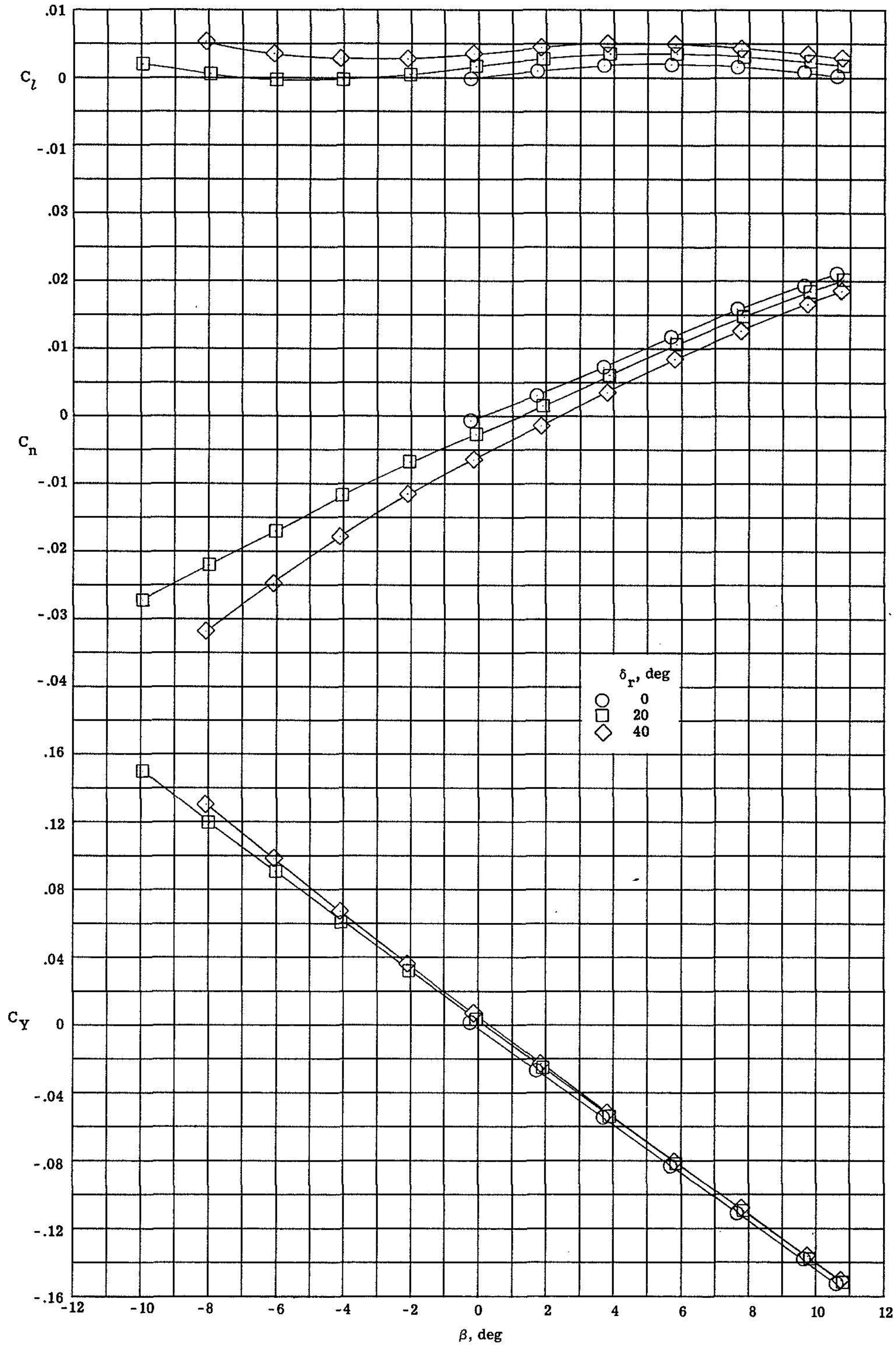

(a) α = -0.1°, straight sting.

Figure 22.- Variation of directional and lateral characteristics with sideslip angle for various deflection angles of center fin rudder, R_1.

[redacted]

[redacted]

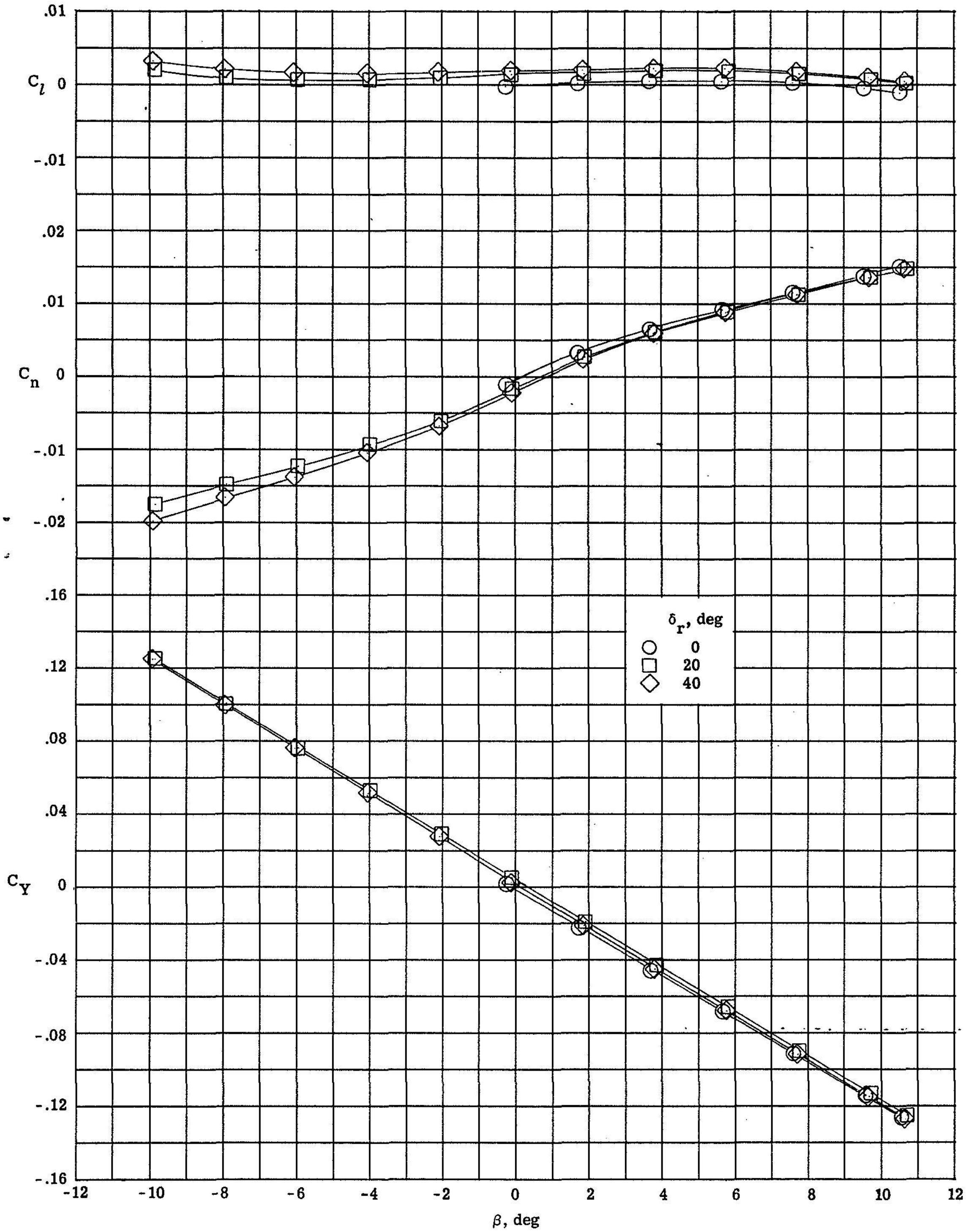

(b) $\alpha = 10.0^0$, straight sting.

Figure 22.- Continued.

[redacted]

[redacted]

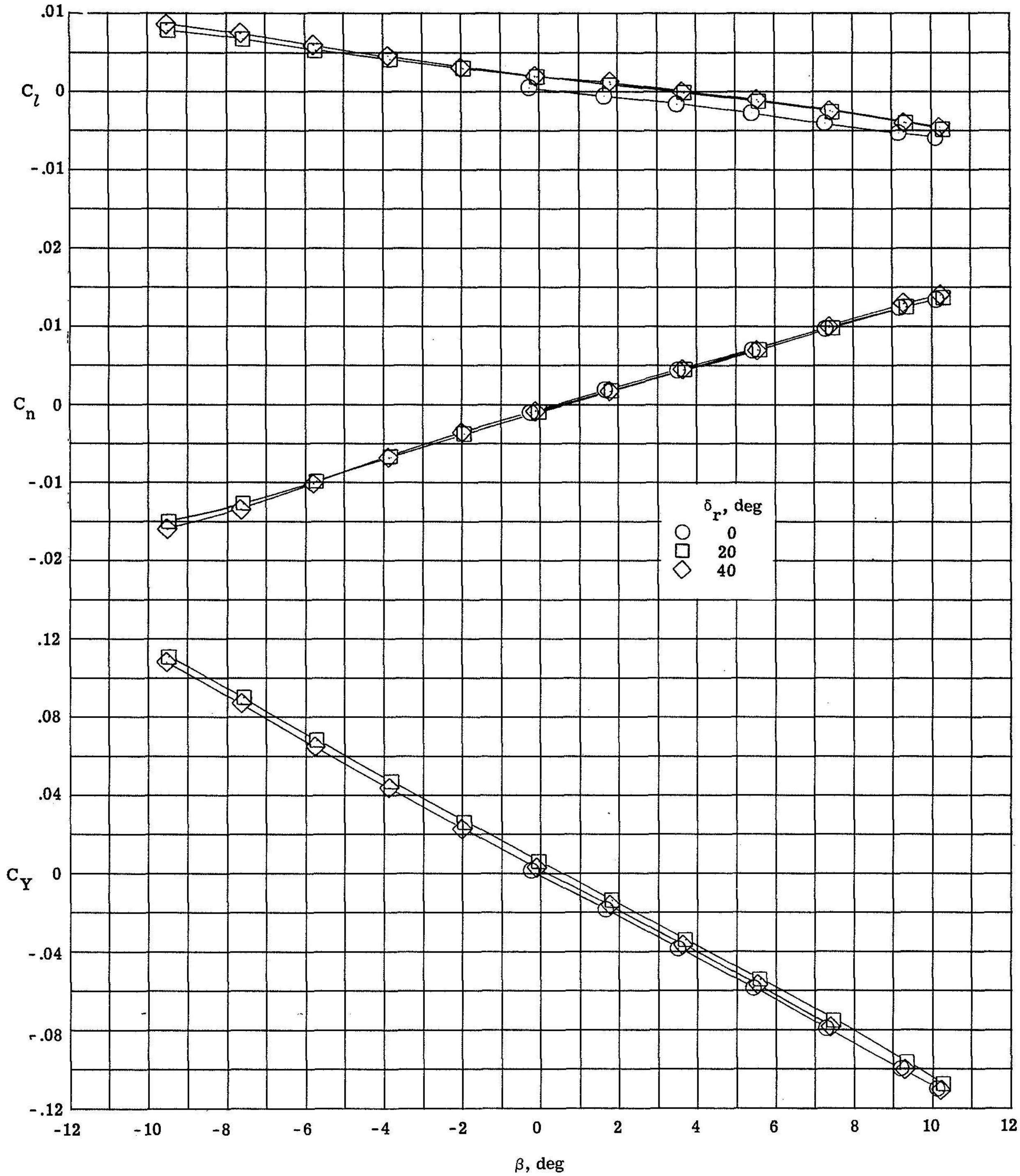

(c) α = 20.2^o, straight sting.

Figure 22.- Continued.

[redacted]

[redacted]

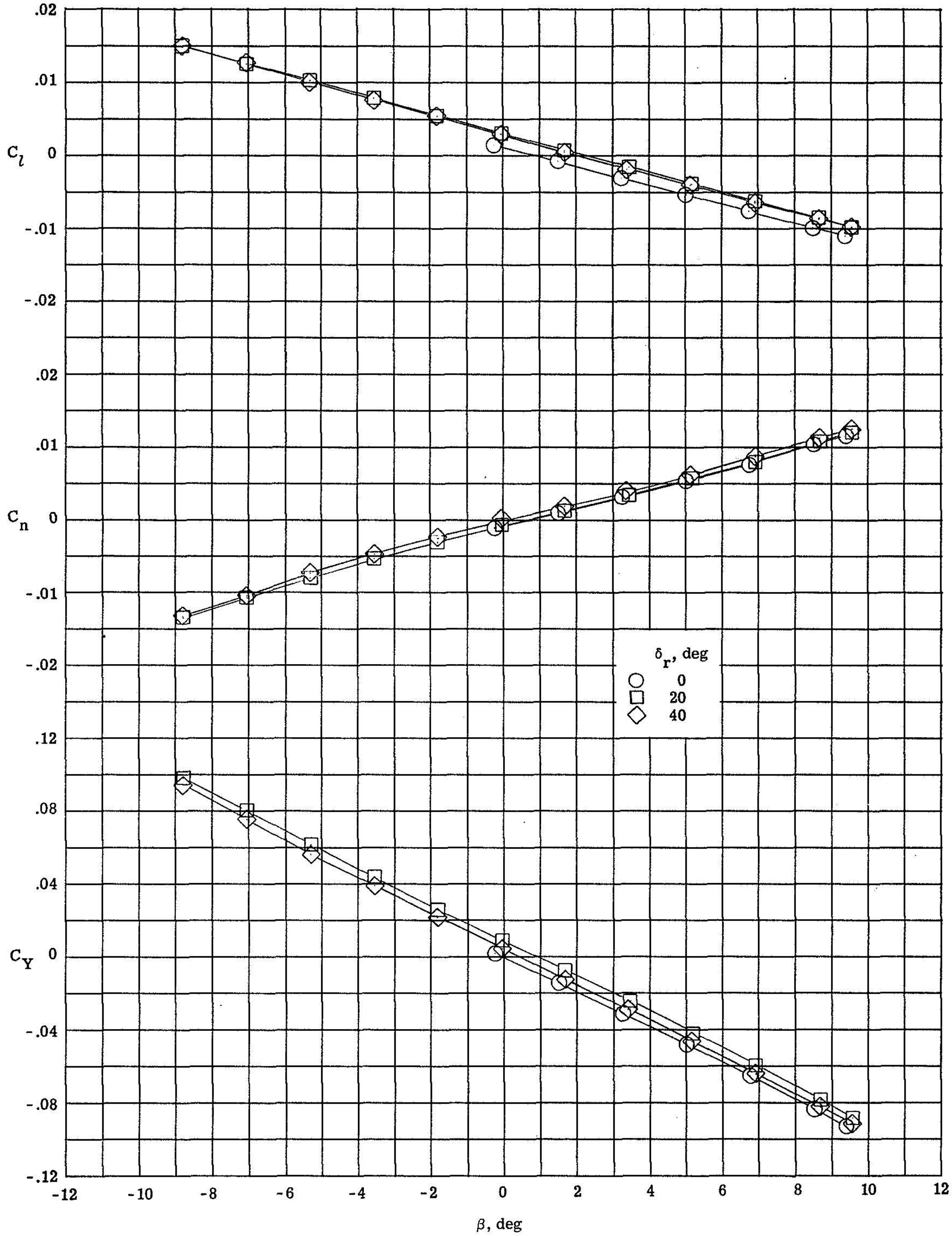

(d) $\alpha = 30.3^0$, straight sting.

Figure 22.- Concluded.

[redacted]

[redacted]

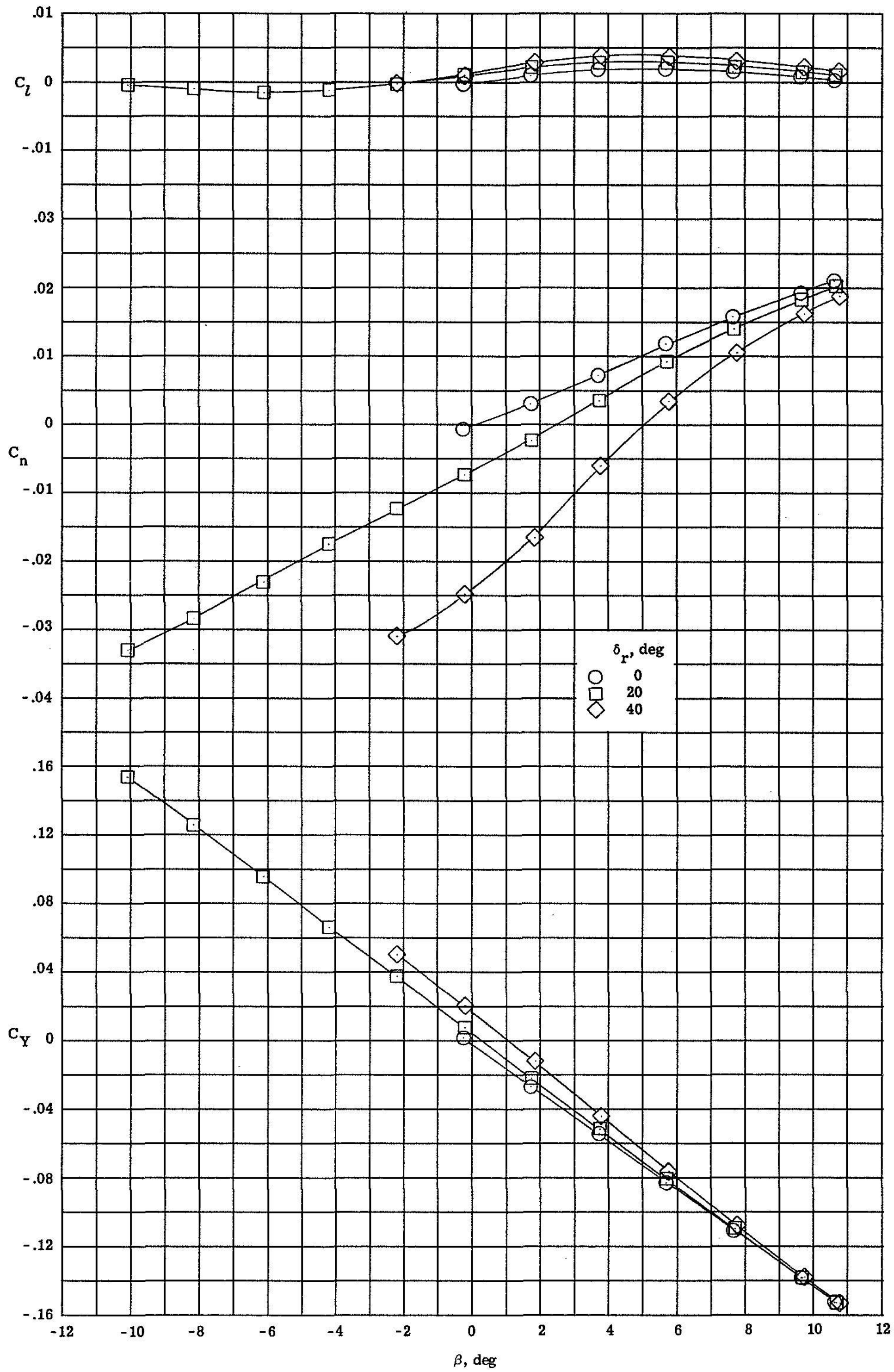

(a) $\alpha = -0.1^{0}$, straight sting.

Figure 23.- Variation of directional and lateral characteristics with sideslip angle for various deflection angles of the tip-fin rudder, R_4.

[redacted]

[redacted]

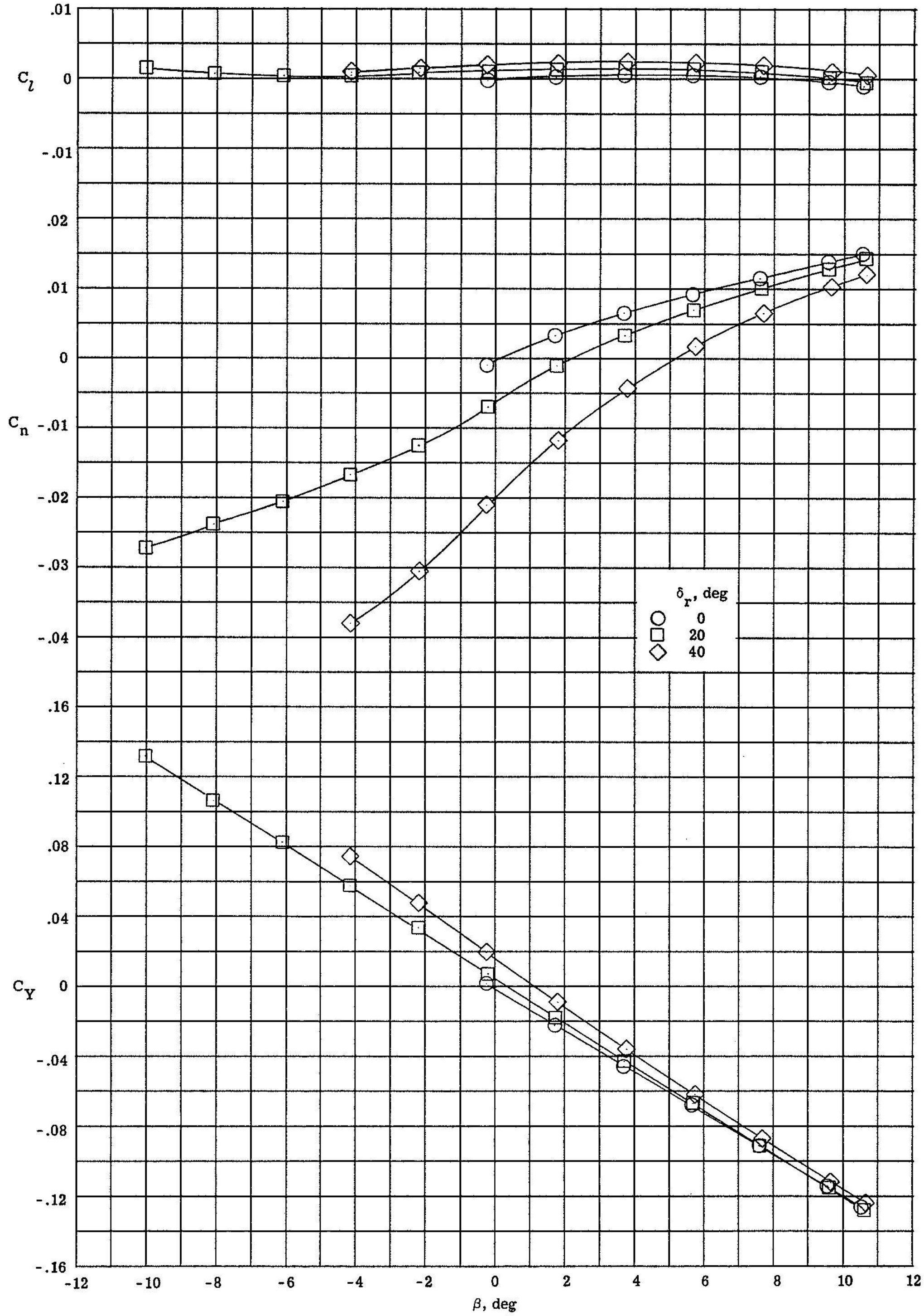

(b) $\alpha = 10.0^0$, straight sting.

Figure 23.- Continued.

[redacted]

[redacted]

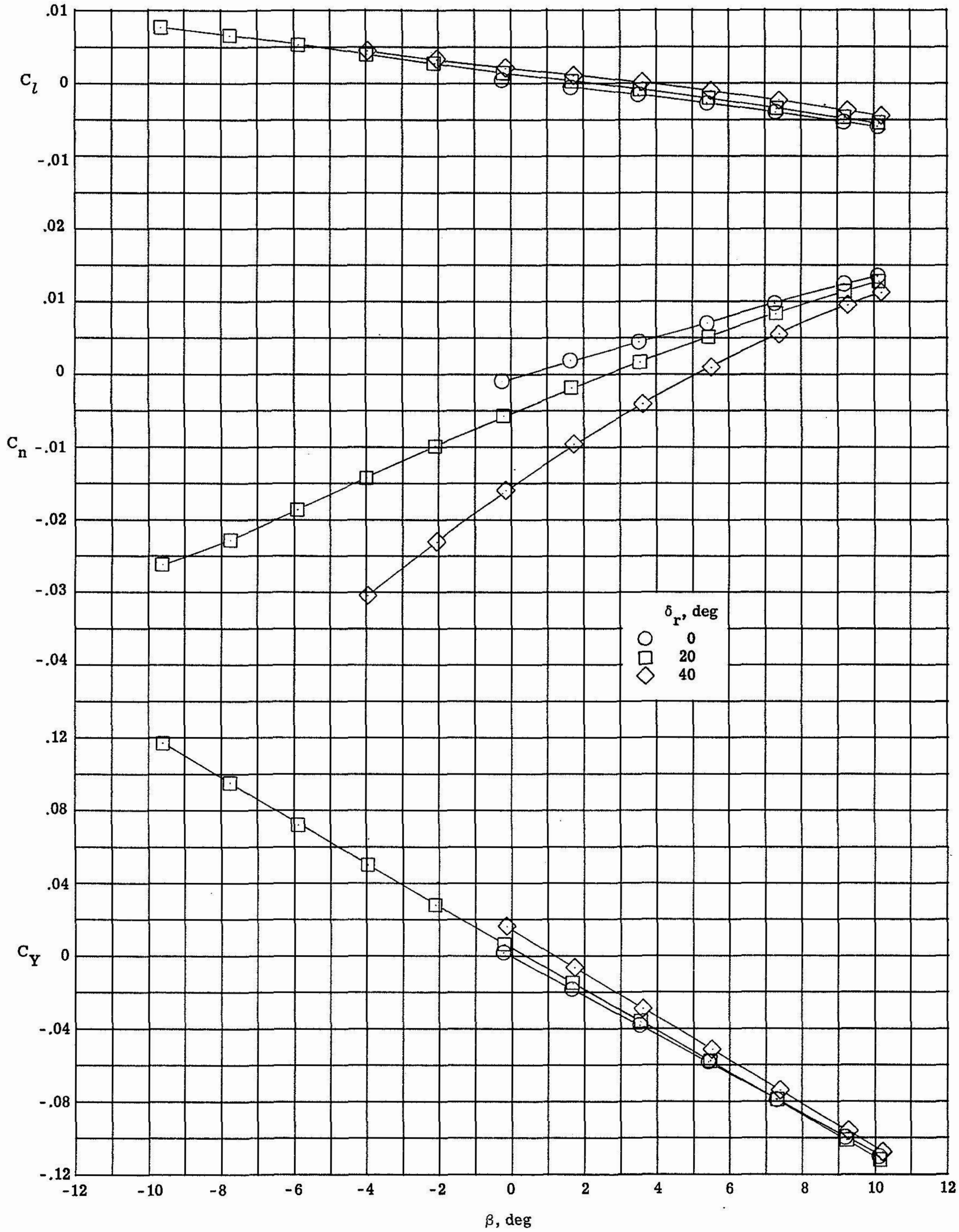

(c) $\alpha = 20.2^o$, straight sting.

Figure 23.- Continued.

[redacted]

[redacted]

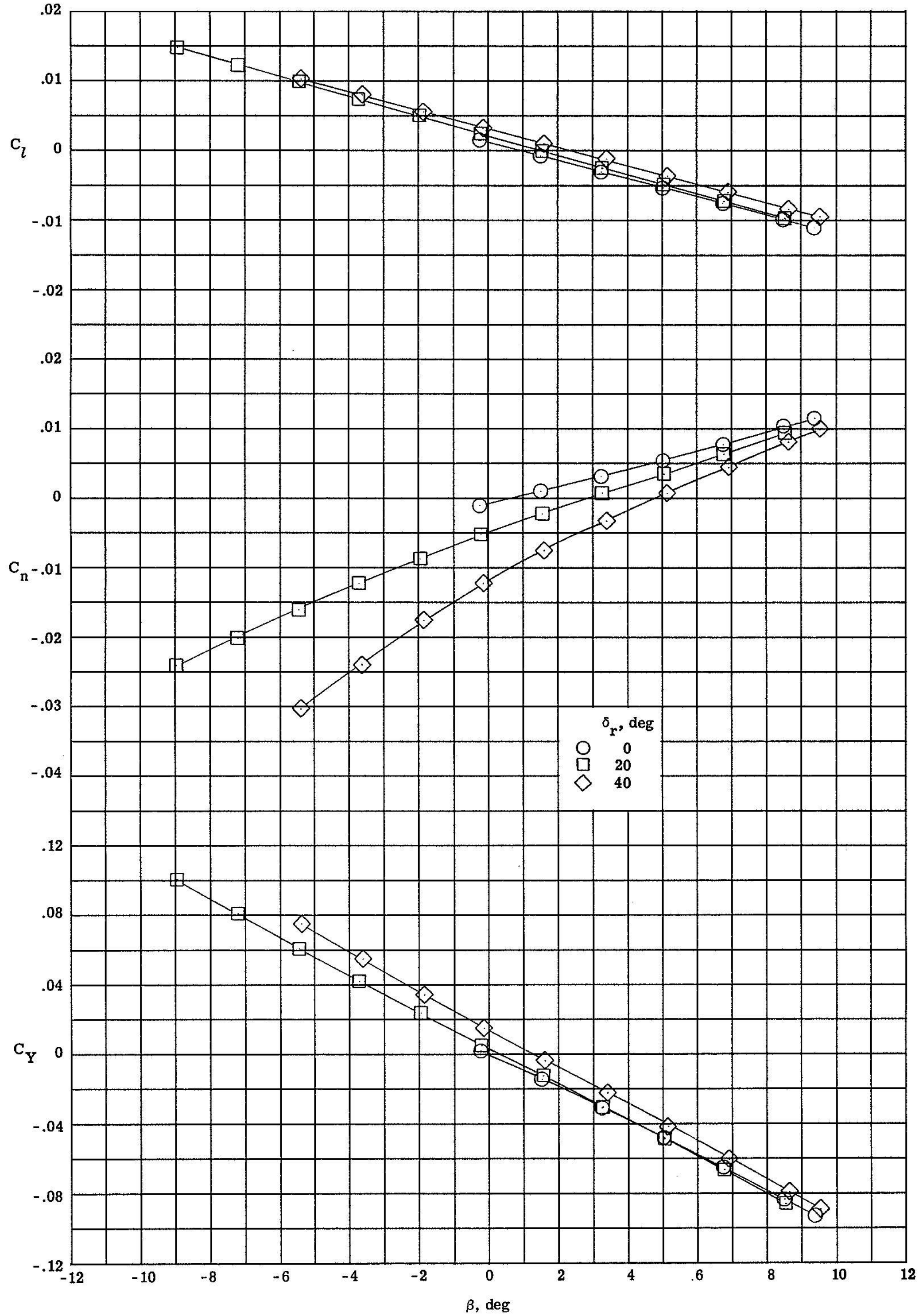

(d) $\alpha = 30.3^{\circ}$, straight sting.

Figure 23.- Continued.

[redacted]

[redacted]

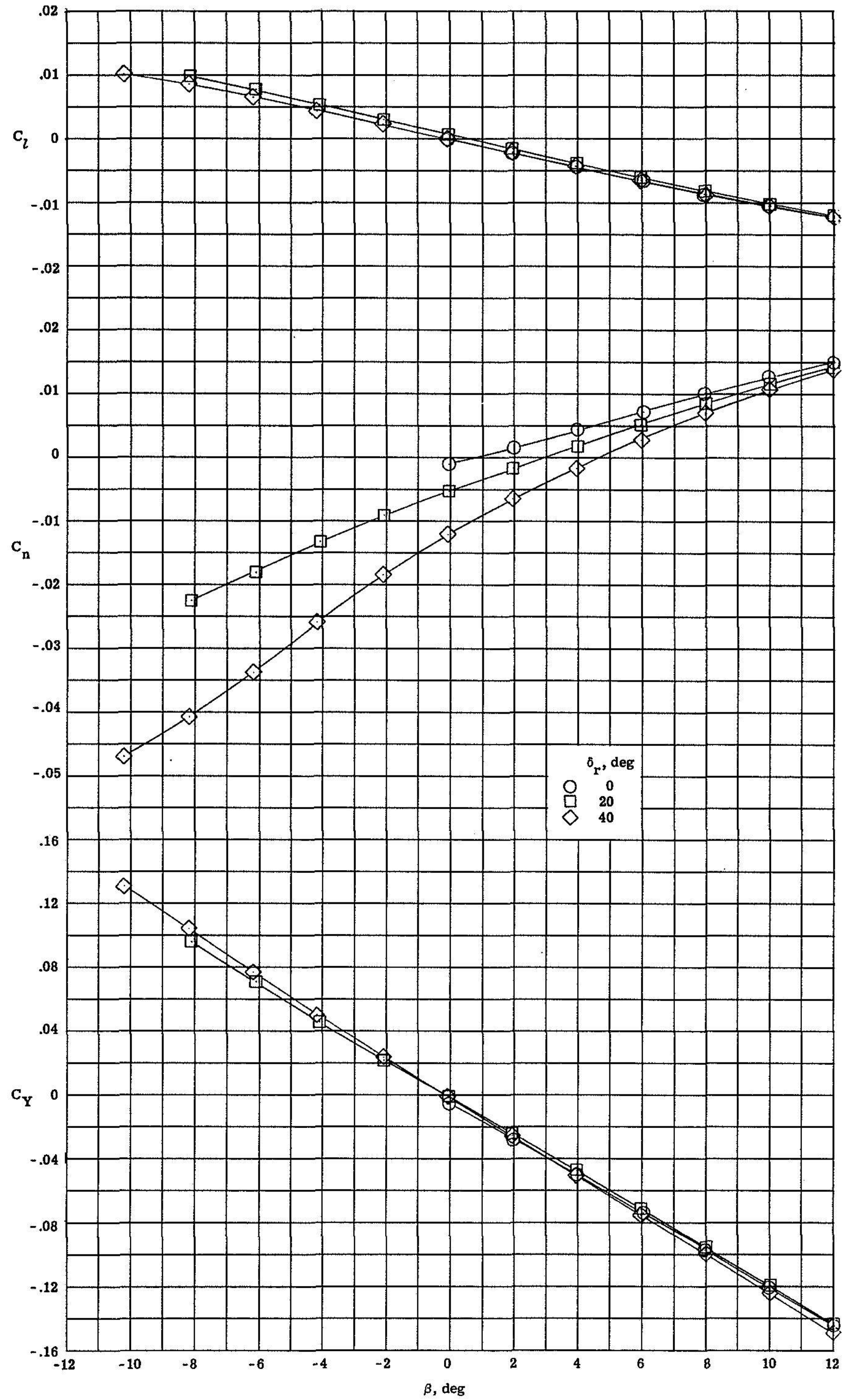

(e) $\alpha = 29.3^{\circ}$, bent sting.

Figure 23.- Continued.

[redacted]

[redacted]

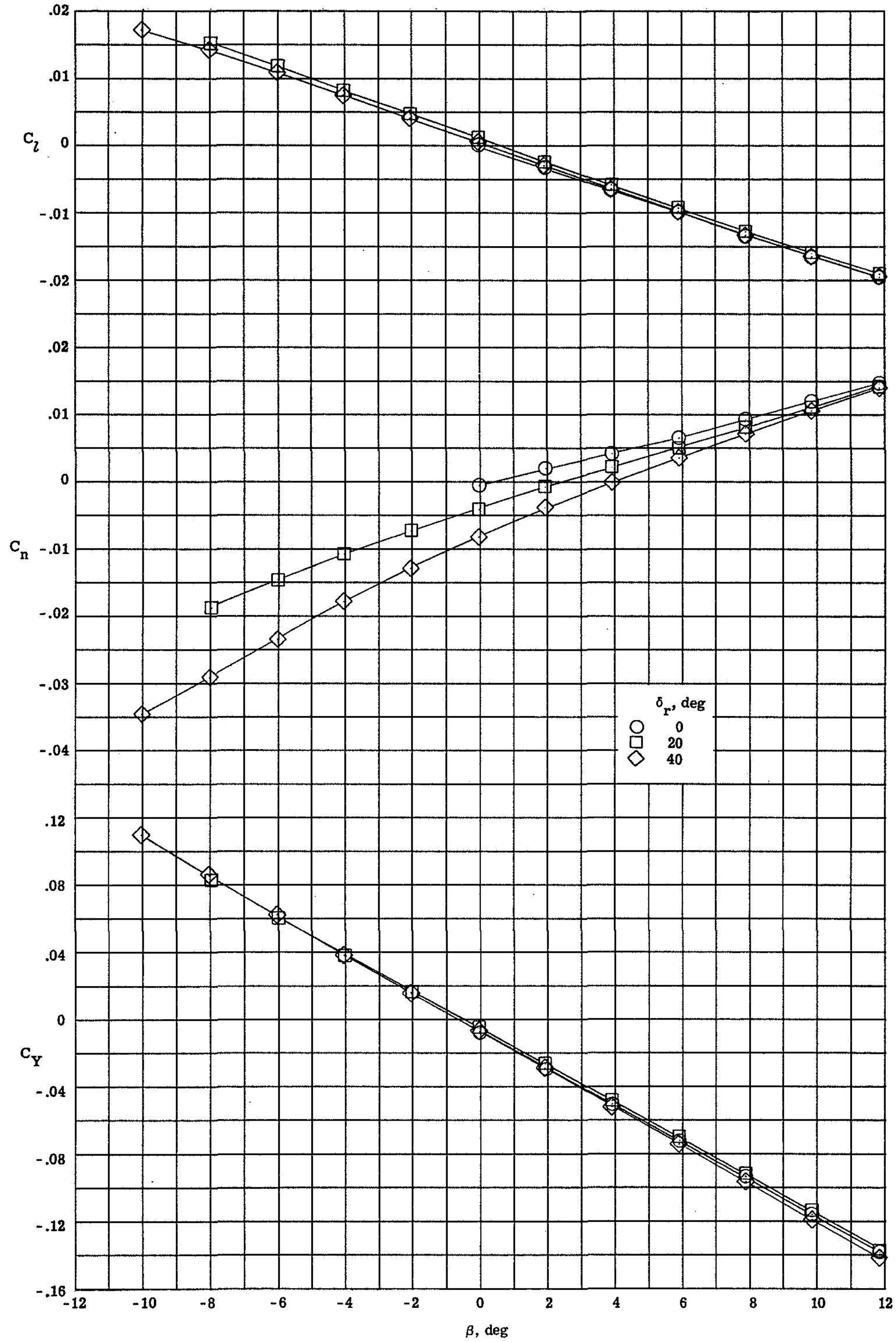

(f) $\alpha = 39.3^0$, bent sting.

Figure 23.- Continued.

[redacted]

[redacted]

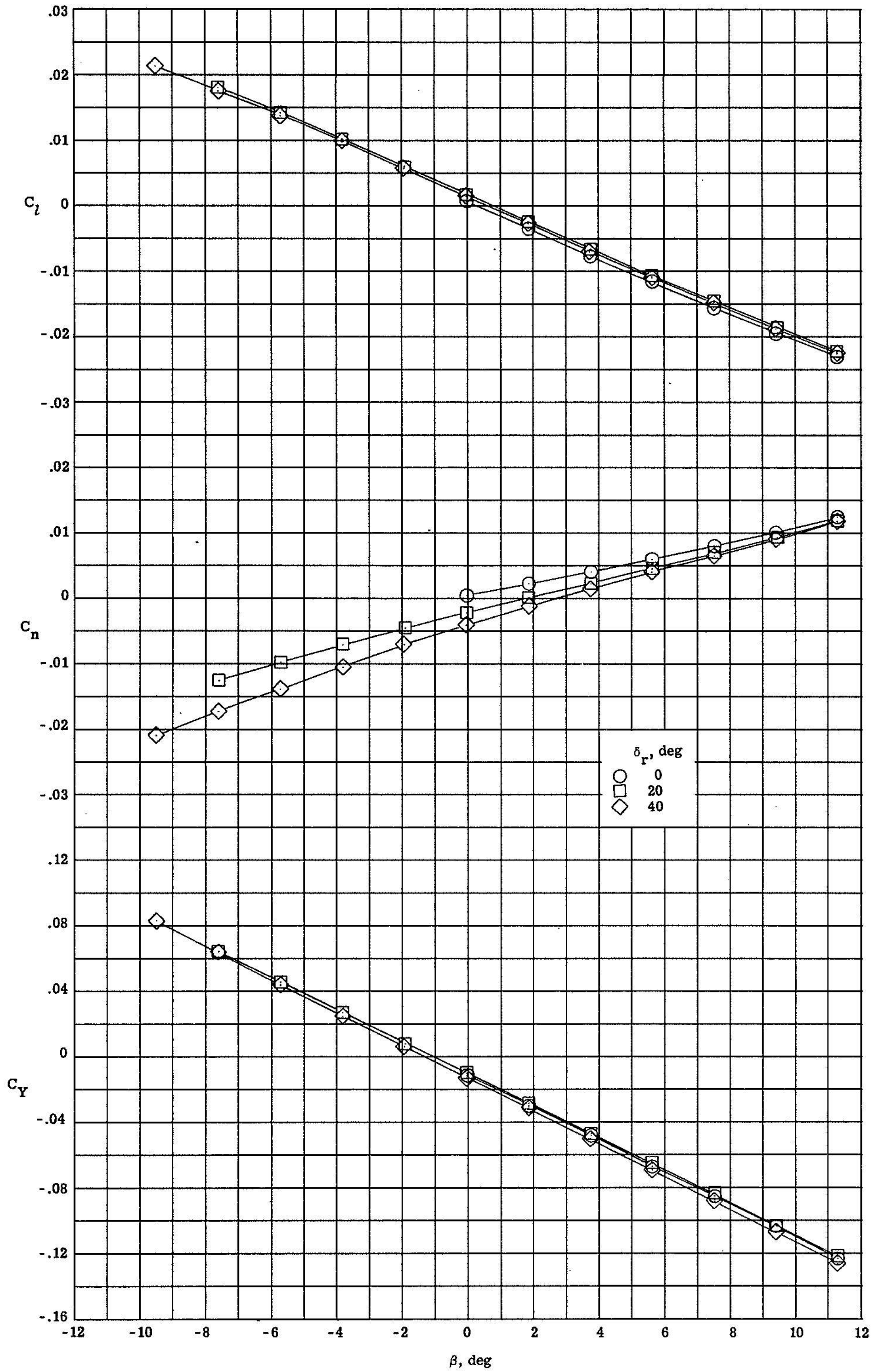

(g) $\alpha = 49.3^0$, bent sting.

Figure 23.- Continued.

[redacted]

[redacted]

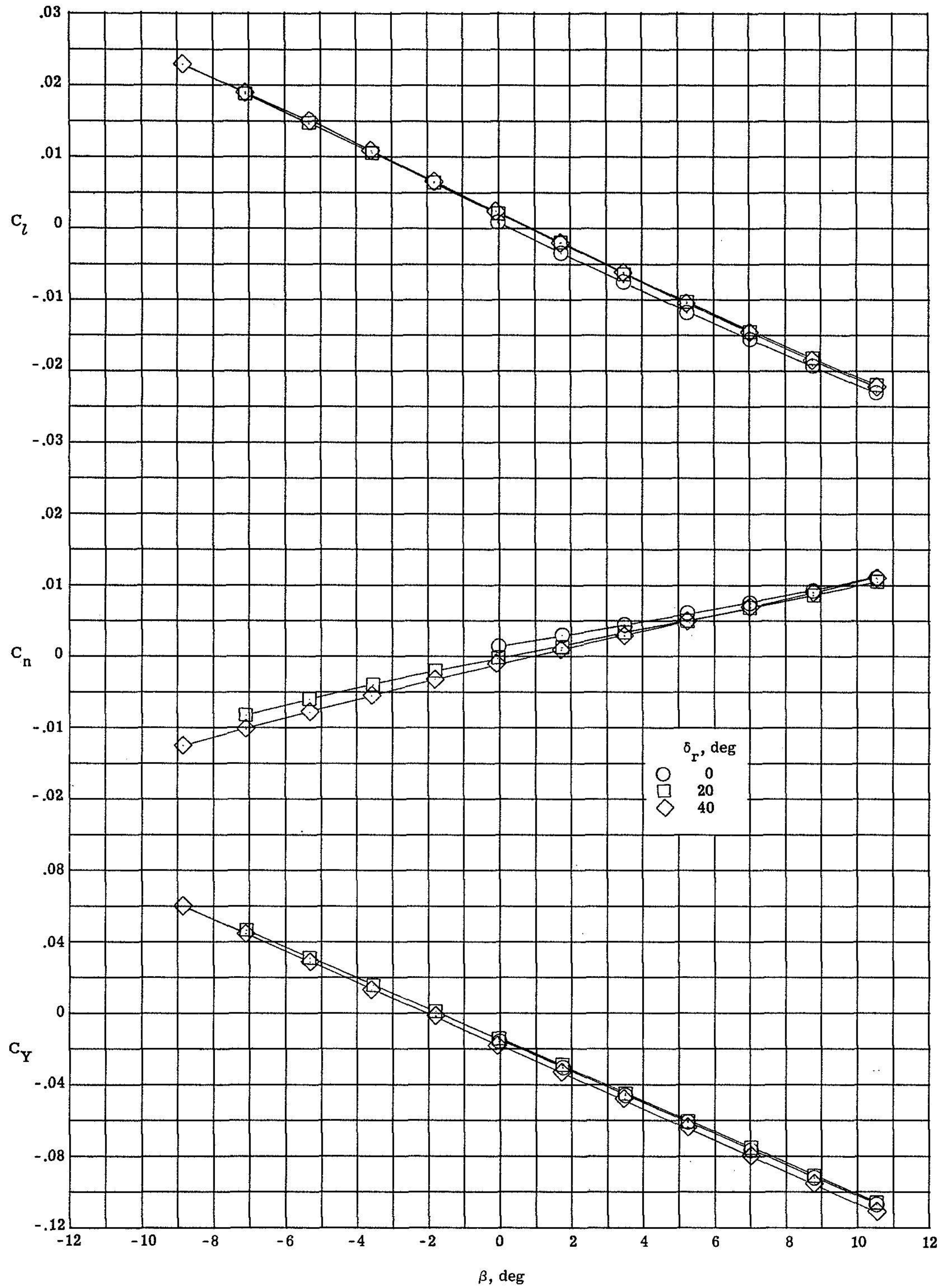

(h) $\alpha = 57.7^{0}$, bent sting.

Figure 23.- Concluded.

[redacted]

[redacted]

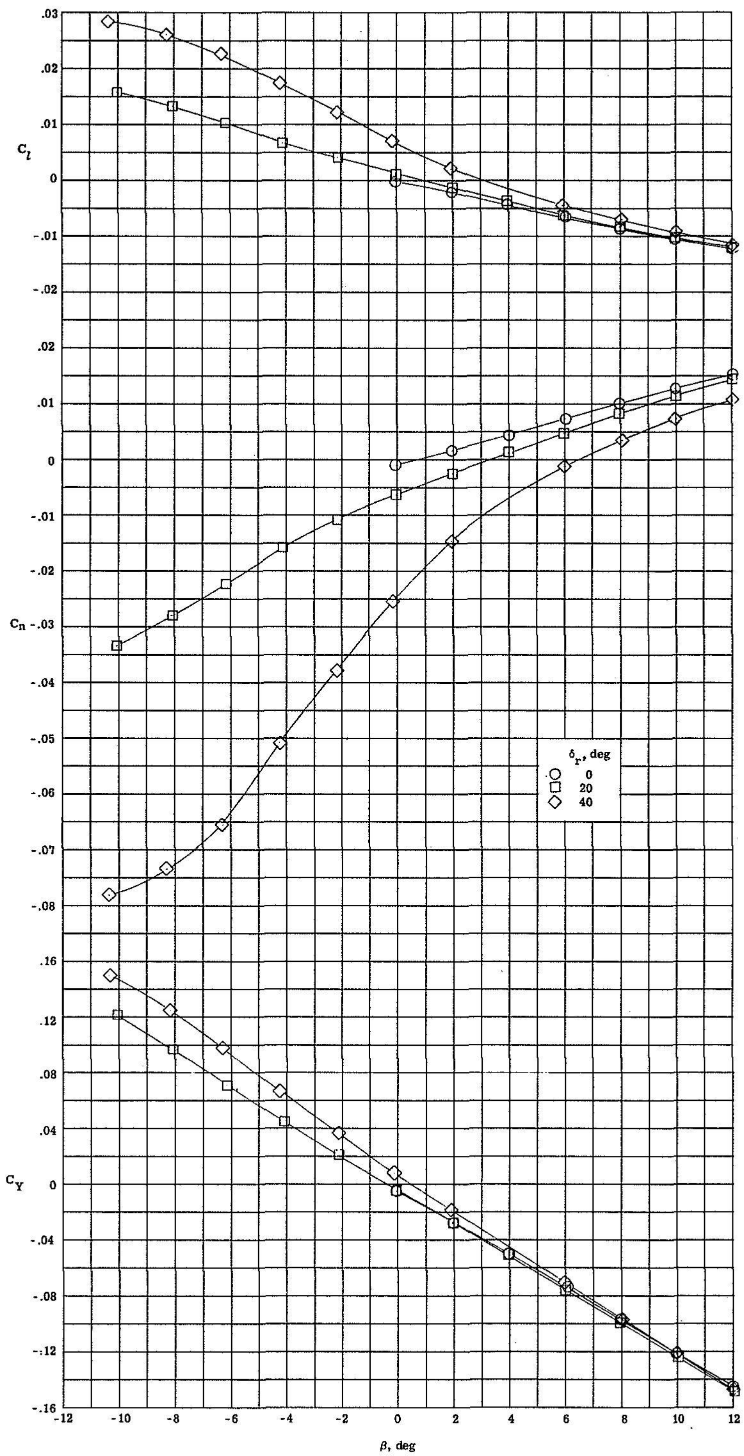

(a) $\alpha = 29.3^{\circ}$, bent sting.

Figure 24.- Variation of directional and lateral characteristics with sideslip angle for various deflection angles of the tip-fin rudder, R_5.

[redacted]

[redacted]

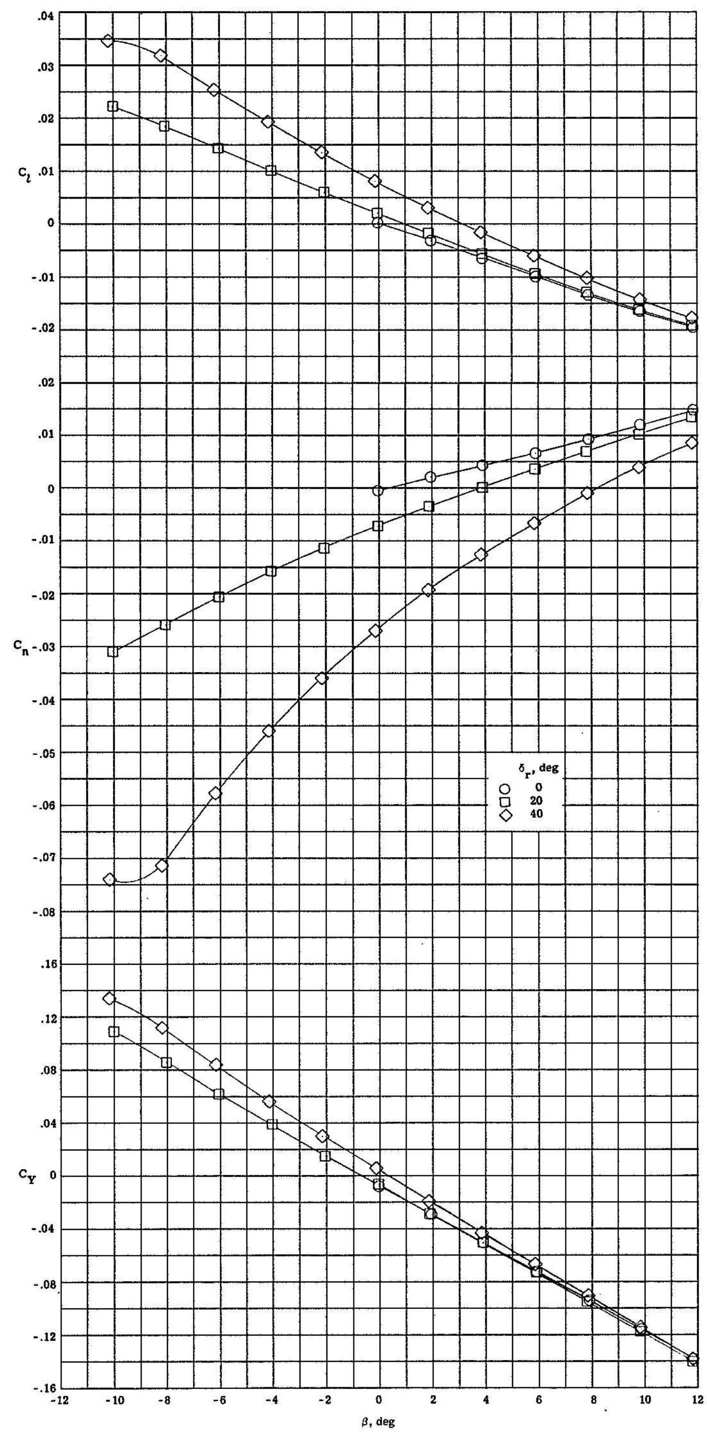

(b) $\alpha = 39.3^0$, bent sting.

Figure 24.- Continued.

[redacted]

[redacted]

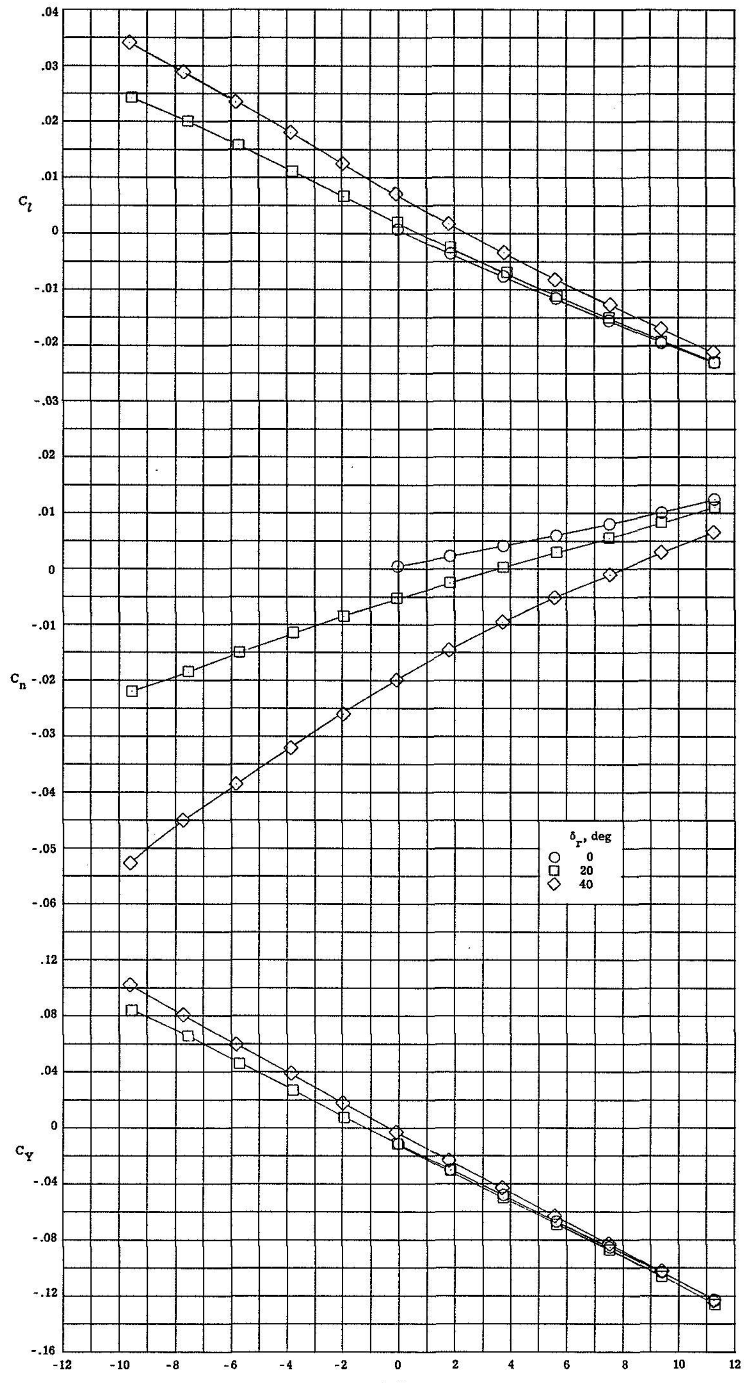

(c) $\alpha = 49.3^0$, bent sting.

Figure 24.- Continued.

[redacted]

[redacted]

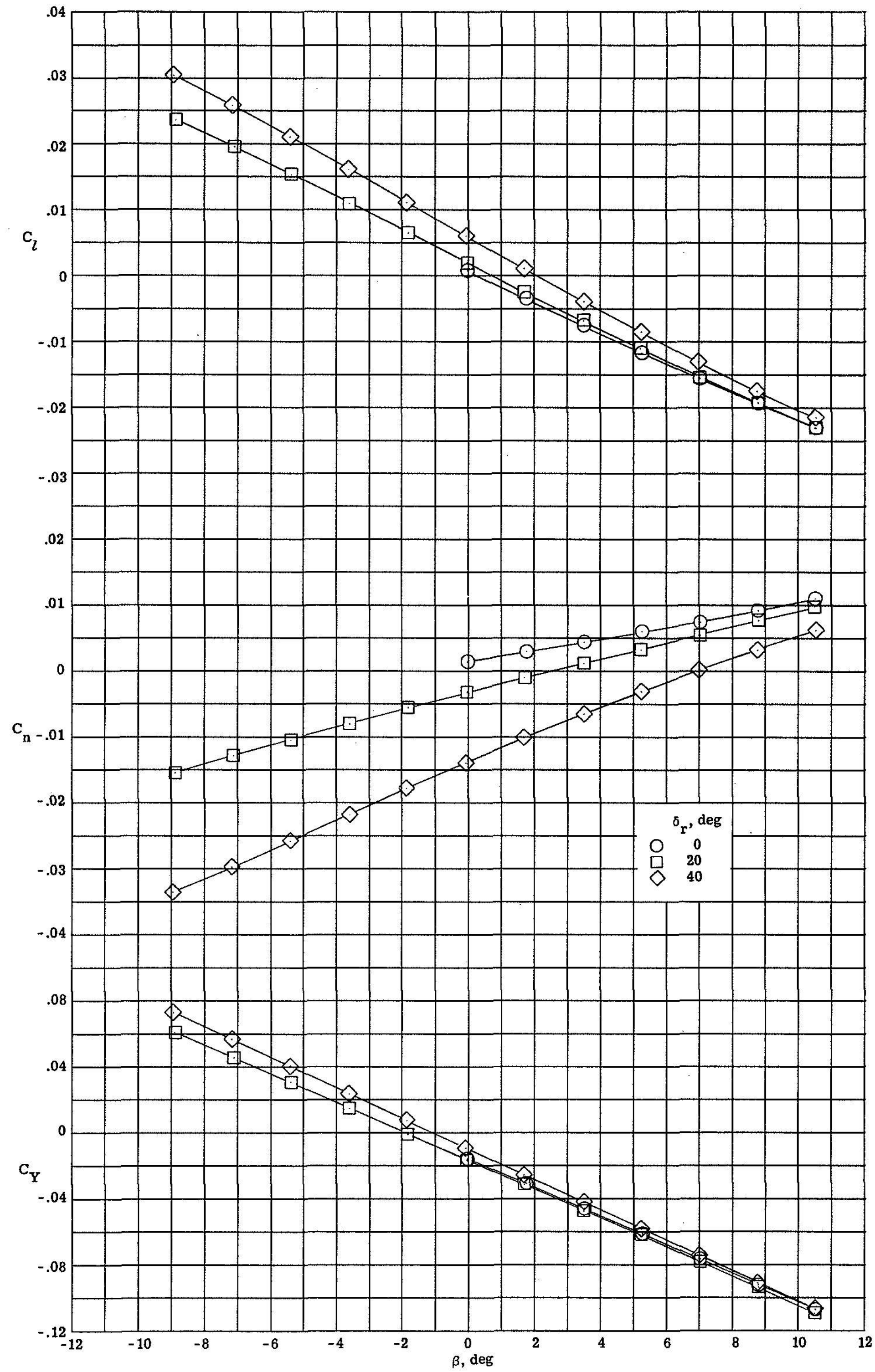

(d) α = 57.7°, bent sting.

Figure 24.- Concluded.

[redacted]

[redacted]

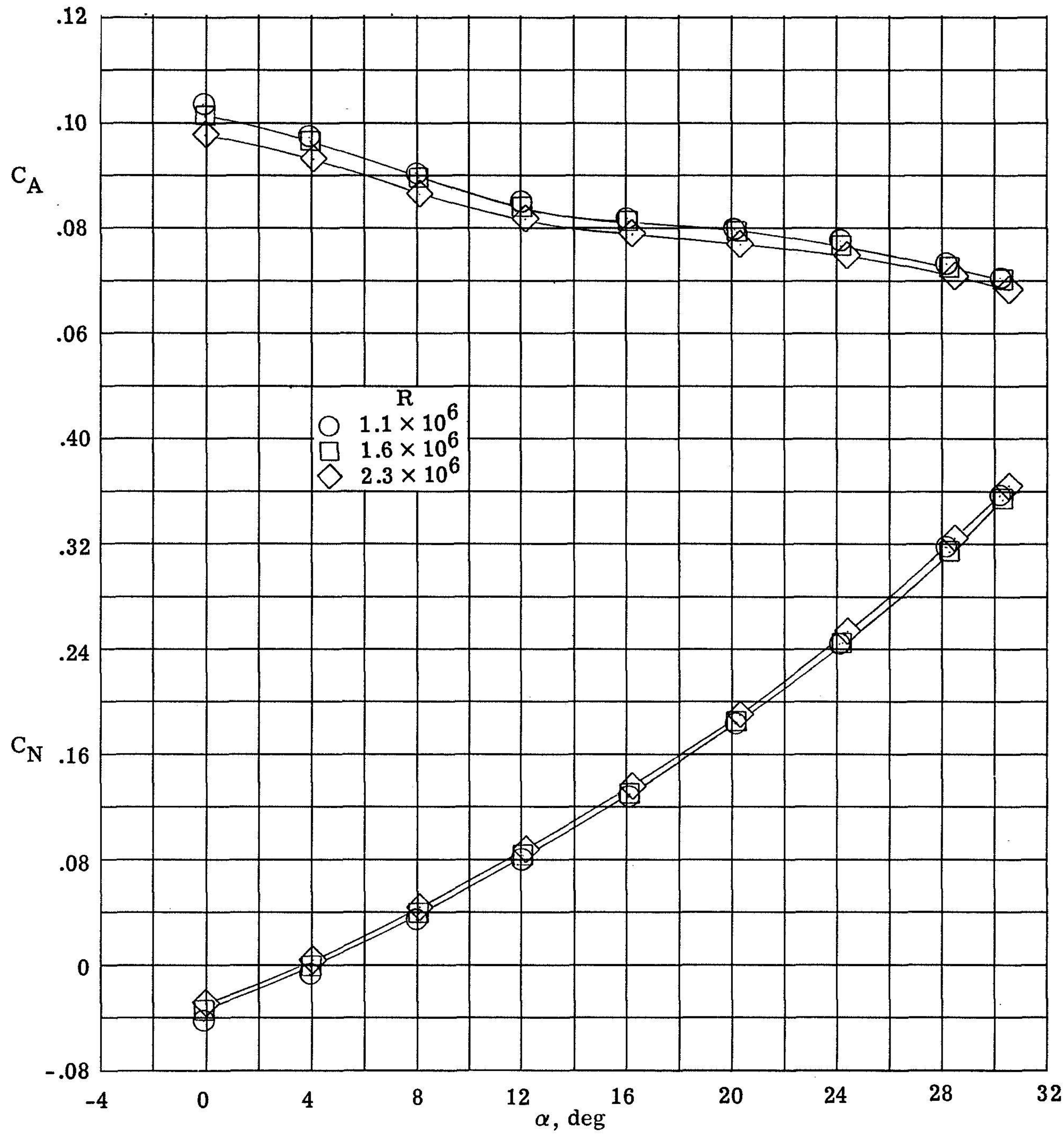

(a) $\delta_e = 0^o$.

Figure 25.- Effects of Reynolds number on the body-axis longitudinal characteristics for various elevon deflection angles.

[redacted]

[redacted]

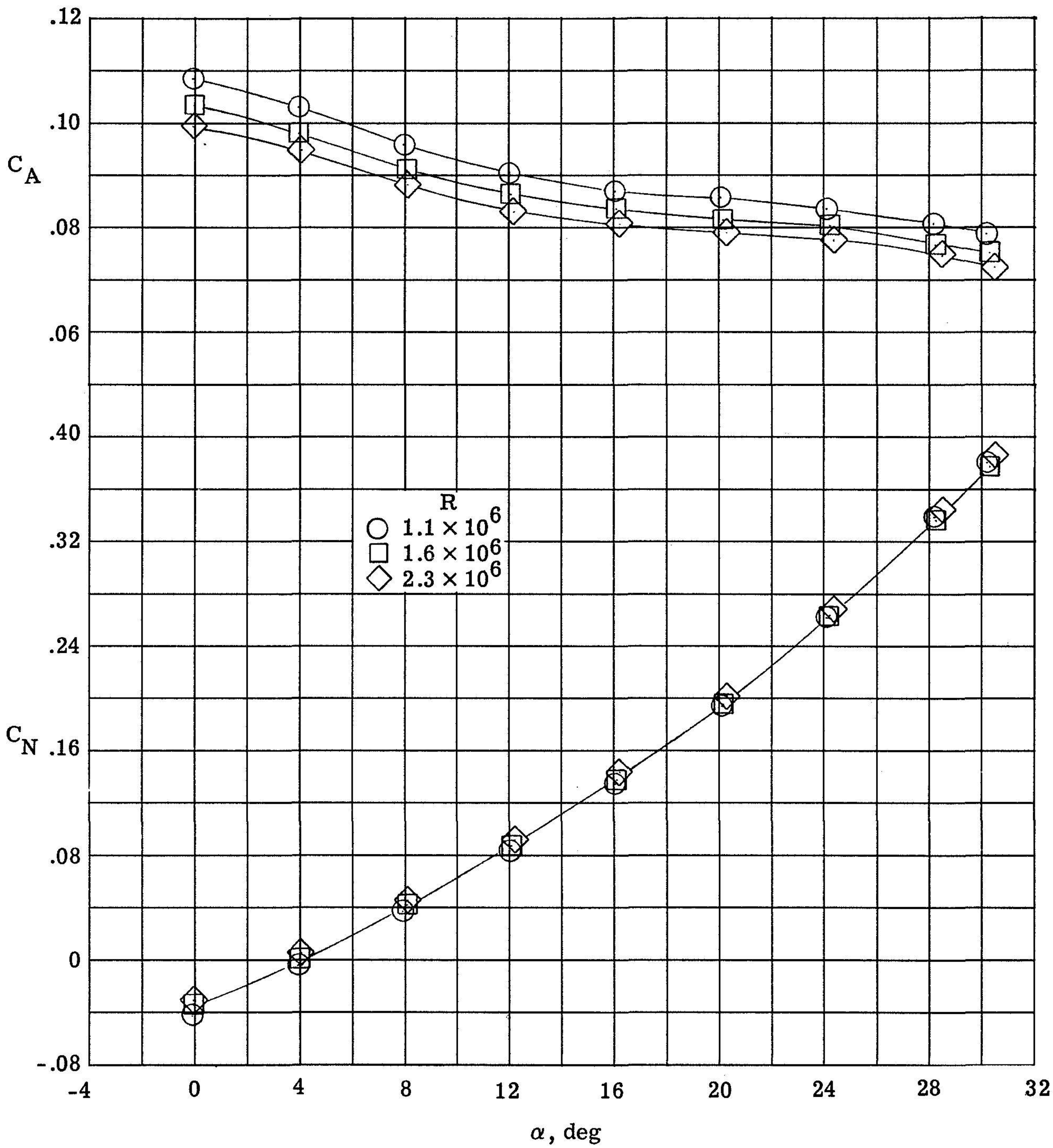

(b) $\delta_e = 15^0$.

Figure 25.- Continued.

[redacted]

[redacted]

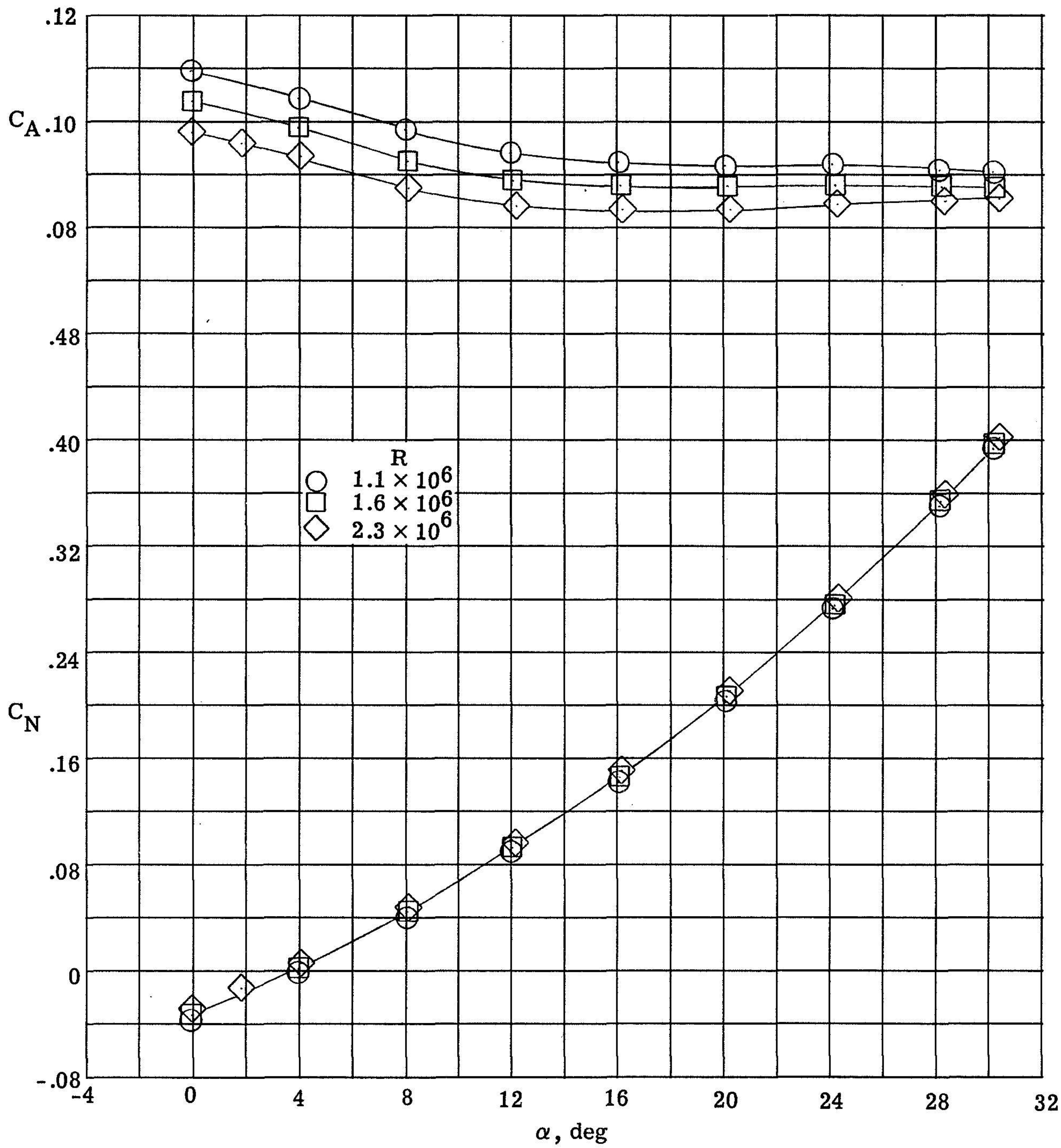

(c) $\delta_e = 30^o$.

Figure 25.- Continued.

[redacted]

[redacted]

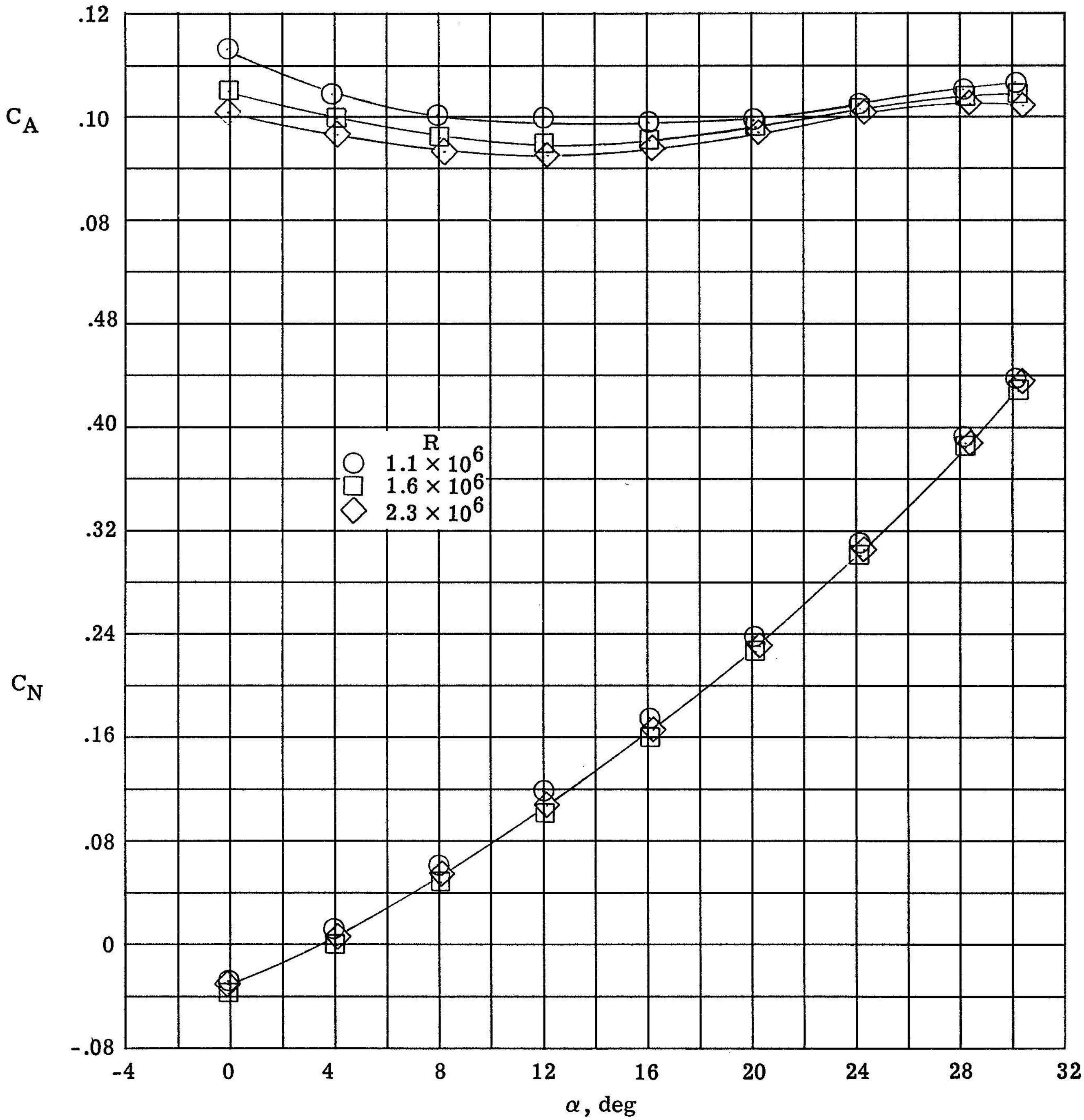

(d) $\delta_e = 45^0$.

Figure 25.- Concluded.

[redacted]

[redacted]

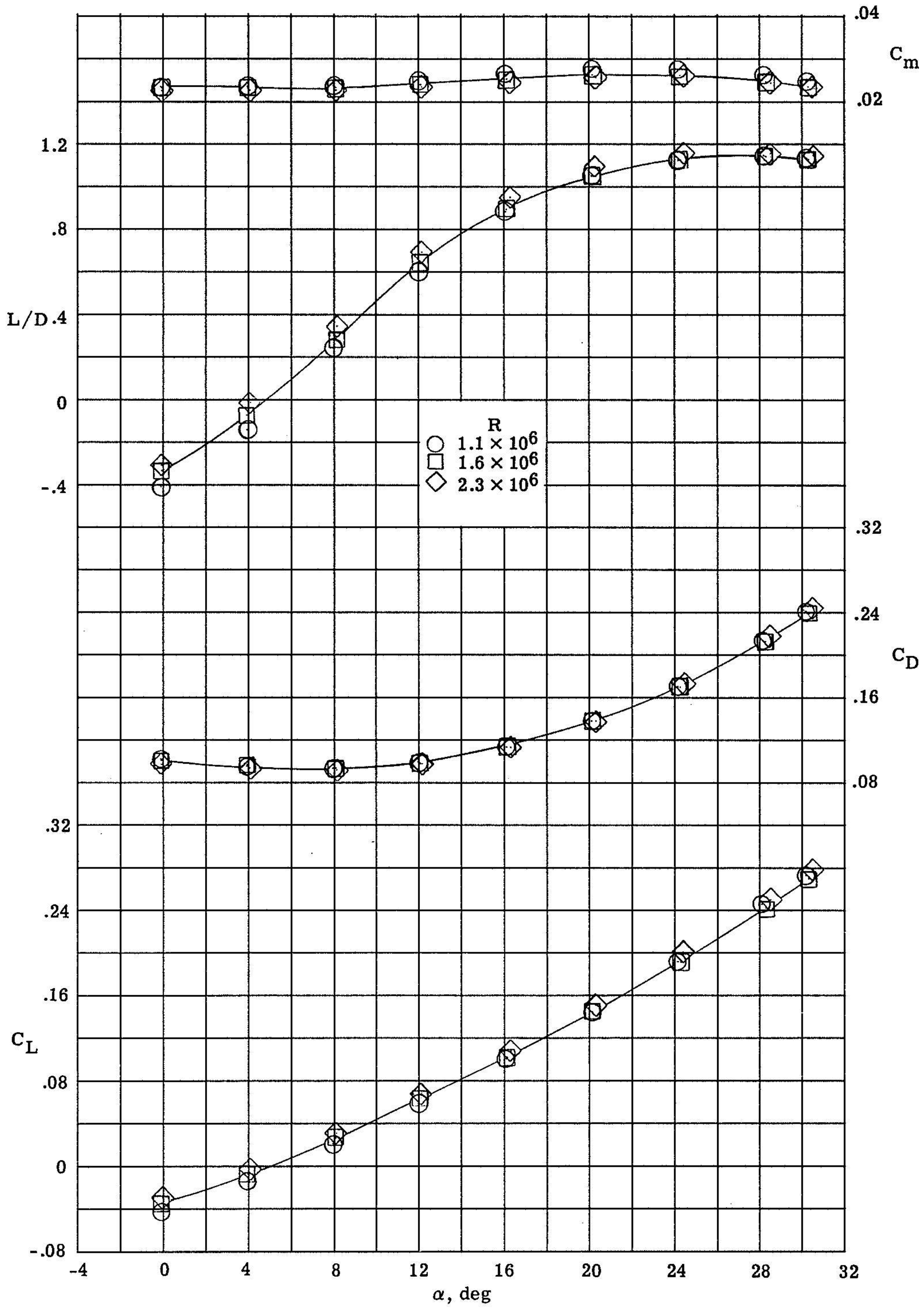

(a) $\delta_e = 0^{0}$.

Figure 26.- Effects of Reynolds number on the stability-axis longitudinal characteristics for various elevon deflection angles.

[redacted]

[redacted]

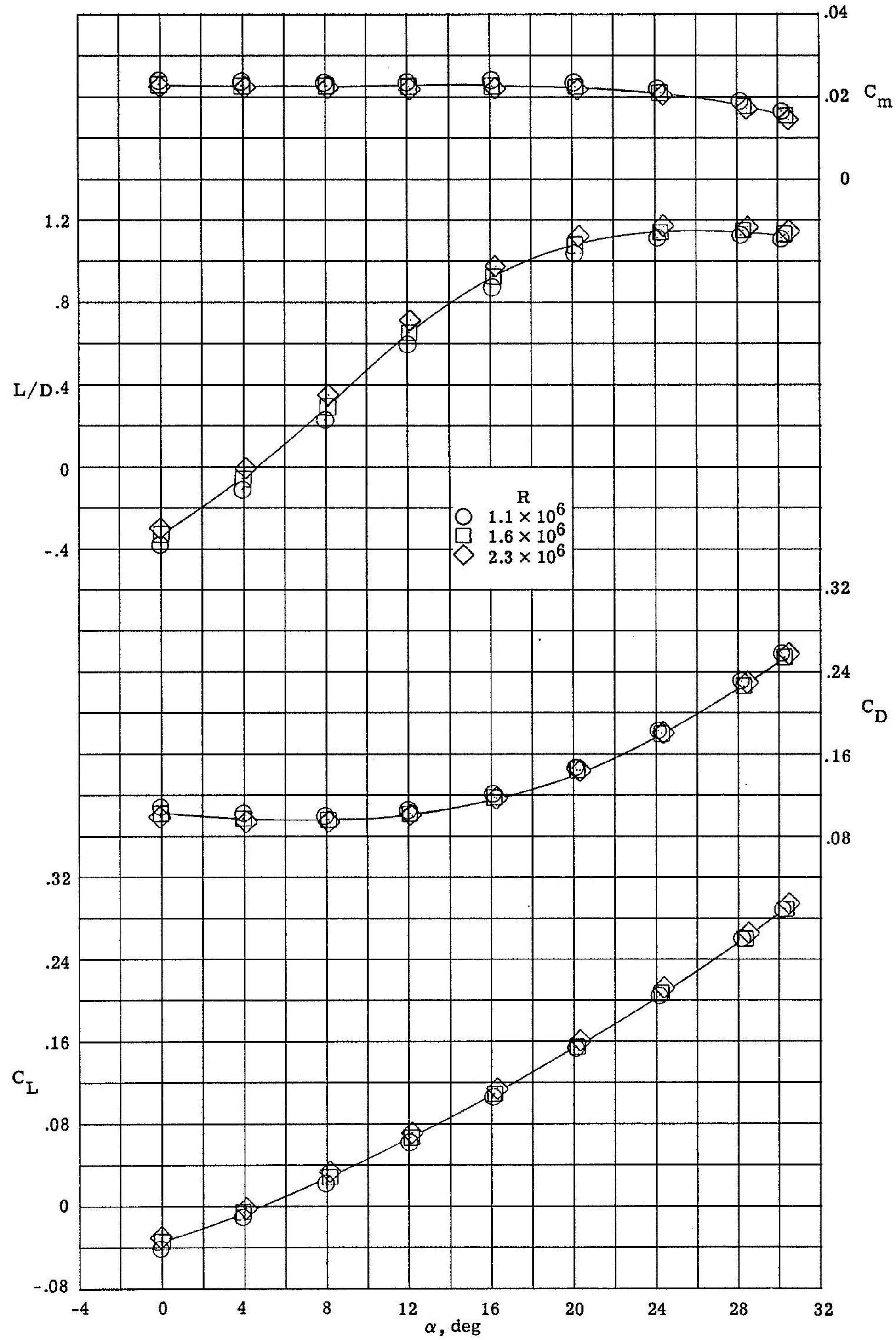

(b) $\delta_e = 15^0$.

Figure 26.- Continued.

[redacted]

[redacted]

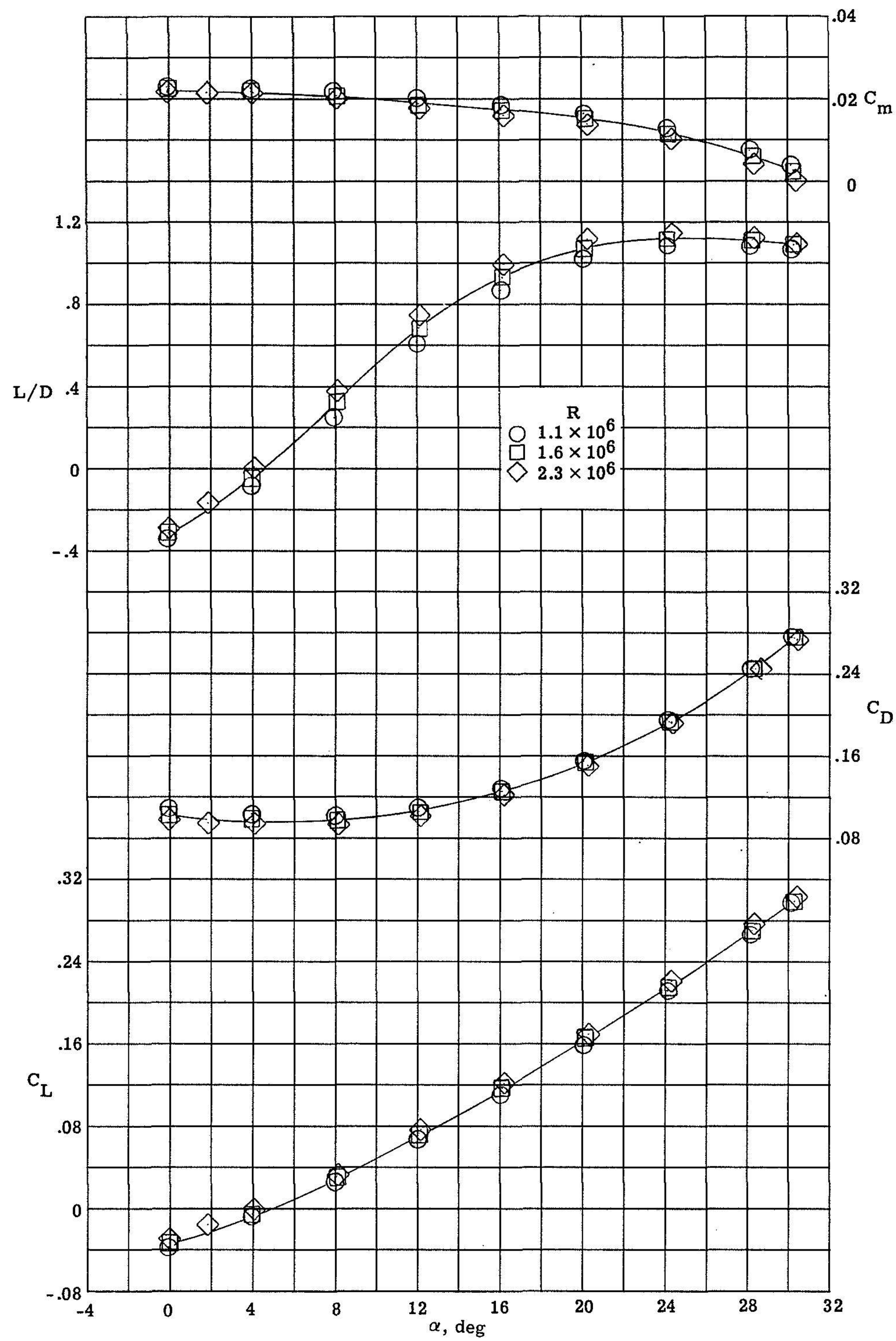

(c) $\delta_e = 30^0$.

Figure 26.- Continued.

[redacted]

[redacted]

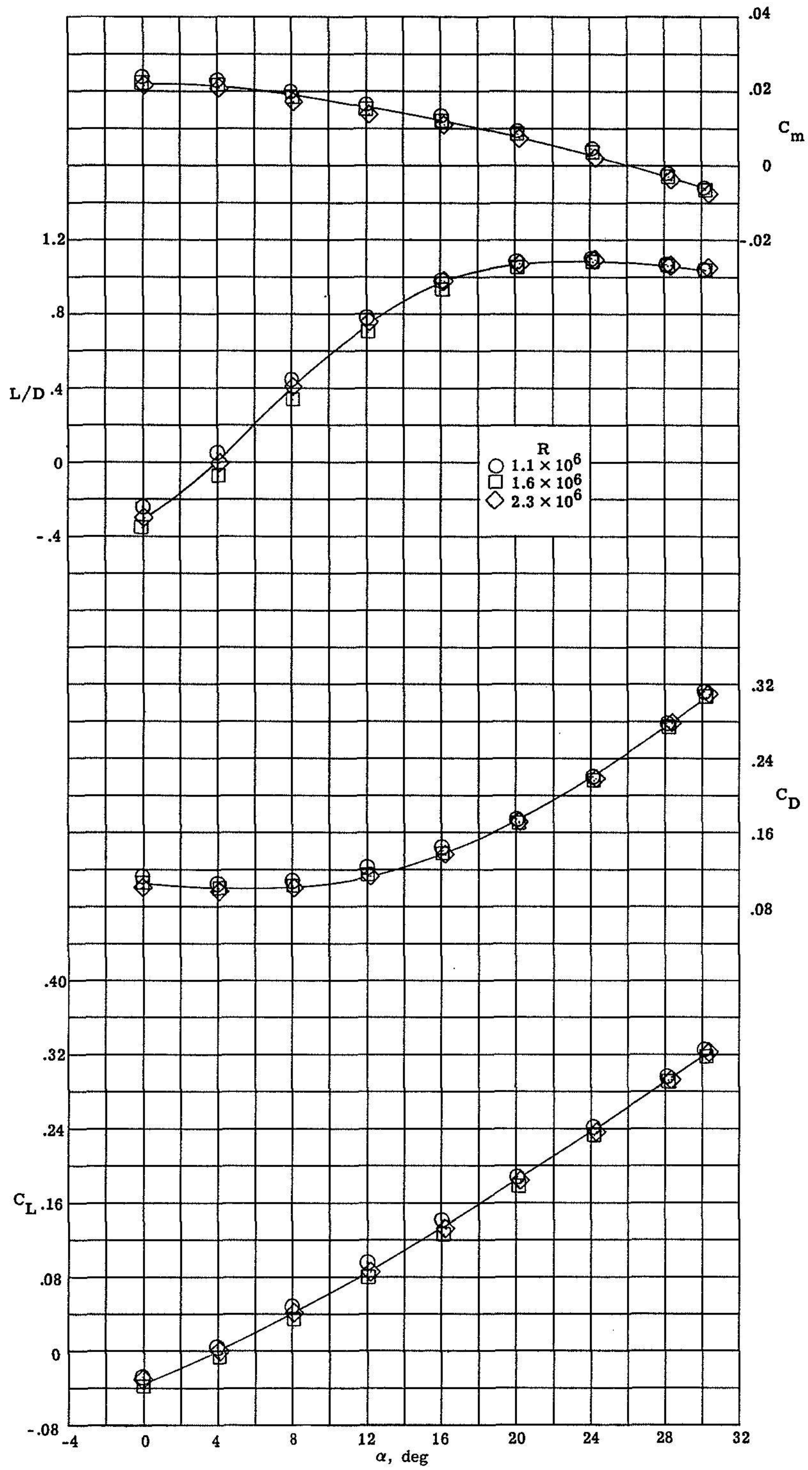

(d) $\delta_e = 45^0$.

Figure 26.- Concluded.

[redacted]

[redacted]

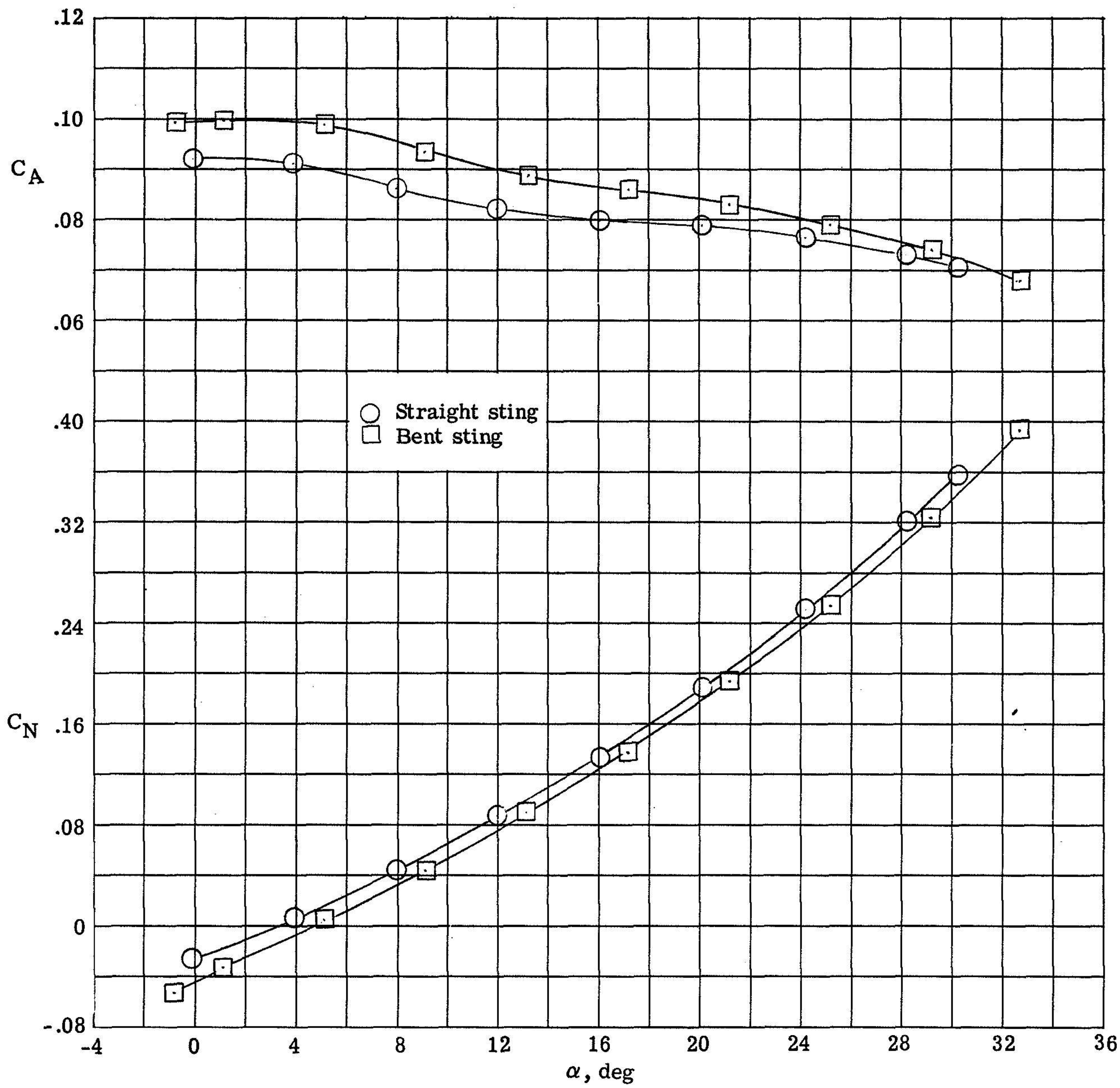

(a) Body-axis data.

Figure 27.- Comparison of longitudinal aerodynamic characteristics obtained with straight sting and bent sting at the lower angles of attack with tip fin I_4.

[redacted]

[redacted]

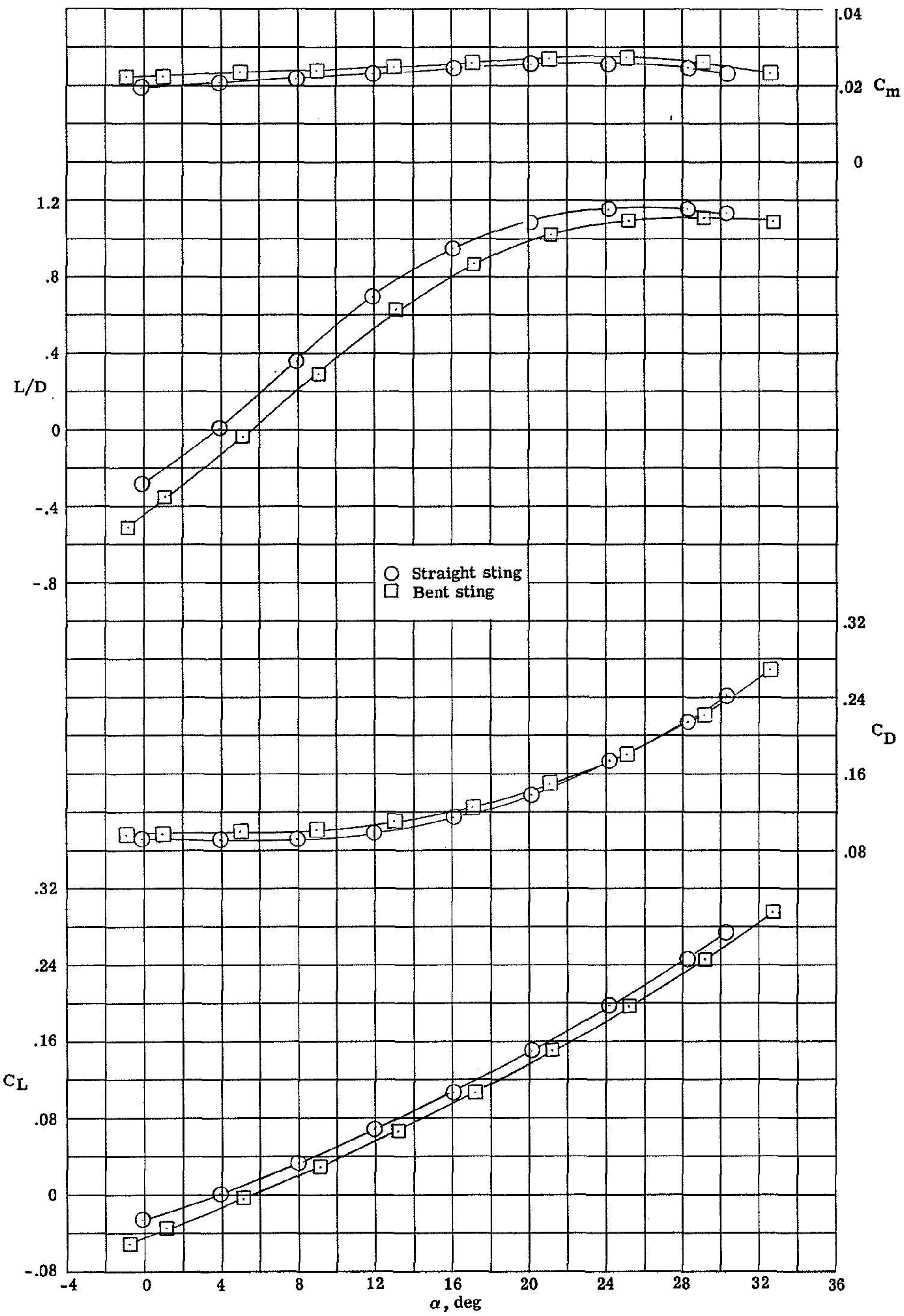

(b) Stability-axis data.

Figure 27.- Concluded.

[redacted]

[redacted]

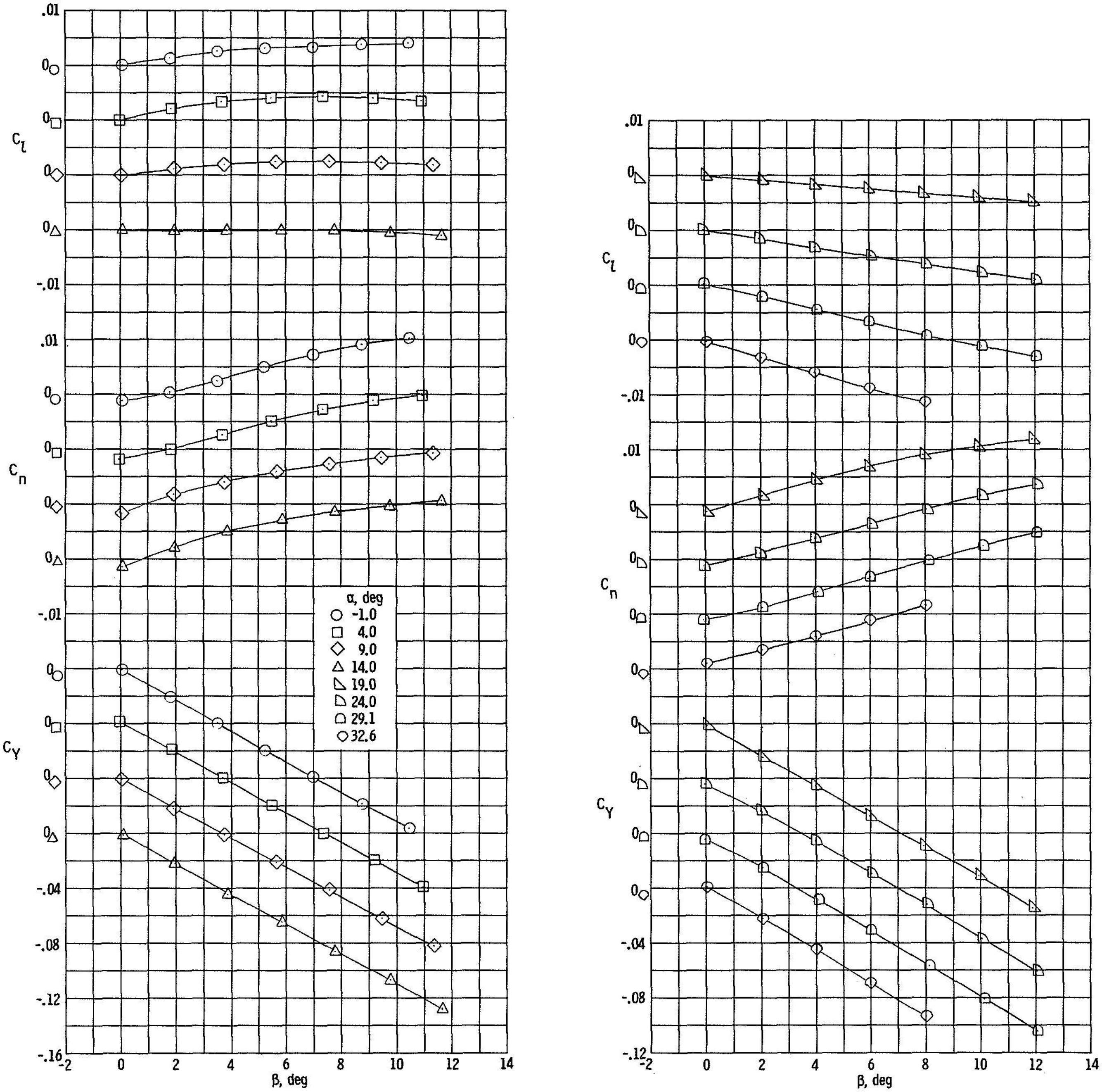

Figure 28.- Variation of directional and lateral characteristics with sideslip angle obtained with bent sting, $\delta_e = 0^0$.

[redacted]

[redacted]

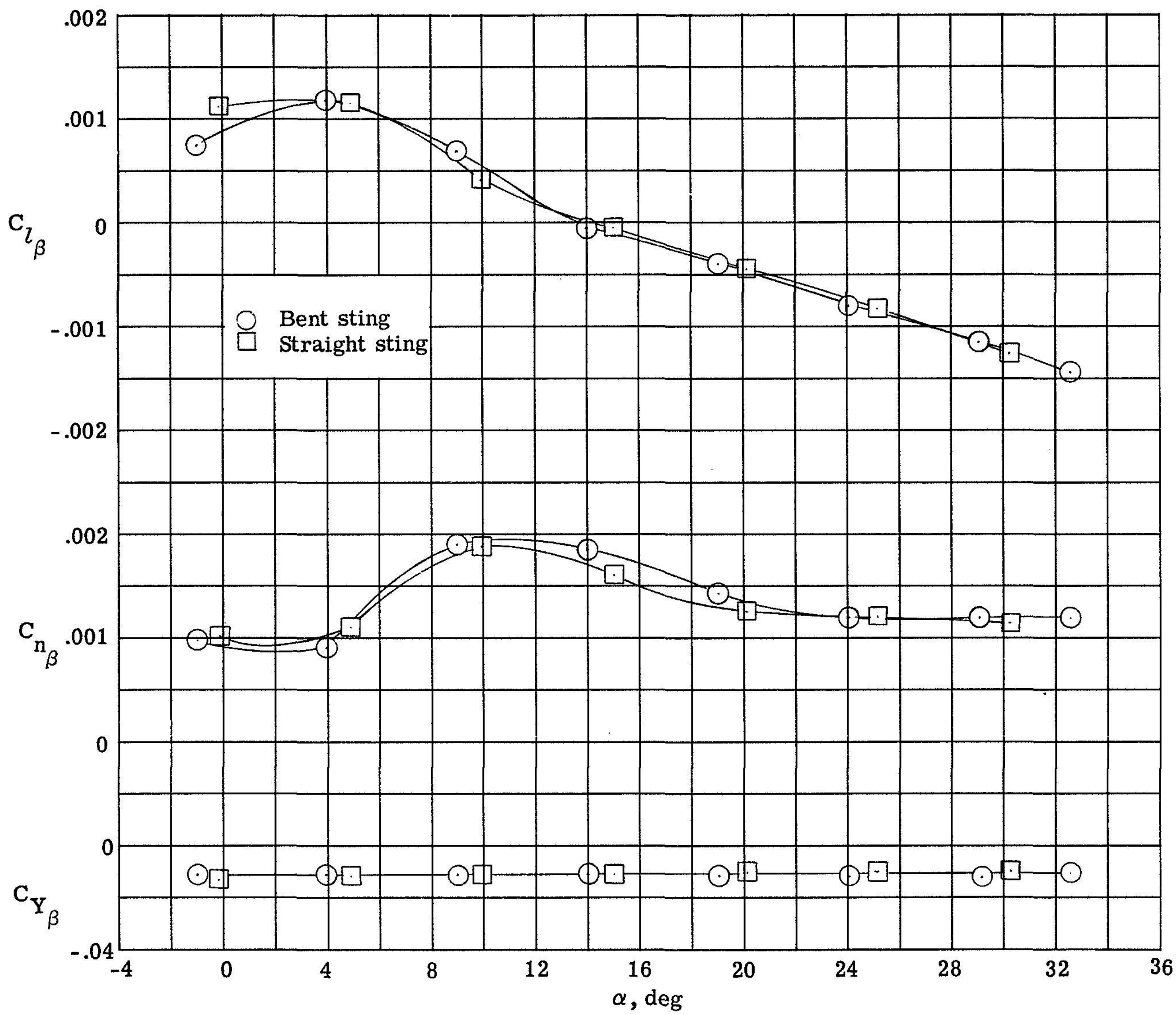

Figure 29.- Comparison of directional and lateral stability characteristics obtained with straight sting and bent sting at the lower angles of attack.

[redacted]

[redacted]

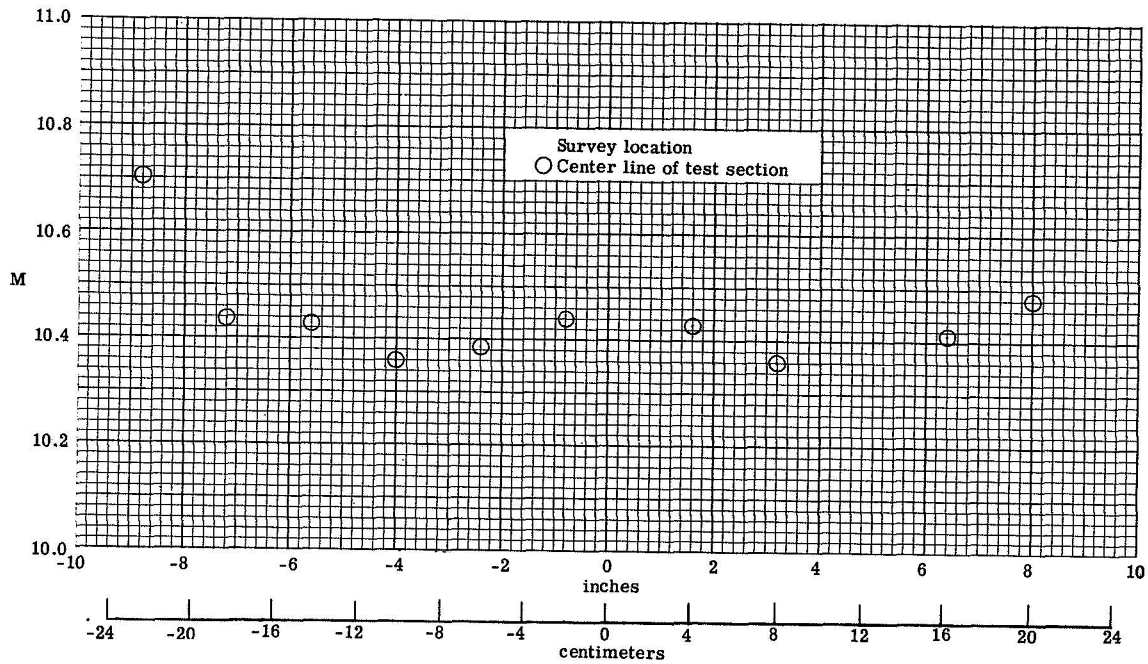

(a) Horizontal distribution.

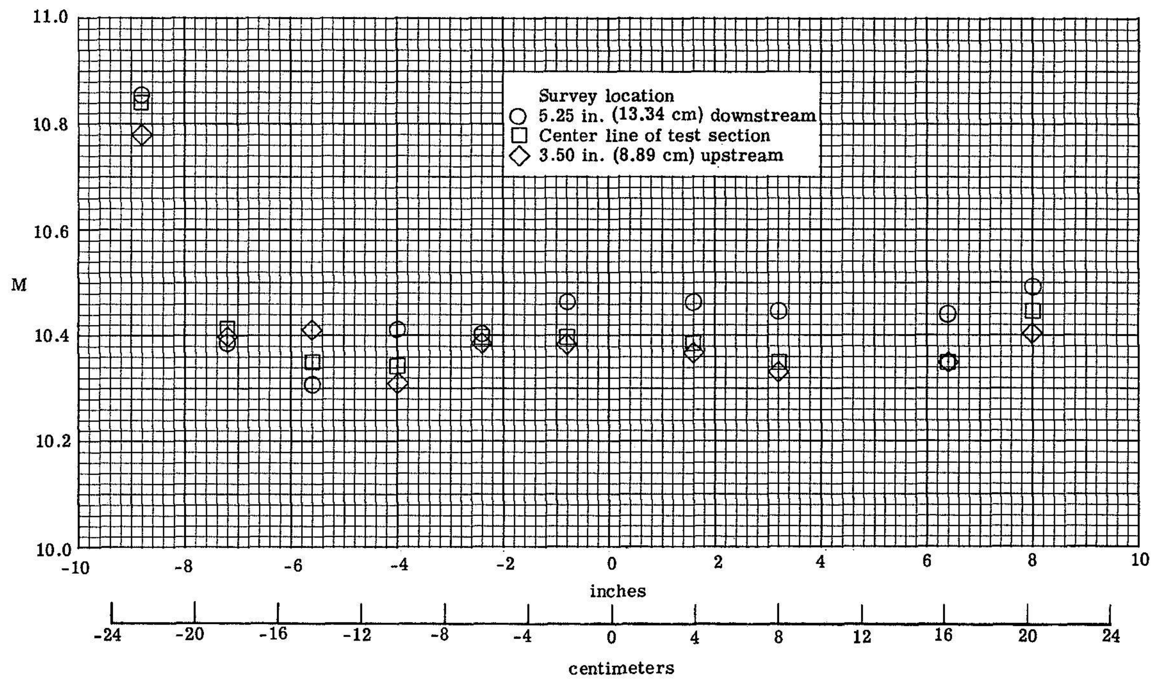

(b) Vertical distribution.

Figure 30.- Mach number distribution at a stagnation pressure of 750 psia (5.171 MN/m^2).

[redacted]

[redacted]

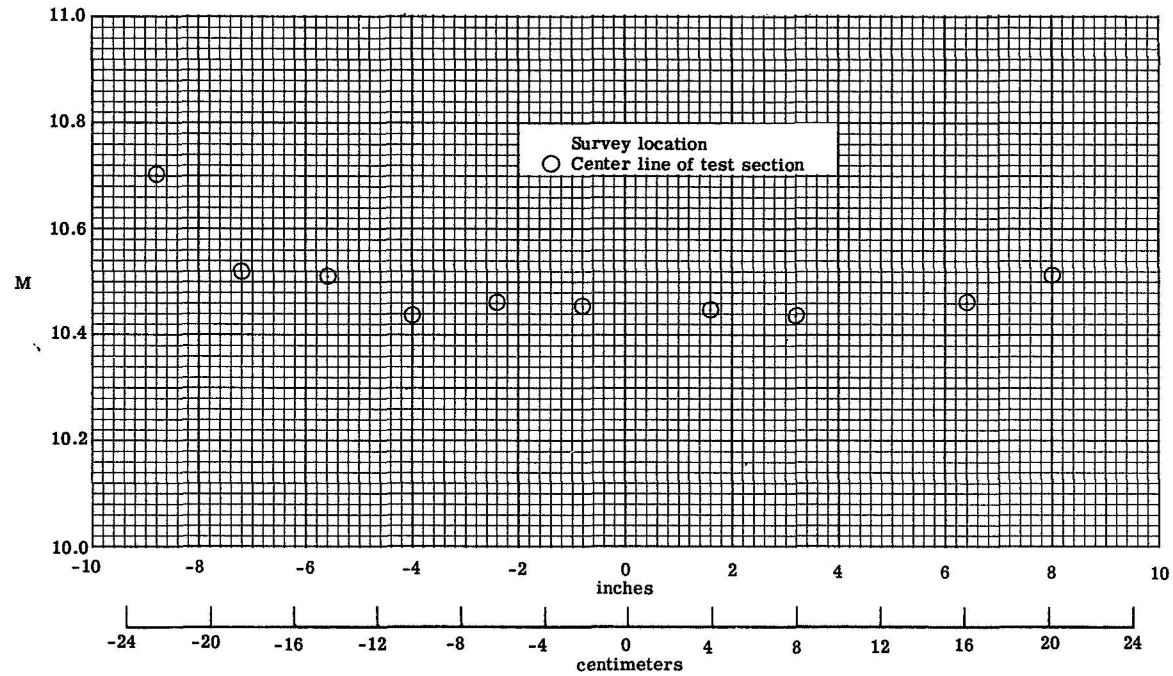

(a) Horizontal distribution.

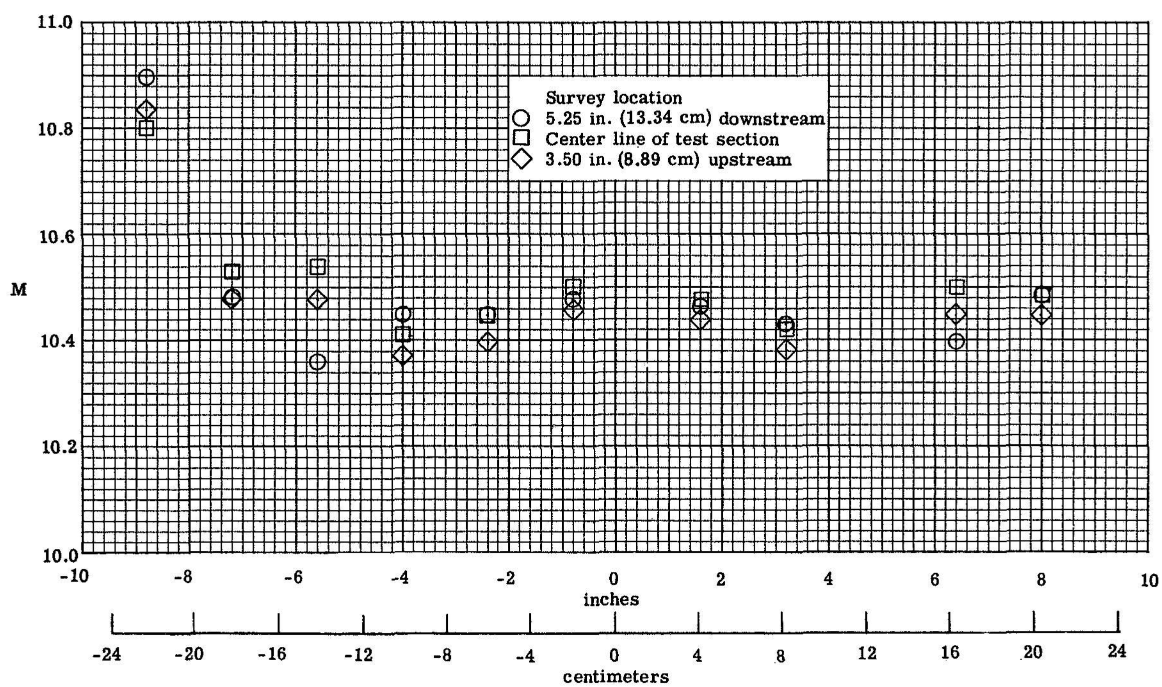

(b) Vertical distribution.

Figure 31.- Mach number distribution at a stagnation pressure of 1200 psia (8.274 MN/m^2).

[redacted]

[redacted]

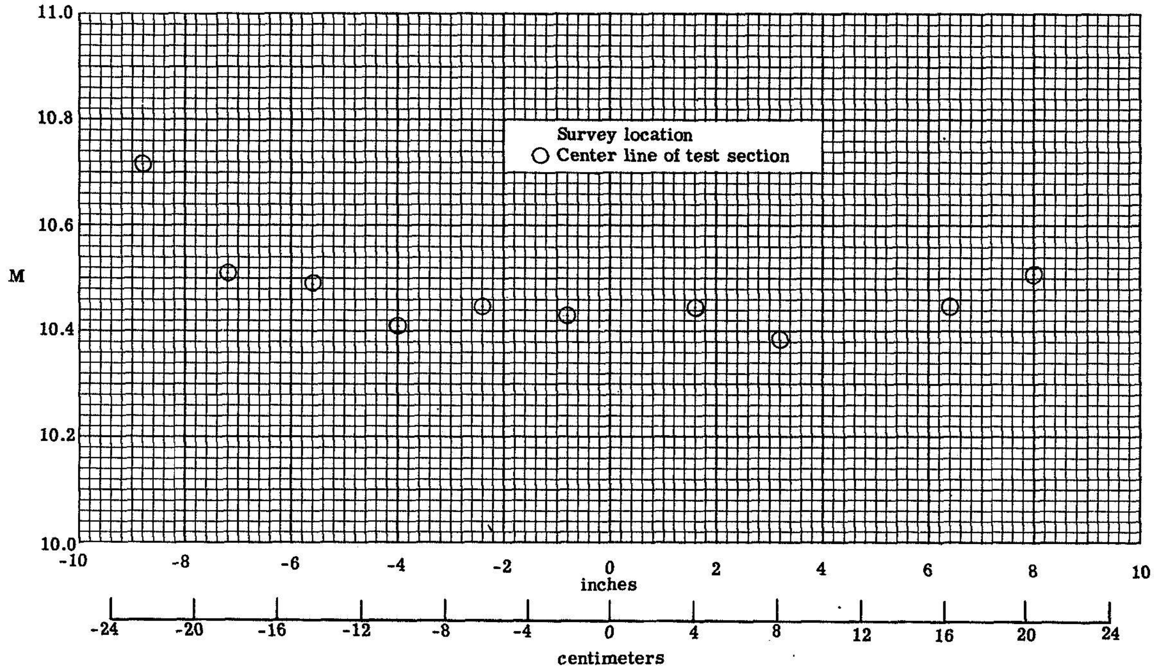

(a) Horizontal distribution.

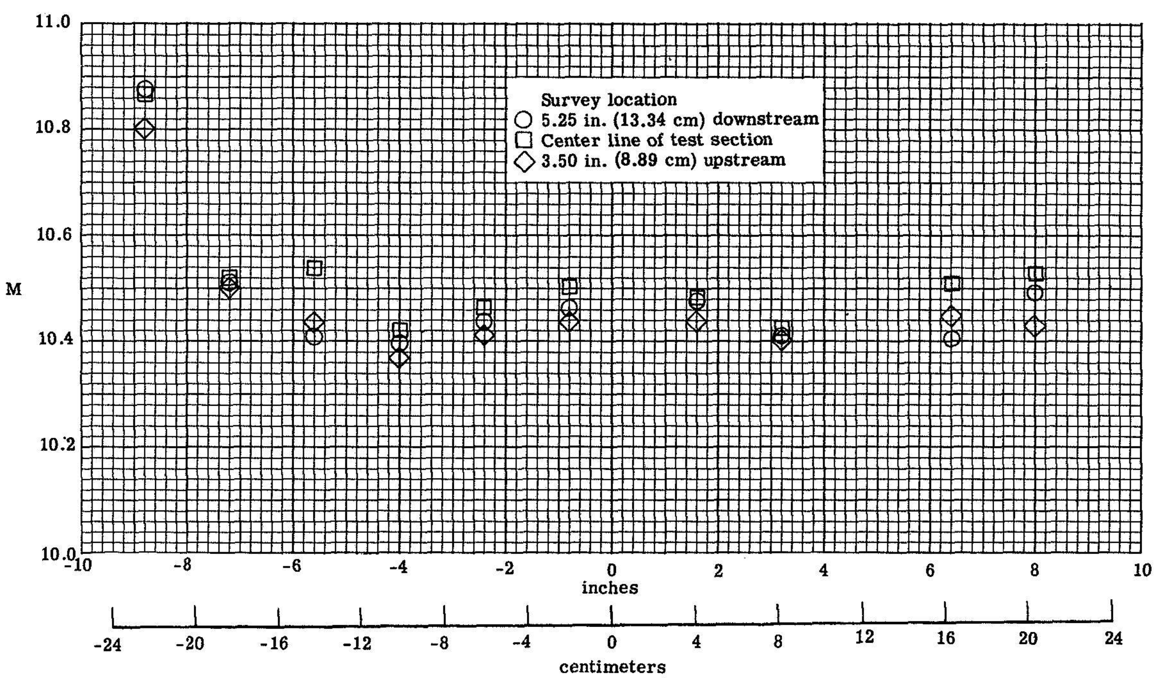

(b) Vertical distribution.

Figure 32.- Mach number distribution at a stagnation pressure of 1500 psia (10.342 MN/m2).

[redacted]

[redacted]

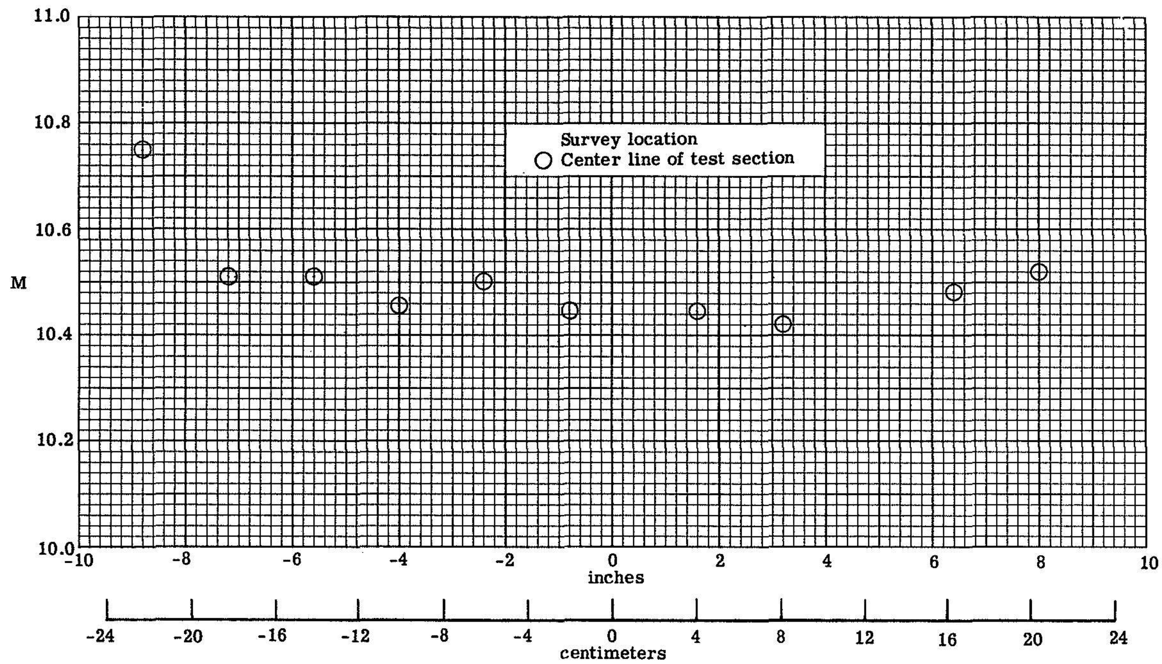

(a) Horizontal distribution.

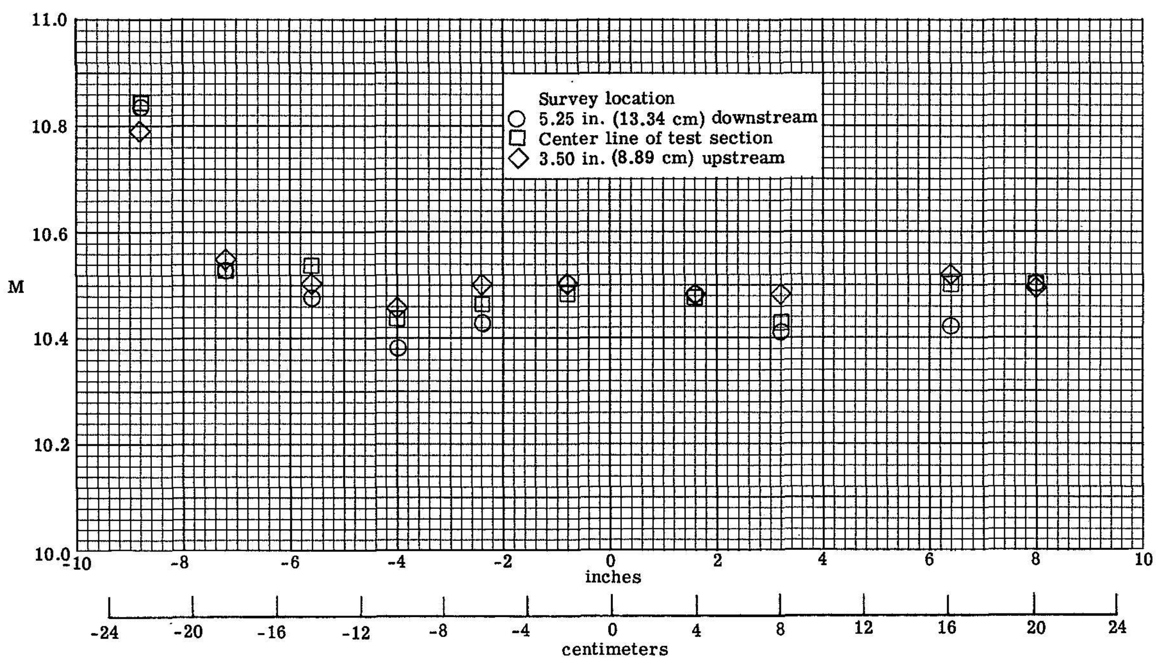

(b) Vertical distribution.

Figure 33.- Mach number distribution at a stagnation pressure of 1800 psia (12.411 MN/m2).